TRANSPORT OF DISSOLVED ORGANIC CARBON FROM SOIL TO SURFACE WATER

IDENTIFICATION AND MODELING OF PATHWAYS AND CONTROLLING FACTORS

Nele VAN GAELEN

Supervisors:
Prof. dr. ir. J. Diels
Prof. dr. G. Govers
Prof. dr. ir. J. Vanderborght

Members of the
Examination Committee:
Prof. dr. O. Batelaan
Prof. dr. T.A. Bogaard
Prof. dr. K. Kalbitz
Prof. dr. ir. B. Sels
Prof. dr. ir. E. Smolders

Dissertation presented in partial fulfilment of the requirements for the degree of Doctor in Bioscience Engineering

June 2016

Doctoraatsproefschrift nr. 1355 aan de faculteit Bio-ingenieurswetenschappen van de KU Leuven

Acknowledgments

A finalized PhD thesis is never the effort of just one person. For what is presented here, I had the help of many people, without whom I would have never been able to finish this work. I'd like to take the opportunity here to give them the credit they deserve.

First of all, I am grateful to Jan Vanderborght, who introduced me to scientific research in the final year of my Master studies. It was the positive experience of my Master thesis that showed me the pleasure of submerging myself into a specific research topic.

After these Master studies Jan Diels, Gerard Govers and Jan Vanderborght joined in a team effort to guide me through my PhD research. Each with a different perspective on the matter and a different working approach, I would like to thank all three of my promotors for their continuous input.

I'm also grateful to the chairman and the members of the jury for their critical but constructive comments on the first version of this PhD thesis.

Thanks go out to Wim Clymans, for starting up the research in de study catchments, and to Benedicta Ronchi and Dries Verheyen, who joined me in the work conducted at the LUSI sites. Thank you An Van den Putte, Christoph Langhans and Veerle Verschoren, for the help with the rainfall simulations.

I couldn't have presented these results without the efforts of Lore Fondu, who collected and analyzed an endless amount of water samples, or without Bjorn Dieu, who presented an infinite energy in the lab. I'm also grateful to Valentijn, Mustapha, Jos, Karla, Kristien en Peter for their practical and technical support both in the lab and on the field.

I had the pleasure of being surrounded by colleagues from all over the world in the office. Some who were only there for a few months, some who sat through it with me for the final run. I'd like to say thanks to all of them, for the joyful notes during break times and the listening ear in times of distress. A special note for Joachim, steady as a rock at the desk across the room.

Thank you Astrid Bryon, Pieter Vandermeeren and Yann de Mey. I don't think one of you has ever realized, neither do I remember the exact words you said, but each of you has at one point during my research reassured me that I would be able to finish this.

I'd especially like to say thanks to all my family and friends. I greatly appreciate your never-ending interest, your encouraging words, all the practical help and the shoulders to lean on. An extra thank you goes out to Hanne. As both a sister and a colleague, I have frequently relied on her. With a sixth sense for procrastination and a better sense for decision making than I have, she often lovingly called me to order.

Most importantly, I couldn't have done this without Michaël. Our live together started off at the exact same time I started this PhD, and look where we are now! Over all these years, he's been my greatest support. With his indestructible positive view on everything in life, he has continuously helped me wherever he could. Thank you Mike! For everything…

Finally, a big hug for Nore, for her always-energizing smile.

Abstract

Dissolved organic carbon (DOC) in the surface water is an important component of the global carbon cycle. Due to its active and mobile nature, it affects aquatic ecosystems in several ways and plays a significant role in the cycling and distribution of carbon within and between ecosystems. Although the estimated annual flux of DOC from the land to the oceans is ±0.4 Pg C $year^{-1}$, almost half the current net terrestrial uptake of ±0.9 Pg C $year^{-1}$, the factors controlling the transport of DOC from the soil to the surface water are not clear.

Previous research on the transport of DOC in the soil and on the factors controlling DOC export towards the river system has mostly been carried out in forest and wetland areas. However, agricultural land use can lead to significant surface runoff and thereby enable a surface runoff pathway for the transport of DOC. Little information is available on the transport of DOC through surface runoff from agricultural fields and on the factors controlling this transport. At the catchment scale, previous work has mainly focused on either regular sampling during baseflow conditions or high-frequency monitoring during a limited number of events, leading only to a partial understanding of the factors controlling the DOC transport. Although experimental data on DOC export from catchments are available, efforts to model the DOC export are scarce. Therefore, the general aim of this work was to determine the factors controlling the transport of dissolved organic carbon from the soil to the surface water and to identify and model the transport pathways.

Field experiments were conducted at different temporal and spatial scales. At the plot scale, rainfall simulations were carried out to identify the effect of soil properties, field characteristics and hydrological conditions on DOC export by surface runoff from agricultural fields. Additionally, the temporal evolution of DOC concentrations and specific UV absorbance (SUVA) values in runoff water during a rainfall event was observed. SUVA is an indicator of the aromaticity and the recalcitrant nature of DOM, whereby higher SUVA values are measured when the DOM is more aromatic.

Four small headwater catchments contrasting in land use and hydrogeology were monitored to study the transport pathways delivering DOC towards the surface water at the catchment scale. Stream water was sampled on a regular base during dry weather conditions and at high frequency during rainfall events, to observe the temporal variation of DOC concentrations both seasonally and at the time scale of a rain event. Stream water, groundwater, soil pore water, precipitation/throughfall and riparian zone water samples were additionally analyzed for silica and major cations, allowing an end-member mixing analysis that gained insight into the contributing pathways delivering DOC at the catchment outlet during different flow regimes.

For the Blégny grassland catchment, stream water DOC concentrations were modeled as a simple mixture of DOC from the different transport pathways delivering water at the catchment outlet. Therefore, discharge measured at the catchment outlet was modeled as a combination of discharge from different components using the FLEX hydrological model and the WETSPRO model.

Results from the rainfall simulations showed that the antecedent rainfall conditions are the most important control on DOC concentrations and quality in surface runoff water from agricultural fields. Lower amounts of rainfall before the experiment, or lower initial moisture content of the soil lead to high concentrations of low aromatic DOC in the runoff water. Soil and field characteristics only have

limited effect on DOC concentrations in runoff. Overall, DOC concentrations in runoff water are highest and SUVA values are lowest at the start of a rainfall event.

In the stream water from small headwater catchments, DOC concentrations and SUVA values were higher in forest catchments than in pasture catchments. In our study catchments, no seasonal variation in baseflow stream DOC concentrations was observed. During rainfall events in all catchments however, both DOC concentrations and SUVA values increased with discharge, reached a maximum and decreased again as discharge returned to pre-event baseflow values. Overall, the majority of the total annual export of DOC from the study catchments was transported to the catchment outlet during times when discharge was elevated in response to a rainfall event. The changes in concentrations and quality of DOC during discharge events could be attributed to a change in contributions of transport pathways of water to the stream. In the forested catchments with deep groundwater tables and thick unsaturated zones, the main contributions to the stream water during baseflow was via the groundwater. Rising stream DOC concentrations during rainfall events were attributed to additional throughfall and riparian zone transport pathways. In the grassland catchments with shallow groundwater tables, stream flow mainly originated from shallow groundwater discharged at seeps. During rain events, an additional transport pathway through the organic rich top soil layer and water from the riparian zone caused DOC concentration to rise. The importance of the contributing pathways in the grassland catchment changed seasonally and depended on the degree of saturation of the catchment soils.

The WETSPRO model calculating DOC concentrations in the stream water as a mixture of DOC from the different transport pathways, was able to reproduce DOC concentrations observed in the Blégny catchment. As the FLEX hydrological model however did not succeed in an accurate prediction of discharge measured in the field, modeled subflows of the FLEX model did not allow a good prediction of the observed variation in stream water DOC concentrations.

Overall, this research showed that on agricultural soils that generate considerable amounts of surface runoff during a rainfall event, surface runoff is an important pathway for the transport of DOC from the soil to the surface water. In future research, this transport pathway thus deserves our increased interest. At the catchment scale, the majority of the total annual export of DOC for the study catchments was transported to the catchment outlet during times when discharge was elevated in response to a rainfall event. This proves the value of our work, whereby regular sampling during dry weather baseflow conditions was combined with high-frequency monitoring during a great number of rainfall events. Our results also show that hydrological modeling of observed discharge as the sum of discharges from different transport components, combined with chemical analysis of the contributing sources waters, successfully allows the modeling of DOC concentrations observed in the stream water.

Nederlandstalige samenvatting

Opgeloste organische koolstof (DOC) in het oppervlaktewater is een belangrijke component in de globale koolstofcyclus. DOC beïnvloedt aquatische ecosystemen op verschillende manieren en speelt een significante rol in de uitwisseling van koolstof tussen en binnenin ecosystemen. Hoewel de geschatte jaarlijkse DOC-flux van het land naar de oceaan ±0.4 Pg C $jaar^{-1}$ bedraagt - hetgeen overeenkomt met bijna de helft van de netto terrestrische koolstofopname - is het niet duidelijk welke factoren het transport van DOC van het land naar het oppervlaktewater beïnvloeden.

Eerder onderzoek naar DOC-transport in de bodem en naar welke factoren een invloed hebben op DOC-export naar het oppervlaktewater werd voornamelijk uitgevoerd in bos of moerasgebied. In landbouwgebied is er echter een bijkomende transportweg voor DOC van belang, namelijk de oppervlakkige afstroming. Hierover is slechts weinig informatie beschikbaar. Op de schaal van een rivierbekken concentreerde eerder onderzoek zich ofwel op regelmatige staalname van basisafvoer tijdens droge periodes ofwel op meer frequente staalname tijdens een beperkt aantal regenbuien. Dit heeft slechts geleid tot een gedeeltelijke kijk op de controlerende factoren voor DOC-transport op de schaal van het rivierbekken. Tenslotte zijn er slechts beperkte pogingen ondernomen om de export van DOC te modelleren, hoewel experimentele gegevens van DOC-transport beschikbaar zijn. Het doel van dit werk was daarom om de controlerende factoren voor het transport van DOC van de bodem naar het oppervlaktewater te bepalen en de transportwegen te identificeren en modelleren.

Veldexperimenten werden uitgevoerd op verschillende ruimtelijke en temporele schalen. Op de schaal van kleine proefvlakken werden experimenten met regenvalsimulatie opgezet om na te gaan wat het effect is van bodemeigenschappen, veldkarakteristieken en hydrologische randvoorwaarden op DOC-export via oppervlakkige afstroming van landbouwvelden. Daarnaast werd de evolutie van DOC-concentraties en specifieke UV absorbantie (SUVA) bestudeerd tijdens de duur van een regenbui. SUVA is een maat voor de aromaticiteit van DOC, waarbij hogere SUVA-waarden duiden op meer aromatische DOC.

Om de transportwegen van DOC naar het oppervlaktewater op de schaal van het klein rivierbekken (bovenstroom) te bestuderen en de variatie van DOC-concentratie en -kwaliteit in de tijd na te gaan, werden vier kleine rivierbekkens opgevolgd. Deze verschilden van elkaar in landgebruik en hydrogeologie. In elk rivierbekken werden regelmatige staalnames van rivierwater tijdens droge periodes gecombineerd met meer frequente staalnames tijdens regenbuien. Hierdoor kon de seizoensvariatie van DOC in het oppervlaktewater worden nagegaan, maar ook de variatie op veel kortere tijdschaal tijdens een regenbui. Stalen van het rivierwater, grondwater, poriewater, regenwater en water uit de verzadigde oeverzone werden geanalyseerd op DOC, maar ook op silicium en verschillende kationen. Dit liet toe een '*end-member mixing*' analyse uit te voeren, waardoor de transportwegen die bijdragen tot DOC-export tijdens verschillende hydrologische regimes duidelijk werden.

Voor één van de rivierbekkens onder grasland, het rivierbekken in Blégny, werden de DOC-concentraties in de rivier gemodelleerd als een menging van DOC uit de verschillende transportwegen die bijdragen tot DOC-export. Afstroming van het rivierbekken werd daartoe

gemodelleerd als de som van verschillende watercomponenten met behulp van het FLEX-model en het WETSPRO-model.

Resultaten van de regenvalsimulaties toonden aan dat op de schaal van het proefvlak, de vochtigheidsgraad voorafgaand aan een bui de belangrijkste controlerende factor is voor DOC-concentraties en DOC-kwaliteit (SUVA) in oppervlakkige afstroming van landbouwgronden. Minder regen voorafgaand aan de regensimulatie of een lager initieel vochtgehalte in de bodem zorgden voor hogere DOC-concentraties met een lagere aromaticiteit in oppervlakkige afstroming. Bodem- en veldkarakteristieken hadden daarentegen slechts een beperkte invloed. DOC-concentraties in oppervlakkige afstroming van landbouwgronden waren het hoogst en SUVA-waarden waren het laagst aan het begin van een regenbui.

Op de schaal van een rivierbekken werden hogere DOC-concentraties en hogere SUVA-waarden gemeten in de bekkens onder bos dan in de bekkens onder grasland. In geen van de vier rivierbekkens werd een seizoensvariatie van de DOC-concentraties in de rivier gemeten. Op kortere tijdschaal werden echter wel grote variaties in DOC-concentraties en SUVA-waarden vastgesteld tijdens een regenbui. Wanneer het debiet in de rivier steeg tijdens een regenbui stegen zowel DOC-concentraties als SUVA-waarden. Beiden bereikten een piekwaarde en daalden opnieuw wanneer het debiet daalde naar de waarde geobserveerd voor de start van de regenbui. Deze veranderingen in DOC-concentraties en -kwaliteit konden worden toegeschreven aan een verandering in de bijdrage van de verschillende transportwegen via dewelke het water de rivier bereikte. In de rivierbekkens onder bos werden diepe grondwatertafels en dikke onverzadigde zones teruggevonden. Tijdens droge periodes leverde de grondwaterstroming de belangrijkste bijdragen aan de totale afvoer in deze rivierbekkens. Hogere DOC-concentraties in de rivier tijdens een regenbui werden dan veroorzaakt door een bijdrage van regenwater en water uit de verzadigde oeverzone. In de rivierbekkens onder grasland kwamen de grondwatertafels op een veel beperktere diepte voor. Daar was het ondiepe grondwater dat op verschillende plaatsen op de hellingen aan de oppervlakte kwam, de belangrijkste transportweg voor afvoer tijdens droge periodes. Tijdens een regenbui werd de stijging in DOC-concentraties veroorzaakt door bijdragen van de verzadigde oeverzone en van een transportweg doorheen de bovenste bodemlagen die rijk zijn aan organische stof. In het rivierbekken onder grasland varieerde het belang van de verschillende transportwegen per seizoen.

In Blégny konden met behulp van het WETSPRO-model de gemeten DOC-concentraties goed gereproduceerd worden. De DOC-concentraties in de rivier werden daarbij bepaald als een menging van DOC in de verschillende transportwegen. Aangezien het FLEX-model niet in staat was om de afvoer in het rivierbekken afdoende te modelleren, konden de gemodelleerde componenten van het FLEX-model ook de variaties in geobserveerde DOC-concentraties niet goed voorspellen.

De resultaten uit dit onderzoek gaven aan dat oppervlakkige afspoeling significant bijdraagt aan het transport van DOC van de bodem naar het oppervlaktewater in landbouwgebieden. Deze transportweg verdient dus bijkomende aandacht in toekomstig onderzoek. Op de schaal van het rivierbekken werd in de studiegebieden het overgrote deel van de DOC getransporteerd tijdens periodes met verhoogde afvoer ten gevolge van een regenbui. Dit toont het belang van ons werk aan, waarbij regelmatige staalnames van rivierwater tijdens droge periodes werden uitgevoerd én meer frequente staalnames werden gedaan tijdens een groot aantal regenbuien. Bovendien toonde dit werk aan dat de hydrologische modellering van afstroming als de som van watercomponenten in

combinatie met chemische analyse van de verschillende componenten, toelaat DOC-concentraties in de rivier goed te beschrijven.

List of figures

Figure 1.1. DOC concentrations measured in arable land in soil leachate at 40 cm depth, versus time-averaged water velocity (Mertens et al., 2007). 3

Figure 1.2. Flowchart representing the thesis outline. 8

Figure 2.1. Experimental set-up, showing the nozzle-type rainfall simulator. The inset shows the runoff collecting gutter, the collection tank and the experimental plot (0.85m by 0.85m) bounded by metal plates and surrounded by 4 rain gauges. 12

Figure 2.2. [DOC] (left) and SUVA values (right) versus time for 6 rainfall experiments on field site 2PE (maize) on June 17 and 18, 2010. Conventional tilled data: Open diamonds - dashed connection lines; Reduced tilled data: solid diamonds and connection lines. 18

Figure 2.3. Modeled versus measured [$\overline{DOC}$] for each individual field experiment. The full line is the 1:1 line. a) model with fixed and random effects, b) model with fixed effects only. 21

Figure 2.4. Modeled versus measured $\log_{10}\overline{SUVA}$ values for each individual field experiment. The full line is the 1:1 line. a) model with fixed and random effects, b) model with fixed effects only. 22

Figure 2.5. DOC concentrations versus time in surface runoff (solid diamonds) and percolation water (open diamonds) during the first (left) and second (right) rainfall application. Rainfall applications were separated by a 7 day air drying period. 23

Figure 2.6. SUVA values versus time in surface runoff (solid diamonds) and percolation water (open diamonds) during the first (left) and second (right) rainfall application. Rainfall applications were separated by a 7 day air drying period. 24

Figure 3.1. Location of the study sites on the elevation map of Belgium. For each catchment a detailed map shows the topography, roads and the position of the V-notch weir and automatic sampler (blue square). 31

Figure 3.2. Cross-section (SSE to NNW) of the landscape in the Meerdaal catchment, with an indication of the groundwater table, deduced from the piezometer data and from field observations. 32

Figure 3.3. Cross-section (W to E) of the landscape in the Blégny catchment, with an indication of the groundwater table, deduced from the piezometer data and from tensiometer measurements between March 2013 and September 2013. 33

Figure 3.4. Hydrology and DOC concentrations in the stream at the outlet of the Meerdaal catchment (January 2010 - July 2013). The inset shows an enlargement of the baseflow discharge during one month (July 2010). The bottom graph shows groundwater depth measured in 3 piezometers. Discharge was not measured during the large rainfall event on 03/05/2012 due to malfunctioning of the equipment.....39

Figure 3.5. General representation of discharge, precipitation and solute concentrations measured in the stream outlet of the Meerdaal catchment during a rainfall event (29/06/2011).....40

Figure 3.6. Hydrology and DOC concentrations in the stream outlet of the Blégny catchment (January 2010 - July 2013). The bottom graph shows groundwater depth measured in 3 piezometers. 41

Figure 3.7. General representation of discharge, precipitation and solute concentrations measured in the stream outlet of the Blégny catchment during the spring-summer period (20/05/2012, left) and the fall-winter period (05/12/2012, right). 42

Figure 3.8. PCA results for the Meerdaal catchment. Baseflow and event stream water samples are shown with mean values and standard deviations of potential end-members.....45

Figure 3.9. PCA results for the Blégny catchment. Baseflow and event stream water samples are shown with mean values and standard deviations of potential end-members.....46

Figure 3.10. Estimated contributions based on the EMMA of the different end-members at sample time during the event on 29/06/2011 in the Meerdaal catchment. The full line shows the measured discharge data (recorded every 15 minutes). Estimated fractions were multiplied with the measured discharge to be able to show them on the discharge axis. 48

Figure 3.11. Estimated contributions based on the EMMA of the different end-members at sample time during the events on 20/05/2012 (top) and 05/12/2012 (bottom) in the Blégny catchment. The full line shows the measured discharge data (recorded every 15 minutes). Estimated fractions were multiplied with the measured discharge to be able to show them on the discharge axis.....48

Figure 4.1. The Blégny catchment with indication of the position of the V-notch, suction cups transects, piezometers and seeps, and elevation contour lines (m above sea level). 57

Figure 4.2. Structure of the hydrological model. Symbols are explained in detail in Table 4.2. 59

Figure 4.3. Discharge and precipitation measured at the site between April 2010 and December 2013 aggregated over intervals of 1 hour. Hourly potential evapotranspiration from a station nearby. Discharge data corresponding to a level of >15cm are indicated in grey, and are not included for the calibration of the hydrological model. 64

Figure 4.4. Stream water DOC concentrations measured during baseflow and peak flow conditions. The inset shows the enlargement of a two week period (indicated in red) in the summer of 2011, clearly illustrating the rising DOC concentrations during rain events. 65

Figure 4.5. Histograms showing the parameter posterior probability distribution. The parameter set with the lowest sum of squared residuals, as inferred from the DREAM calibration procedure, is indicated in red. 67

Figure 4.6. Hourly aggregated measured (full blue line) and modeled (FLEX, full black line) discharge data. The grey band indicates the 95 % confidence interval of the modeled discharge values due to parameter uncertainty. 68

Figure 4.7. Hourly aggregated measured discharge values (full blue line) and discharge modeled by the FLEX model consisting of its three components namely Q_S (light grey), Q_F (dark grey) and Q_R (red). The inset shows the enlargement of the same two week period in the summer of 2011 as was the case in Figure 4.4. 69

Figure 4.8. DOC concentration at the catchment outlet, with measured values represented by black dots and hourly modeled values using the FLEX subflow results represented by the full line. The inset shows the enlargement of the same two week period in the summer of 2011 as was the case in Figure 4.4. 70

Figure 4.9. Measured DOC concentrations versus DOC concentrations modeled using the subflow results of the FLEX model. 71

Figure 4.10. Hourly discharge consisting of its three subflow components separated by the WETSPRO tool: slow flow (light grey), interflow (dark grey) and overland flow (red). The inset shows the enlargement of the same two week period in the summer of 2011 as was the case in Figure 4.4. 72

Figure 4.11. DOC concentration at the catchment outlet, with measured values represented by black dots and hourly modeled values using the WETSPRO subflow results represented by the full line. The

inset shows the enlargement of the same two week period in the summer of 2011 as was the case in Figure 4.4.....73

Figure 4.12. Measured DOC concentrations versus DOC concentrations modeled using the subflow results of the WETSPRO model. 74

Figure 5.1. Discharge, $\delta^{18}O$ and $\delta^{2}H$ measured in the stream outlet of the Meerdaal catchment. Open circles indicate values measured in samples collected during baseflow conditions, full circles indicate values measured in event samples. 80

Figure 5.2. Discharge, $\delta^{18}O$ and $\delta^{2}H$ measured in the stream outlet of the Blégny catchment. Open circles indicate values measured in samples collected during baseflow conditions, full circles indicate values measured in event samples. 81

Figure 5.3. Discharge, $\delta^{18}O$ and $\delta^{2}H$ measured in the stream outlet of the Meerdaal catchment during a rainfall event. Open circles indicate values measured in samples collected during baseflow conditions, full circles indicate values measured in event samples. 82

Figure 5.4. Discharge, $\delta^{18}O$ and $\delta^{2}H$ measured in the stream outlet of the Blégny catchment during a two-week period in the summer of 2011. Open circles indicate values measured in samples collected during baseflow conditions, full circles indicate values measured in event samples. 82

List of tables

Table 1.1. Range of DOC concentrations observed in natural waters according to Thurman (1985). 2

Table 1.2. Average riverine DOC fluxes from catchments with different land uses. 4

Table 2.1. Overview of crop type and soil properties of the surface soil layer of the field sites where simulated rainfall experiments were conducted. Numbers in bold indicate a significant difference ($P<0.05$) between conventional and reduced tilled parts. 12

Table 2.2. Characteristics of the soil used in the laboratory experiments. 14

Table 2.3. Overview of measured class and numerical variables and their mean values and standard deviation for the field experiments. Subscript s = measured in soil; r = measured in sediment. 16

Table 2.4. Pearson correlation coefficients between the different numerical variables and $[\overline{DOC}]$ and $\overline{SUVA}$ per experiment. s= measured in soil; r = measured in sediment. 19

Table 2.5. ANOVA results for the effect of tillage technique, season, field and their interaction effects on different measured variables. P-values from type III F-test are given. Statistically significant values are indicated in bold. s = measured in soil. 20

Table 2.6. $[\overline{DOC}]$ and $\overline{SUVA}$ results of the different factors tested in the laboratory experiments. For the drying-rewetting factor tested, values during the second rainfall application (after the drying period) are given. For all other factors tested mean values of the 2 replicates are given. 22

Table 3.1. Overview of the collected samples and the analyses carried out, per catchment. 34

Table 3.2. Filter depth of the piezometers installed in the Meerdaal and Blégny catchment, mean groundwater depth and distance to the stream. 35

Table 3.3. Mean values and standard deviations of DOC, Si and cation concentrations measured in the stream water baseflow, soil pore water, groundwater, riparian water, seeps (Blégny only) and throughfall/precipitation samples. For stream water event samples minimum and maximum are given. 43

Table 3.4. Percentage of variance explained by principal components. 44

Table 3.5. Discharge weighted mean fractions and standard deviations of contributing end-members in the Meerdaal and Blégny catchments as calculated by the EMMA. For the events, the mean and standard deviation of the discharge weighted mean values calculated per event are given. 47

Table 3.6. Coefficients of determination (R^2) and Pearson correlation coefficient (P_{corr}) of measured and predicted concentrations based on the EMMA. 49

Table 3.7. Annual DOC loads reaching the stream of the Meerdaal (forest) catchment via the different transport pathways during dry weather baseflow conditions and during peak event conditions. 49

Table 3.8. Annual DOC fluxes reaching the stream of the Blégny (grassland) catchment via the different transport pathways during dry weather baseflow conditions and during peak event conditions. 50

Table 4.1. State and flux equations of the FLEX hydrological model. 60

Table 4.2. States, fluxes and model parameters of the FLEX hydrological model. For the model parameters, calibration ranges are indicated. 61

Table 4.3. Mean values and standard deviations (in parentheses) of DOC concentrations measured in the stream water during baseflow conditions, soil pore water, groundwater, riparian water, seeps and precipitation samples. For stream water event samples minimum and maximum values are given. 66

Table 4.4. Parameter set with lowest sum of squared residuals, as inferred from the DREAM calibration procedure. 66

Table 4.5. Calibrated parameters of the WETSPRO filter for each subflow. 71

List of acronyms and symbols

A_{254}	Absorbance at 254 nm
ANOVA	Analysis of variance
b	Path length
C_j	Concentration of solute j
$C_{j\ new}$	Standardized concentration of solute j
C_{kj}	Concentration of solute j in the k^{th} end-member
C_R	Runoff coefficient, i.e. proportion of water that cannot be stored in S_U and that recharges S_F and S_S
CT	Conventional tillage
$Ctot_{ij}$	Modeled concentration of solute j in the stream at time i
$Ctot_{ij\ measured}$	Measured concentration of solute j in the stream at time i
D	Proportion of water that recharges S_S
DOC	Dissolved organic carbon
[DOC]	Dissolved organic carbon concentration
$[DOC]_F$	DOC concentration in the water from the fast component
$[DOC]_R$	DOC concentration in the water from the riparian component
$[DOC]_S$	DOC concentration in the water from the slow component
$[DOC]_{TOT}$	Total modeled stream DOC concentration at the catchment outlet
$[\overline{DOC}]$	Discharge weighted mean DOC concentration
EMMA	End-member mixing analysis
E_p	Potential evapotranspiration
E_R	Actual evapotranspiration from S_R
E_U	Actual evapotranspiration from S_U
E_{tot}	Total actual evapotranspiration
f	Proportion of catchment covered by riparian zone/wetland
k_F	Storage coefficient of S_F
k_R	Storage coefficient of S_R
k_S	Storage coefficient of S_S
L_P	Relative soil moisture below which evapotranspiration is moisture constrained
n	Number of samples
p	Probability

P	Precipitation
P_{corr}	Pearson's linear correlation coefficient
PC	Principal component
PCA	Principal component analysis
PET	Polyethylene terephthalate
POC	Particulate organic carbon
Q	Discharge
Q_F	Flow from S_F
Q_{mod}	Modeled discharge
Q_{obs}	Observed discharge
Q_R	Flow from S_R
Q_S	Flow from S_S
Q_{tot}	Total runoff
R^2	Coefficient of determination
RC	Runoff coefficient
R_F	Recharge to fast responding reservoir
R_P	Recharge to slow responding reservoir
RT	Reduced tillage
S_F	Storage in the fast responding component
SOC	Soil organic carbon
S_R	Storage in the riparian/wetland component
S_S	Storage in the slow responding component
S_U	Storage in the unsaturated reservoir
S_{Umax}	Maximum storage capacity in unsaturated zone
SUVA	Specific UV absorbance
$\overline{SUVA}$	Discharge weighted mean SUVA value
TOC	Total organic carbon
v_{ki}	Discharge volume fraction of the k^{th} end-member at time i
x_i	Measured value
$\bar{x}$	Mean of measured values
y_i	Modeled value
$\bar{y}$	Mean of modeled values
α	Level of significance
β	Shape parameter

$\delta^{2}H$	Relative deviation of the ratio of stable isotopes ^{2}H and ^{1}H measured in a sample, from the ratio of isotopes measured in a standard
$\delta^{18}O$	Relative deviation of the ratio of stable isotopes ^{18}O and ^{16}O measured in a sample, from the ratio of isotopes measured in a standard
λ	Shape parameter
μ	Mean concentration of solute j in the stream water
σ	Standard deviation of solute j in the stream water

Table of contents

Acknowledgments i
Abstract iii
Nederlandstalige samenvatting v
List of figures ix
List of tables xiii
List of acronyms and symbols xv
Table of contents xix
Chapter 1. Introduction 1
1.1 Research background 1
1.1.1 Dissolved organic carbon: definition, composition and environmental importance 1
1.1.2 Dissolved organic carbon in the surface water 3
1.2 Problem statement 5
1.3 Research questions, objectives and hypotheses 6
1.4 Thesis outline 7
Chapter 2. Controls on dissolved organic carbon export through surface runoff from loamy agricultural soils 9
2.1 Introduction 9
2.2 Materials & methods 11
2.2.1 Study area 11
2.2.2 Field rainfall experiments 11
2.2.3 Laboratory rainfall experiments 14
2.2.4 Statistical analysis 15
2.3 Results 17
2.3.1 DOC concentrations and SUVA values during rainfall event 17
2.3.2 Weighted mean DOC concentration per experiment 18
2.3.3 Regression equation 20
2.3.4 Laboratory rainfall simulations 22
2.4 Discussion 24
2.5 Conclusion 27
Chapter 3. Identifying the transport pathways of dissolved organic carbon in contrasting catchments 29
3.1 Introduction 29

3.2 Material and methods 31
3.2.1 Study area 31
3.2.2 Experimental set-up 33
3.2.3 Laboratory analysis 35
3.2.4 Statistical analysis 36
3.2.5 End-member mixing analysis 36
3.2.6 Load and flux calculations 38
3.3 Results 38
3.3.1 Hydrology 38
3.3.2 Solute concentrations 41
3.3.3 End-member mixing analysis 44
3.3.4 DOC loads and fluxes 49
3.4 Discussion 50
3.5 Conclusion 53
Chapter 4. Modeling the export of dissolved organic carbon from a pasture catchment 55
4.1 Introduction 55
4.2 Materials and methods 56
4.2.1 Study area 56
4.2.2 Experimental set-up 57
4.2.3 Sample collection and analysis 58
4.2.4 Modeling of catchment hydrology 58
4.2.5 Modeling of DOC concentrations 63
4.3 Results 64
4.3.1 Rainfall-runoff characteristics 64
4.3.2 DOC dynamics 65
4.3.3 Results of the FLEX hydrological model 66
4.3.4 Results of the WETSPRO hydrological model 71
4.4 Discussion 74
4.5 Conclusion 76
Chapter 5. General discussion, conclusions and future perspectives 77
5.1 Suggestions for future research 86
References 87
Publications 97

Chapter 1. Introduction

1.1 Research background

1.1.1 Dissolved organic carbon: definition, composition and environmental importance

Dissolved organic matter (DOM) is the term used for the complex of organic molecules of various origin and composition present in the aquatic system, originating from partial decomposition of, and exudation from living organisms including plants, animals and soil microorganisms (Kalbitz et al., 2000; Evans et al., 2005). It is operationally defined as comprising any organic compound that passes through a filter of 0.45 µm pore size (Thurman, 1985; Kalbitz et al., 2000) and is often quantified in terms of its carbon content, referred to as dissolved organic carbon (DOC) and expressed in mg l^{-1} C.

DOC plays an important role in the cycling and distribution of carbon both within and between ecosystems (Kaiser and Kalbitz, 2012). The estimated annual flux of DOC from the land to the oceans is ±0.4 Pg C $year^{-1}$ (Aitkenhead and McDowell, 2000) which equals almost half the current net terrestrial uptake of ±0.9 Pg C $year^{-1}$ (Regnier et al., 2013), indicating it is a significant component in the global carbon cycle (Jardine et al., 2006). DOC provides energy and nutrients to biota and has a part in soil formation (Dawson et al., 1978) and mineral weathering. Due to its complexation capacity, it can affect the solubility, toxicity and transport of heavy metals and organic contaminants (Tipping, 1993; Kalbitz et al., 2000). Although DOC is only a small fraction (<1 %) of the total soil organic carbon (SOC) (Qualls and Haines, 1991), it is a highly mobile carbon component (Neff and Asner, 2001) and therefore an early indicator of changes in SOC (Haynes, 2000). In the surface water, DOC accounts for 10 to 90 % of the total organic carbon (Meybeck, 1982). Stream water DOC has an effect on stream pH and light penetration (Morris et al., 1995). By attenuating both visible and UV light, it can decrease the growth of autotrophs, but at the same time protect aquatic organisms against UV radiation (Akkanen, 2002). At a practical level, DOC in the surface water poses problems for drinking water production, as it can lead to the formation of carcinogenic disinfection by-products such as trihalomethanes and haloacetic acids (Liang and Singer, 2003).

Observed DOC concentrations in the soil are the result of processes that release DOC such as desorption from the solid phase and inputs from plant litter, root exudates and microbial biomass and processes that remove DOC such as adsorption and decomposition. The different processes involved are controlled by both biotic and abiotic factors and depend on environmental factors such as temperature, precipitation and physical and chemical soil characteristics (Kalbitz et al., 2000).

Because DOM is defined operationally, and as the number of organic compounds it comprises is limitless, it is impossible to give a general chemical definition of DOM (Kalbitz et al., 2000; Evans et al., 2005). In general however, a small proportion of DOM consists of low molecular weight substances such as organic acids, sugars and amino acids (Kalbitz et al., 2000), which can be identified chemically. The greatest part of DOM consists of complex molecules of high molecular weight, called humic substances. Humic substances are a mixture of aromatic and aliphatic hydrocarbon structures with attached amide, carboxyl, ketone and other functional groups (Leenheer and Croué, 2003). They strongly absorb visible light at the blue end of the spectrum, thereby causing the characteristic brown color of water with high DOM content (Evans et al., 2005).

Besides the quantification of DOM, which is done by measuring its carbon content (DOC), different methods are available to provide a measure of the quality (i.e. the chemical and structural features) of the DOM, by fractionating it into classes with distinct chemical or physical properties. The most frequently used fractionation method is based on the sorption of acidified DOM on resin XAD-8, separating hydrophobic from hydrophilic DOM fractions (Amery et al., 2009). By passage through anion and cation exchange columns, these fractions can be subsequently subdivided into acid, basic and neutral fractions (Leenheer and Croué, 2003). Other methods to fractionate the DOM are based on molecular size, e.g. sequential ultrafiltration and size exclusion chromatography (Leenheer and Croué, 2003). Furthermore, the measurement of spectrophotometric characteristics such as fluorescence or ultraviolet (UV) absorbance, can be used to characterize DOM. The specific UV absorbance (SUVA), defined as the UV absorbance of a water sample measured at 254 nm normalized for the DOC concentration (Weishaar et al., 2003), is an indicator of the aromaticity and the recalcitrant nature of DOM, whereby higher SUVA values are measured when the DOM is more aromatic (Leenheer and Croué, 2003; Weishaar et al., 2003). Measurements of fluorescence on the other hand can be used to estimate the degree of humification (Zsolnay et al., 1999).

DOC concentrations observed in natural waters (Table 1.1) show great variation from <1 mg l^{-1} to >50 mg l^{-1} (Thurman, 1985; Leenheer and Croué, 2003). The concentrations are lowest in oceans, groundwater and lakes and rivers draining bare rock or thin soils with low organic content. Observed values are highest in rivers draining wetlands or peatlands and in organic soil pore waters (Evans et al., 2005).

Table 1.1. Range of DOC concentrations observed in natural waters according to Thurman (1985).

Type of water	DOC concentration (mg l^{-1})
Seawater	0.5
Groundwater	0.7
Rivers/lakes	2-10
Precipitation	1
Soil pore water	2-30
Swamps/marches/bogs	10-60

In general, DOC concentrations in the soil vary in the order forest soil > grassland soil > arable soil (Chantigny, 2003), which is mainly due to the vegetation type. Moreover, DOC concentrations are generally higher in coniferous forest soils than in deciduous forest soils. Similarly, the quality of DOC depends on the land use type, with greater proportions of low molecular weight DOC reported in agricultural areas compared to natural or forested systems (Cronan et al., 1999). Observed DOC concentrations are typically higher in the upper soil horizons than in lower, mineral soil horizons (Futter et al., 2007) which is a result of adsorption of DOC onto Al- and Fe- oxides and clay minerals as water percolates into lower soil horizons during transport. Also the quality of the DOC changes with soil depth. SUVA values are high in the litter layer, but decline with increasing soil depth (Jaffrain et al., 2007), indicating that DOC becomes less aromatic and thus more biodegradable as soil depth increases. This is due to preferential adsorption of the aromatic portion of DOC by soil solids (Jaffrain et al., 2007). Similarly, the ratio of hydrophobic to hydrophilic compounds decreases with soil depth (Siemens et al., 2003).

Previous research on vertical transport of DOC in the soil has reported an inverse relation between DOC concentration and water fluxes (Mertens et al., 2007 and Don and Schulze, 2008). Besides a baseline DOC concentration, Mertens et al. (2007) found a decrease in DOC concentration in leachates from a bare field plot with increasing pore water velocities (Figure 1.1). Fast flowing water results in a limited contact time with the soil matrix and therefore lower DOC concentrations compared with slow flow. De Troyer (2011) also showed in the field that vertical DOC transport is mainly controlled by the water flux, and that environmental conditions and land management practices only have a limited effect.

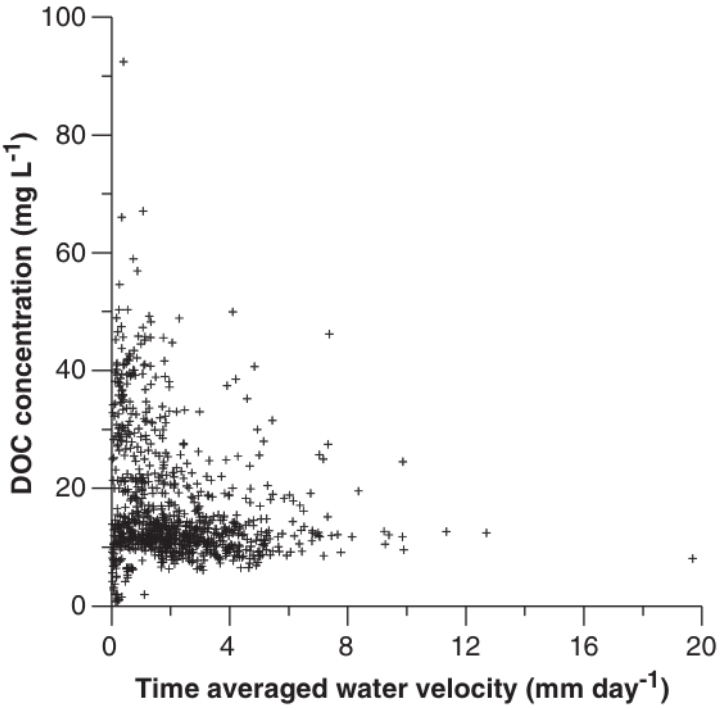

Figure 1.1. DOC concentrations measured in arable land in soil leachate at 40 cm depth, versus time-averaged water velocity (Mertens et al., 2007).

1.1.2 Dissolved organic carbon in the surface water

At the catchment scale, DOC can reach the stream water via different hydrological transport pathways such as groundwater flow, which is typically the main contributor to the stream during baseflow conditions, interflow, consisting of rapid subsurface flow, and surface runoff. The fate of DOC differs along these different flow paths. Therefore, the way the transport pathways connect geographically distributed source areas of DOC plays a critical role for the DOC export from the catchment (McGlynn and McDonnell, 2003; Inamdar and Mitchell, 2006).

Several studies have reported relationship between stream discharge and DOC concentrations measured in the stream (Lewis and Grant, 1979; Dawson et al., 2002, 2011; McGlynn and McDonnell, 2003), whereby higher discharge leads to increasing DOC concentrations (Boyer et al., 1996; Dalzell et al., 2007). In some cases, this relationship depended on the season (Dawson et al., 2002, 2008a).

Considerable spatial variation was found in DOC export from different catchments. Average annual riverine DOC fluxes from catchment with different land uses as previously reported in literature are given in Table 1.2. A number of studies have demonstrated positive relationships between the DOC export and the % wetland area (Hinton et al., 1998; Xenopoulos et al., 2003; Mattsson et al., 2009) or peat cover (Hope et al., 1997) in the catchment. Additionally, DOC fluxes are positively correlated with the amount of organic matter present in the catchment soils (Aitkenhead et al., 1999) and the soils C/N ratio (Aitkenhead and McDowell, 2000). However, the strongest relationships between catchment characteristics such as soil carbon pools and percentage peat cover and DOC concentrations measured in the stream water are found in small catchments (Aitkenhead et al., 1999). Negative relationships between DOC export and the proportion of agricultural land in the catchment were reported by Mattsson et al. (2009), which can be attributed to lower buildup of organic matter due to harvesting in agricultural areas.

Table 1.2. Average riverine DOC fluxes from catchments with different land uses.

Land use	Average DOC flux ($kg\ ha^{-1}yr^{-1}$)
Cool grasslands [a]	3.86
Taiga [a]	7.00
Agricultural land (USA) [b]	9.50
Tropical savannah [a]	10.90
Siberian steppe [a]	12.90
Warm deciduous forests [a]	14.10
Agricultural land (Denmark) [c]	16.57-30.27
Warm mixed woodlands [a]	17.14
Cool deciduous forests [a]	19.27
Warm conifer forests [a]	36.84
Cool conifer forests [a]	42.26
Northern mixed forests [a]	52.60
Heath/moorlands [a]	56.50
Tropical forests [a]	63.36
Boreal/peat mix [a]	63.49
Peatlands [a]	85.67
Swamp forests [a]	99.13

[a]Data from 15 biome types, based on published literature on mean annual DOC fluxes from 164 watersheds ranging in size from 0.38 ha to 3.2 10^8 ha, as summarized by Aitkenhead and McDowell (2000)
[b]Data published by Royer et al., 2005
[c]Data published by Stedmon et al., 2006

Besides the spatial variation in DOC export, concentrations measured at the catchment outlet also greatly vary temporally. Several authors have reported seasonal variation in baseflow stream water DOC concentrations, with peaks in fall and minima in spring (Dawson et al., 2002, 2008a, 2011; Halliday et al., 2012). This can be attributed to the rewetting of the catchment after a period of high biological activity in the summer (Halliday et al., 2012) and the input of fresh organic matter caused by leaf fall and decomposition (Mulholland and Hill, 1997). However, seasonal differences in stream DOC concentrations are also dependent on the seasonal changes in sources and production mechanisms and whether DOC export from the catchment is production or transport limited (Lambert et al., 2013). On a shorter time scale, DOC concentrations measured at the catchment outlet generally increase during periods of elevated discharge caused by rain events or snowmelt, compared to baseflow concentrations (McDowell and Likens, 1988; Boyer et al., 2000; Hagedorn et

al., 2000; Dawson et al., 2002; Kaiser and Guggenberger, 2005; Shanley et al., 2011; Halliday et al., 2012). DOC concentrations in the stream water during a discharge event have been reported to reach their maximum before (Boyer et al., 2000), at the same time, or only after (Brown et al., 1999; Hagedorn et al., 2000; Inamdar and Mitchell, 2006) discharge reaches its peak. Additionally, contradictory hysteresis patterns have been observed. Boyer et al. (2000) and Zhang et al. (2007) reported clockwise hysteresis, with higher DOC concentrations on the rising limb of the hydrograph than on the receding limb at equivalent discharges. In other cases concentrations of DOC were higher on the descending limb of the hydrograph than on the rising limb, resulting in counterclockwise hysteresis (Brown et al., 1999; Hagedorn et al., 2000). Also properties of DOC such as UV absorptivity can change during rainfall events. Hagedorn et al. (2000) reported that UV absorptivity reached a maximum on the descending limb of the hydrograph during rainfall events, caused by large contributions of highly aromatic DOC from topsoil water in later stages of the storm.

The temporal variations in DOC concentrations and quality during periods of elevated discharge have previously been attributed to changes in contributions of the hydrologic flow paths. High DOC concentrations during peak events are then attributed to near-surface water flow paths that interact with the organic carbon-rich forest floor or surficial soil layers in riparian or wetland areas (Boyer et al., 1997; Hagedorn et al., 2000; Inamdar and Mitchell, 2006). Other authors also found a role for in-stream processes such as stream channel expansion at increasing discharge, or throughfall directly onto the stream that can affect the DOC concentrations (Tate and Meyer, 1983; Mulholland and Hill, 1997; Hagedorn et al., 2000). However, the range of possible controls makes it challenging to define the controlling factors for the DOC transport towards the surface water. Different transport mechanisms can lead to similar solute patterns measured in the stream, while a single export mechanism can produce dissimilar solute concentration patterns (Inamdar and Mitchell, 2006).

1.2 Problem statement

Besides the aforementioned seasonal and rainfall induced variations in surface water DOC concentrations, several authors have reported long-term increases in DOC concentrations in surface water in the UK, northern Europe and North America over the last decades (Freeman et al., 2001; Worrall et al., 2004; Evans et al., 2005). Causal factors for this increase might be recovery from acidification after major reductions in acidifying emissions at an international level (Evans et al., 2005), CO_2 enrichment (Freeman et al., 2004) and rising temperatures (Freeman et al., 2001; Gruau and Jardé, 2005). However, to be able to fully comprehend these rising DOC concentrations, we need a complete understanding of (1) how DOC is formed and how this process depends on the properties of the system (2) the mechanisms controlling the transport of DOC from the soil to the surface water and the pathways delivering DOC at the catchment outlet. In this work, we focus on gaining insight in the latter.

Previous research on the factors controlling DOC transport at the catchment scale has found a role for the hydrological transport pathways present in the catchment (Boyer et al., 1997; Hagedorn et al., 2000; Inamdar and Mitchell, 2006). However, it remains a question whether varying contributions of the different pathways delivering DOC to the stream water can fully explain the temporal variations in DOC concentrations and quality observed at the catchment outlet during discharge

events. In addition, earlier attempts to get insight into the factors controlling DOC transport at the catchment scale have mostly focused either on low frequency (mostly weekly) sampling over a longer term (Boyer et al., 1997; Dawson et al., 2002, 2008b; Laudon et al., 2004; Hernes et al., 2008), or high frequency sampling during a single or a limited number of events (Bishop et al., 2004; Kaiser and Guggenberger, 2005; Inamdar and Mitchell, 2006). Although it has already been demonstrated that the combination of long-term regular baseflow sampling and high frequency event sampling can lead to unique insights into the hydrogeochemistry of a catchment (Shanley et al., 2011; Halliday et al., 2012), only few studies have reported on this (Hagedorn et al., 2000; Shanley et al., 2011). Yet, by only sampling during baseflow conditions, a major part of the DOC export is unaccounted for, as DOC export during rainfall events can be a great part of the total catchment DOC export (Hinton et al., 1997). Sampling exclusively during a selection of events will on the other hand overlook long-term trends and seasonal baseflow differences.

Most research on the factors controlling DOC transport has focused on forest, wetland and peat areas, with little information available on arable land. However, arable land typically has lower C/N ratios than forest or grassland soils, which likely affects the DOC dynamics (Aitkenhead and McDowell, 2000). It also allows for different management strategies of which the effects on DOC export are not know. Furthermore, agricultural land use can lead to significant surface runoff, but only little information is available concerning composition and concentration of DOC in this transport pathway. Studies by Cronan et al. (1999) and Royer et al. (2007) suggest that DOC concentrations in surface runoff are at least of the same magnitude as those found in subsurface flow and that the quality of DOM in surface runoff is substantially different from that of DOM in subsurface or groundwater flow. Therefore, the DOC transport via surface runoff in agricultural areas and the effect of land management on DOC export deserve our increased interest.

Lastly, although experimental data on DOC export from catchments are available, efforts to model the DOC concentration in the catchment streams are scarce (Hornberger et al., 1994; Boyer et al., 1996; Futter et al., 2007; Ledesma et al., 2012). Most of the modeling attempts have focused on a description of DOC variations on the larger time scale, successfully reproducing annual and monthly variations in DOC concentration (Boyer et al., 1996; Futter et al., 2007; Ledesma et al., 2012). Only limited modeling efforts have been made to predict the dynamics of DOC concentrations during rain event conditions (Xu et al., 2012).

1.3 Research questions, objectives and hypotheses

The overall aim of this research is to gain insight in the transport of dissolved organic carbon from the soil to the surface water and identify and model the transport pathways. To meet this objective, we set out to answer the following research questions.

Q1. What are the controls for the transport of DOC through surface runoff from arable land? What is the effect of soil properties, hydrological conditions and field characteristics on the concentrations and quality of DOC in surface runoff?
Q2. At the catchment scale, what are the factors controlling the temporal variation in DOC concentrations and quality observed at the stream outlet?
Q3. Which transport pathways contribute to the transport of DOC to the surface water at the watershed scale during baseflow conditions and during discharge peak events?

Q4. Can hydrological modeling of the different water pathways at the catchment scale lead to an adequate modeling of DOC concentrations in the stream outlet during different flow regimes?

Coupled with these four research questions, following hypotheses were formulated.

H1. The export of DOC via surface runoff from agricultural fields in the Belgian loam belt is limited by the source term or the DOC production rate in the surface soil. The consequences of this hypothesis are twofold.
  H1.1. Greater antecedent soil moisture contents and higher rainfall intensities lead to lower DOC concentrations in surface runoff.
  H1.2. Field management characteristics such as tillage technique affect the DOC concentrations measured in surface runoff. Reduced tillage techniques whereby crop residues are left at the soil surface, lead to greater DOC concentrations in surface runoff water.

H2. At the catchment scale, the temporal variation in DOC concentrations and quality observed in the stream during periods of elevated discharge caused by rain events can be explained by a change in contributions of different pathways delivering water and thus DOC at the catchment outlet, assuming equilibrium conditions of DOC concentrations in the water in the different pathways. For this to be confirmed, we tested the following hypotheses.
  H2.1. An end-member mixing analysis using cation and DOC concentrations measured in the different transport pathways, allows the identification of the contribution of each pathway for the transport of DOC to the surface water at different flow regimes.
  H2.2. Discharge to the stream during baseflow conditions is mainly via the groundwater. During discharge peaks caused by rainfall events, additional transport pathways such as precipitation/throughfall, soil pore water and riparian zone water additionally contribute to the transport of DOC to the surface water.
  H2.3. In a small headwater catchment with quick discharge responses to rainfall events, stream water DOC concentrations during baseflow conditions and peak events can be adequately predicted by combining hydrological modeling of the different water pathways with a simple mixing equation of DOC concentrations measured in these transport pathways.

1.4 Thesis outline

This thesis consists of 5 chapters, whereof the first is the present introductory chapter (Figure 1.2). Three following chapters each address a separate part of the research questions, testing the aforementioned hypotheses (Section 0). The last chapter presents the general conclusion of the research.

In **Chapter 1**, a general introduction provides the necessary background information on DOC, as well as the problem statement and the research questions and hypotheses addressed in this thesis.
Chapter 2 presents the results of field and laboratory rainfall experiments carried out to identify the factors controlling DOC export by surface runoff and the processes releasing DOC into surface runoff

during a rainfall event at the interrill plot scale. It assesses the effect of soil properties, hydrological conditions and field characteristics on the concentrations and quality of DOC in surface runoff.
In **Chapter 3**, the contributing pathways for the transport of DOC at the watershed scale were identified in catchments differing in land use and hydrogeology. Data collected in 4 headwater catchments in Belgium during different hydrological regimes over a period of 4 years are presented. The temporal change in contributions from different transport pathways was used to explain variations in DOC concentrations and quality measured at the catchment outlet.
In **Chapter 4** the hydrological modeling of discharge in one of the headwater catchments yields fluxes of water reaching the catchment outlet via the different transport pathways. Using the results of Chapter 3, these fluxes of water, each with their own geochemical signal, are used to model the concentrations of DOC measured at the stream outlet.
In **Chapter 5**, the general conclusions to the research questions are summarized. Furthermore, unresolved issues and suggestions for future research are formulated.

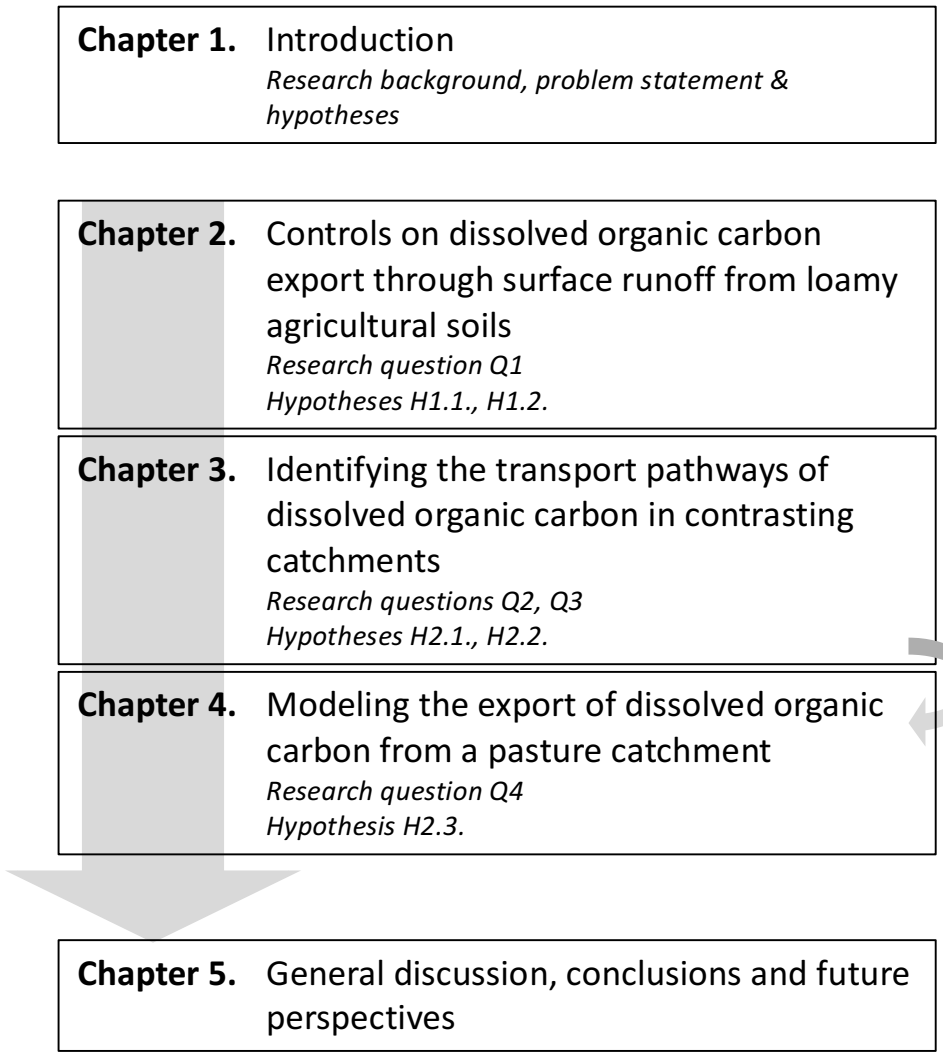

Figure 1.2. Flowchart representing the thesis outline.

Chapter 2. Controls on dissolved organic carbon export through surface runoff from loamy agricultural soils

Adapted from: Van Gaelen, N.; Verschoren, V.; Clymans, W.; Poesen, J.; Govers, G.; Vanderborght, J. and Diels, J. 2014. Controls on dissolved organic carbon export through surface runoff from loamy agricultural soils. Geoderma 226-227, 387-396.

2.1 Introduction

Dissolved organic carbon (DOC) is one of the most active and mobile carbon pools and consequently plays an important role in the global carbon cycle (Jardine et al., 2006). Due to its high mobility and reactivity, it plays a significant role in the cycling and distribution of nutrients and carbon both within and between ecosystems. Dissolved organic matter provides energy and nutrients to biota, but can also increase the bioavailability of trace metals or organic pollutants (Kalbitz et al., 2000). In drinking water production, it can lead to the formation of unwanted disinfection by-products, such as trihalomethanes (Liang and Singer, 2003). The yearly flux of DOC from land to the oceans was estimated to be ±0.4 Pg C $year^{-1}$ (Aitkenhead and McDowell, 2000), about half the current net terrestrial uptake of ±0.9 Pg C $year^{-1}$ (Regnier et al., 2013).

Over the last decades, increasing DOC concentrations have been reported in the surface waters of agricultural areas. The causal factors remain unclear (Freeman et al., 2004; Gruau and Jardé, 2005; Evans et al., 2005) as most research on DOC transport in soils and on factors controlling DOC export towards the river system focused on forests and wetland areas. Results from agricultural sites remain scarce. Although DOC concentrations in the soil typically decrease with land use from forest soils over grassland soils to arable soils (Chantigny, 2003), agricultural systems deserve our increased attention. In agricultural catchments, the proportion of low molecular weight DOC is larger than in natural or forested catchments (Cronan et al., 1999). As a strong relationship exists between DOC flux and soil C/N on a catchment scale (Aitkenhead and McDowell, 2000), the transition from a natural system to an agricultural system with typically lower C/N, will likely alter the DOC dynamics.

De Troyer (2011) has studied the vertical flux of DOC in agricultural land, and the soil characteristics controlling this export. Examining pore waters of different agricultural soils, it was found that soil properties can only weakly explain DOC concentrations in the soil solution. Likewise, data from her field study indicated a limited effect of environmental conditions and land management practices on DOC concentrations in vertical transport. Instead, vertical DOC transport was mainly controlled by the water flux. This confirmed the findings of Mertens et al. (2007) and Don and Schulze (2008), who reported an inverse relation between DOC concentration and water fluxes from agricultural and grassland soils.

However, agricultural land use does not only lead to changes in DOC dynamics within the soil, but also leads to significant surface runoff and thereby enables a new pathway for DOC transfer from terrestrial to aquatic systems. At present, limited information is available on DOC transport by surface runoff. Rainfall experiments with undisturbed soil samples in the lab showed significantly

lower DOC concentrations in runoff than in percolating water (Bajracharya et al., 1998), indicating that a shift in hydrological pathways could alter DOC delivery to streams. DOC concentrations in both runoff and percolation water peaked at the onset of the experiments and diminished toward the end of the event. This suggests that accumulated soluble organic C is rapidly flushed upon rewetting of the soil, both by percolation and runoff water.

Agricultural land is subject to several land management strategies which are successfully applied to increase crop yield and prevent soil degradation, but might also affect the DOC transport. For example, reduced tillage (RT) is being increasingly used as a means to protect soils from erosion and compaction, to conserve soil moisture and to reduce production costs (Holland, 2004). Its effectiveness compared to conventional tillage (CT) in the form of classic mouldboard ploughing for runoff and soil loss reduction in the Belgian Loam Belt has been demonstrated by Leys et al. (2007, 2010). In terms of soil properties, several studies have shown that the impact of the tillage technique on total soil organic carbon (SOC) content is often limited (VandenBygaart et al., 2003; Hermle et al., 2008; Van den Putte et al., 2012). The vertical distribution of SOC however can differ significantly, with higher SOC content near the soil surface at RT sites compared to more evenly distributed SOC at CT sites (VandenBygaart et al., 2003; Hermle et al., 2008; Christopher et al., 2009). The higher SOC contents in the top few centimeters of the soil at RT sites are explained by low mobilization and accumulation of crop residues at the surface (Bertol et al., 2004, 2007). The labile DOC fraction is even more sensitive to tillage disturbance than total SOC (Roper et al., 2010). Cookson et al. (2008) reported higher DOC levels in no-till and conventional-till in comparison to rotary-tilled soils, both within and across soil depths. On grassland, lower DOC concentrations were found in the surface soil after ploughing, compared to neighboring undisturbed grass strips (Don and Schulze, 2008). In addition, lower specific UV absorbance (SUVA) values, indicating lower aromaticity of DOC in the ploughed areas, showed that not only DOC concentrations but also DOC quality shifted upon ploughing.

Whether this enrichment in both SOC and DOC in the top layer of RT fields affects the DOC in runoff, is not clear. Bertol et al. (2004, 2007) found particulate organic carbon enrichment in the runoff sediments of RT compared to CT systems. This can be explained by preferential mobilization of the lighter fractions during low-intensity erosion events (Wang et al., 2013). The dynamics of the dissolved fraction of organic matter is also likely to be affected by the tillage technique (Chantigny, 2003). However, to the best of our knowledge, there are no reports on the export of DOC through runoff from fields under different tillage systems.

Consequently, the controls on the transport of DOC through surface runoff from agricultural fields are largely unknown. It is not clear whether DOC concentrations in runoff water from agricultural fields are mainly determined by the hydrological regime (as is the case for vertical transport), and in what way they are affected by soil properties or management strategies. The effect of these hydrologic, soil and management properties on DOC quality measures such as SUVA is also of major environmental interest, since DOC linked transport of e.g. heavy metals not only depends on concentrations but also on quality of DOC (Amery et al., 2008).

This work aims to define the factors controlling DOC export by surface runoff from loamy agricultural soils and to gain knowledge on the processes releasing DOC into the surface runoff during a rainfall event at the interrill plot scale. The relative importance of different controls is investigated by

studying the effect of soil properties (e.g. SOC, texture, bulk density and gravimetric water content), hydrological boundary conditions (e.g. rain intensity) and field characteristics (e.g. crop cover, tillage technique) on DOC concentrations and quality in surface runoff from simulated rainfall experiments in the field. As we hypothesize antecedent soil moisture conditions, raindrop impact and addition of crop residues to be important controlling factors for the release of DOC in the surface runoff, the effect of these controls was studied in more detail using controlled lab experiments.

2.2 Materials & methods

2.2.1 Study area

Rainfall experiments were conducted on 6 different arable field sites in the Belgian loam belt (central Belgium). The area receives a mean annual precipitation of ca. 800mm and has a mean annual air temperature of ca. 9.7 °C. Soils in the study area are mainly loess-derived Luvisols, which are highly susceptible to erosion processes such as rill and interrill erosion. The fertile loess-derived soils are well suited for arable cropping. The main cultivated crops are sugar beet (*Beta vulgaris* L.), maize (*Zea mays* L.), wheat (*Triticum aestivum* L.), barley (*Hordeum vulgare* L.) and potatoes (*Solanum tuberosum* L.). Field sites selected for the rainfall experiments were split into 2 parts under different management. On one part conventional tillage (CT) was applied, which consists of classic mouldboard inversion ploughing; on the other part reduced tillage (RT) was used. Reduced tillage comprised various techniques such as deep non-inversion tillage, shallow non-inversion tillage and direct drilling. On average, RT had been applied on the trial fields for 6 years.

2.2.2 Field rainfall experiments

Fifty-six field rainfall experiments were conducted in 2010 (Table 2.1). The majority (45) thereof was done from April to June, shortly after crop emergence. Cultivated crops were winter wheat, barley, sugar beet and maize. On two field sites, experiments were repeated in fall, right after harvest, when soil was bare or planted with a green manure (white mustard, *Sinapis alba* L.). On each field site, three representative locations were selected per tillage technique. Wheel tracks and boundaries were avoided. At these locations, runoff plots of circa 0.85 m by 0.85 m were delineated, by installing metal plot boundaries and a runoff collection gutter (Figure 2.1).

Table 2.1. Overview of crop type and soil properties of the surface soil layer of the field sites where simulated rainfall experiments were conducted. Numbers in bold indicate a significant difference (P<0.05) between conventional and reduced tilled parts.

Period	Field site	Years split	Crop	Tillage	n[b]	Slope (%)	Sand [a]	Silt [a]	Clay [a]	SOC	Bulk density (g cm^{-3})
							---------- (g $kg^{-1}_{dry\ soil}$) ----------				
April-June 2010											
	VA1	7	winter	CT	3	8.9	358	557	64	**7.67**	1.38
			wheat	RT	6	9.1	356	585	58	**11.21**	1.33
	VP7	6	barley	CT	3	8.5	485	445	70	**11.98**	**1.47**
				RT	3	11.2	513	424	60	**14.47**	**1.33**
	IWT2	2	sugar	CT	3	1.5	**112**	800	88	**8.52**	2.26
			beet	RT	9	2.1	**124**	792	84	**12.31**	1.17
	PE2	9	maize	CT	3	16.5	**111**	**806**	83	**11.23**	1.18
				RT	3	15.5	**133**	**785**	83	**13.94**	1.16
	GE6	7	maize	CT	3	5.3	442	494	64	**8.27**	1.35
				RT	3	6.1	440	477	83	**11.14**	1.22
	VP10	6	maize	CT	3	10.2	365	557	79	13.96	**1.34**
				RT	3	10.8	399	522	78	13.71	**1.19**
September 2010											
	VA1	7	bare	CT	3	7.5	316	618	66	**7.79**	1.34
				RT	3	8.6	313	625	62	**10.54**	1.34
	VP7	6	green	CT	2	7.9	506	410	84	**11.08**	1.11
			manure	RT	3	8.4	507	425	69	**15.83**	1.06

[a]sand (0.063-2mm), silt (0.002-0.063mm), clay (< 0.002mm), average of three topsoil (0-5cm) samples per tillage technique

[b]Number of conducted rainfall simulations

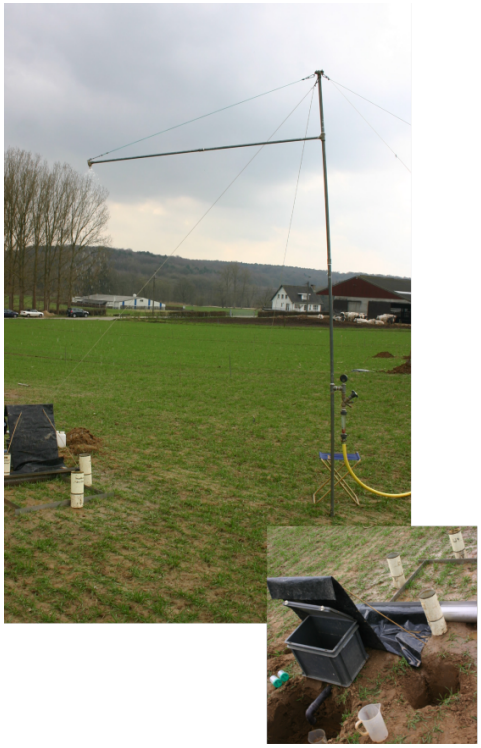

Figure 2.1. Experimental set-up, showing the nozzle-type rainfall simulator. The inset shows the runoff collecting gutter, the collection tank and the experimental plot (0.85m by 0.85m) bounded by metal plates and surrounded by 4 rain gauges.

For all rainfall experiments, a nozzle-type field rainfall simulator was used (Lechler full-cone nozzle, type 460.788, for more details see Poesen et al., 1990) suspended at 3 m height. At its design intensity of 45 mm h^{-1}, the kinetic energy of the simulated rainfall equals ca. 15 J m^{-2} mm^{-1}, which is ca. 65 % of the kinetic energy of natural rainfall occurring at the same intensity (Poesen et al., 1990). Due to variation in wind speed and direction however, the actual rainfall intensity varied and averaged 59±11 mm h^{-1} (n=56). Raindrop-size distribution and hence rainfall kinetic energy can be expected not to be strongly affected by the actual rainfall intensity as the same nozzle and water pressure were used throughout all experiments. The experiments were done using demineralized water, as advised by Borselli et al. (2001), to avoid interactions between simulated rain water quality and physicochemical soil properties. Rainfall was applied for 30-45 min. In most cases steady state runoff was reached by this time.

Several plot characteristics were measured at all sites. The slope gradient (%) along the sowing direction was determined using a clinometer. To estimate the crop cover (%), an orthogonal digital image of the plot was processed by SigmaScan Pro® software, with an existing macro "Turf analysis1-2.BAS" (free for download at http://turf.uark.edu/turfmacro). Cover was geometrically corrected for bias caused by the plant height (Langhans et al., 2011). Before and after every simulation, a sample (Kopecky cylinder; 100 cm^3) of the soil top layer (0-5 cm) was collected for the determination of soil bulk density (g cm^{-3}), initial and final gravimetrically derived volumetric moisture content (cm^3 cm^{-3}), texture, soil organic carbon content (SOC, g $kg^{-1}_{dry\ soil}$) and C/N ratio (%). Texture was determined using a Coulter counter LS 13 320. SOC and C/N ratio were measured using a vario MAX CN Macro Elemental Analyzer.

During the simulations, four rain gauges were placed at the plot borders to measure simulated rainfall intensity (mm h^{-1}). At the effluent gutter outlet, volumetric measurements of runoff were made. By recording time per volume of runoff entering the container, runoff intensity (mm h^{-1}) could be calculated. Total runoff depth was transformed to a runoff coefficient (RC) using the total rainfall depth per experiment (Eq. 2.1) .

$$RC = \frac{Total\ runoff}{Total\ rainfall} \tag{2.1}$$

whereby total runoff and total rainfall depths are in mm and RC is dimensionless.

The first 1000 ml of runoff was subsampled every 200 ml. Subsequently, five more samples were taken, more or less evenly spread over the rest of the duration of the experiment. Two mixed samples were taken from the remainder of the collected runoff water at the end of the experiment. Runoff samples were filtered through a 0.45 µm membrane filter (chromafil®, pre-rinsed with 20 ml of demineralized water) and analyzed for dissolved organic carbon concentrations ([DOC], mg l^{-1}) and specific UV absorbance (SUVA, l g^{-1} cm^{-1}). DOC was measured using an Analytik Jena Multi N/C 2100. The absorbance at 254 nm (A_{254}) was determined with a Perkin Elmer Lambda 20 UV/VIS Spectrophotometer, with a path length (b) of 1 cm. SUVA (l g^{-1} cm^{-1}) was then calculated using Eq. (2.2).

$$SUVA = \frac{A_{254}1000}{b[DOC]} \quad (2.2)$$

where A_{254} is dimensionless, path length b is in cm and [DOC] is the DOC concentration in mg l^{-1}. SUVA is an indicator of the aromaticity and the recalcitrant nature of the DOC, whereby higher SUVA values are measured if the DOC is more aromatic (Weishaar et al., 2003). [DOC] was combined with runoff intensity (mm h^{-1}) to calculate fluxes of DOC (mg $m^{-2}h^{-1}$).

Suspended sediment concentrations in the runoff were measured by evaporating and weighing the runoff samples, and the sediment was analyzed for C content, texture and C/N ratio. Total organic carbon concentrations ([TOC], mg l^{-1}) in the runoff were then determined from the sediment concentrations and C content in the sediment. Particulate organic matter concentrations ([POC], mg l^{-1}) in the runoff were calculated by subtracting [DOC] from [TOC]. From rain gauges placed at the experimental sites, or from weather stations nearby (≤10km), cumulative rainfall depths (mm) were collected for both 30 days and one week preceding the rainfall experiments.

2.2.3 Laboratory rainfall experiments

Under field conditions, the net effect of a single controlling factor on [DOC] in runoff water can be uncertain because several experimental variables can covary and their effects may interact and counterbalance. Therefore, additional laboratory experiments were conducted whereby experimental conditions could be reproduced in an identical way for each experiment. Firstly this allowed to test the effect of raindrop impact, causing turbulent mixing of the pore water and the surface water (Fierer and Gabet, 2000), on [DOC] and SUVA in the runoff and percolating water. Secondly, the isolated effect of leaving crop residues at the soil surface, as is done in reduced tillage practices, was evaluated. Finally, it was tested whether the increase in [DOC] upon rewetting after a dry period, that is consistently observed in leachate water (Kalbitz et al., 2000), is also found in runoff water.

The experimental set-up consisted of an interrill plot box (0.60 m by 0.95 m) that was positioned at a slope of 15 % (Poesen et al., 1990). For each experiment the plot box was filled with top soil that was collected from an arable field near the PE2 experimental field site. To reduce artefacts, the soil was not air-dried but stored outside at ambient temperature until used in the experiments. It was passed through a coarse (5 cm) sieve and packed in the plot box in a layer of 0.15 m. Specifications of the soil are given in Table 2.2. After filling the plot box, the bulk density of the soil was on average 1.18 ±0.07 g cm^{-3} (n=9). An extra buffer strip of identical soil, with a width of 0.2 m next to all 4 sides of the test section, ensured that side-effects were eliminated.

Table 2.2. Characteristics of the soil used in the laboratory experiments.

Sand content[a] ($g\ kg^{-1}_{dry\ soil}$)	Silt content[a] ($g\ kg^{-1}_{dry\ soil}$)	Clay content[a] ($g\ kg^{-1}_{dry\ soil}$)	SOC ($g\ kg^{-1}_{dry\ soil}$)	C/N
105.6	780.0	114.9	7.62	9.16

[a]Sand (0.063-2mm), silt (0.002-0.063mm), clay (< 0.002mm)

The same nozzle-type rainfall simulator as that for the field experiments was used, here with a mean rainfall intensity of 42.9±2 mm h^{-1} (n=9), which more closely resembles the design rainfall intensity of the equipment. Rainfall was applied for 60 min, using demineralized water.

During the experiments, four rain gauges were placed at the plot box's borders to measure simulated rainfall intensity (mm h^{-1}). Samples of the top soil (0-5 cm) were taken before and after each experiment, for the determination of initial and final gravimetrically derived volumetric moisture content (cm^3 cm^{-3}). Volumetric measurements of runoff (mm) were made by collecting the runoff water in a gutter at the lower side of the container. A perforated plate at the bottom of the container also allowed the collection of water that percolated through the soil. The first liter of runoff and leaching water was subsampled every 200 ml. Subsequently, five more samples were taken evenly spread over the rest of the duration of the experiment. At the end of the experiment, mixed samples from the remainder of the runoff and percolation water were collected. All runoff and percolation water samples were analyzed for DOC concentrations, SUVA values and sediment concentrations in the same way as the runoff samples from the field experiments (section 2.2.2).

A total of 9 experiments was carried out, whereby the effect of three factors was evaluated. For each treatment or factor level, DOC concentrations and SUVA values in runoff and leaching water were compared with the results of 2 control experiments. A first factor that was tested was the effect of drop impact. Therefore, in two replicate experiments, a stainless steel wire mesh (mesh size 1.4 by 2.0 mm) was loosely placed on top of the soil surface of the plot box, so that the kinetic energy of the water drops reaching the soil surface was drastically lowered. The second factor tested was the effect of mixing crop residues with the top 5 cm of the soil. The effects of adding maize and sugar beet residues were tested separately, by conducting two replicate experiments for each residue type. Crop residues were collected from our experimental field sites (section 2.2.2) after harvest. A last factor tested was the effect of drying and rewetting of the soil. Therefore, after one of the control experiments, the soil in the plot box was left to air-dry in the lab for 7 days, before conducting a consecutive experiment. To test the effect of drying-rewetting of the soil, only one replication was conducted.

2.2.4 Statistical analysis

In a first part of the analysis, the temporal evolution of DOC concentrations and SUVA values in the runoff water during a single runoff experiment was of interest. [DOC] and SUVA measured in the runoff samples were plotted versus time since the start of the experiment. In a second part of the analysis, discharge weighted mean DOC concentrations and SUVA values per experiment were considered. Statistical analyses were carried out using SAS software (SAS Enterprise Guide 4.3, Copyright © 2010, SAS Institute Inc.).

Table 2.3 gives an overview of mean and standard deviations of all variables measured during the field experiments. SUVA values were not measured for the first 15 experiments. In some experiments, sediment concentrations, SOC, CN-ratio and texture of the sediment could not be determined, due to limited runoff volumes.

Table 2.3. Overview of measured class and numerical variables and their mean values and standard deviation for the field experiments. Subscript s = measured in soil; r = measured in sediment.

CLASS VARIABLES

Variable	n[b]	Classes
Tillage technique	56	CT, RT
Season	56	Spring, Fall
Field site	56	VA1,VP7,VP10,GE6,IWT2, PE2

NUMERICAL VARIABLES

Variable	Unit	n[b]	Mean	Standard deviation
Plot properties				
Slope	%	56	7.98	4.30
Clay content$_s$[a]	g kg$^{-1}_{\text{dry soil}}$	56	73.50	12.14
Silt content$_s$[a]	g kg$^{-1}_{\text{dry soil}}$	56	609.60	143.41
Sand content$_s$[a]	g kg$^{-1}_{\text{dry soil}}$	56	316.90	149.57
Bulk density$_s$	g cm^{-3}	56	1.26	0.12
SOC	g kg$^{-1}_{\text{dry soil}}$	56	11.56	2.47
C/N ratio $_s$	-	56	10.41	1.38
Initial moisture content	cm^3 cm^{-3}	56	20.45	7.74
Crop cover	%	56	23.44	28.03
Experimental drivers				
Rainfall intensity	mm h^{-1}	56	58.97	11.73
Rainfall $_{\text{30 days before experiment}}$	mm	56	51.95	41.08
Rainfall $_{\text{7 days before experiment}}$	mm	56	5.16	5.45
Experimental outcomes				
Total runoff	mm	56	13.63	10.21
Runoff intensity	mm h^{-1}	56	22.52	16.99
Runoff coefficient	-	56	0.36	0.25
$[\overline{DOC}]$	mg l^{-1}	56	8.54	3.90
DOC flux	mg m^{-2} h^{-1}	56	172.01	136.47
$\overline{SUVA}$	l g^{-1} cm^{-1}	41	48.85	33.31
Sediment concentration	g l^{-1}	54	12.38	8.28
[POC]	mg l^{-1}	50	241.97	97.44
Clay content$_r$[a]	g kg$^{-1}_{\text{dry soil}}$	50	105.91	26.16
Silt content$_r$[a]	g kg$^{-1}_{\text{dry soil}}$	50	737.38	67.33
Sand content$_r$[a]	g kg$^{-1}_{\text{dry soil}}$	50	156.67	75.26
C/N ratio $_r$	-	50	10.33	1.41

[a]Sand (0.063-2mm), silt (0.002-0.063mm), clay (< 0.002mm)
[b]Number of simulated rainfall experiments for which this variable was measured

Pearson correlation coefficients were calculated between the different numerical variables and the discharge weighted mean DOC concentration ($[\overline{DOC}]$) per experiment, as well as the logarithm of the discharge weighted mean SUVA ($\log_{10}\overline{SUVA}$) per experiment. SUVA values were log transformed to ensure that residuals were normally distributed. The Pearson correlation coefficients gave an indication of the effect of the measured plot characteristics and rainfall variables on DOC concentrations and SUVA values. An ANOVA analysis was applied to investigate the effect of the class

variables field, tillage technique and season as well as their interactions on $[\overline{DOC}]$, $\log_{10}\overline{SUVA}$ and several other measured variables. Linear mixed models were then constructed, with discharge weighted mean DOC concentrations and the logarithm of the discharge weighted mean SUVA values as the dependent variables of interest. The models describe $[\overline{DOC}]$ or $\log_{10}\overline{SUVA}$ as a function of the measured plot characteristics, rainfall variables and runoff characteristics. The SAS mixed procedure was used, whereby the fixed part consisted of the categorical and continuous explanatory variables and their interactions, while the field variable and its interaction with tillage technique were considered as random effects. As the rainfall simulations in fall were conducted only on 2 out of the 6 field sites, the dataset is unbalanced. Because the 'missingness' (of fall observations) is random, i.e. not correlated with the independent variables, the likelihood-based mixed-model procedure can handle the unbalanced nature and provide valid estimates of the fixed effects (Littell, 2002). Statistical significance of the random effects was evaluated using the likelihood ratio test, whereby the χ^2 test statistic is the difference in '-2 Res Log Likelihood' for the two nested models (Littell et al., 2006). Backward elimination based on the Akaike information criterion (AIC) (Akaike, 1974) led to the final model. The performance of the model was evaluated by calculating the coefficient of determination (R^2), which provides information about the goodness-of-fit of the regression model. R^2 was calculated using Eq. (2.3) (Kvalseth, 1985).

$$R^2 = 1 - \frac{\sum (x_i - y_i)^2}{\sum (x_i - \bar{x})^2} \qquad (2.3)$$

whereby x_i and y_i are respectively the measured and the modeled values, and $\bar{x}$ is the mean of the measured values.

2.3 Results

2.3.1 DOC concentrations and SUVA values during rainfall event

Figure 2.2 shows the general evolution of [DOC] and SUVA as a function of time during a rainfall experiment by showing the results of one representative field site (2PE, sampled on June 17 and 18, 2010). For all experiments, a clear general trend existed whereby DOC concentrations as high as 30 mg l^{-1} during the early stage of the experiments decreased towards a steady level between 4 and 10 mg l^{-1} at the end of the experiments, when steady state runoff was reached. A trend in SUVA values was only observed in 34 % of the experiments, all carried out on just 3 of the 6 field sites (2PE, 6GE and 10VP). On these field sites, SUVA values were low at the beginning of the experiment, which indicated that the initial peak was dominated by labile, low aromatic DOC. When the experiment continued, SUVA values rose, and thus relatively more aromatic fractions of DOC were found in the runoff water. These trends seemed to be independent of applied tillage technique.

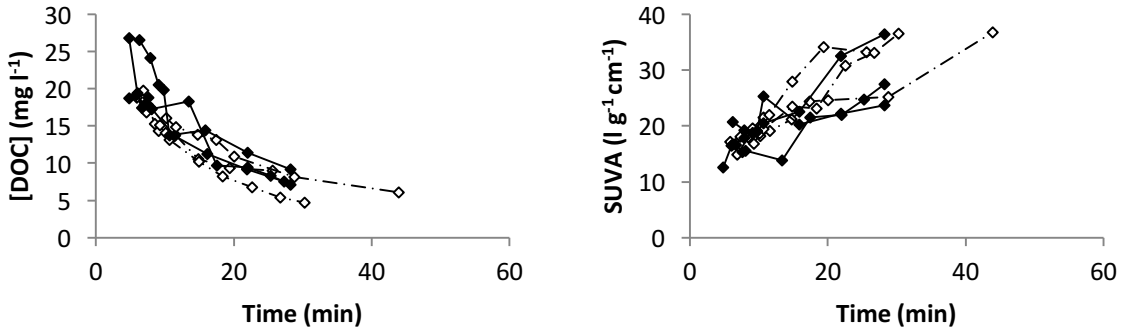

Figure 2.2. [DOC] (left) and SUVA values (right) versus time for 6 rainfall experiments on field site 2PE (maize) on June 17 and 18, 2010. Conventional tilled data: Open diamonds - dashed connection lines; Reduced tilled data: solid diamonds and connection lines.

2.3.2 Weighted mean DOC concentration per experiment

The $[\overline{DOC}]$ in the runoff varied between 1.90 and 17.85 mg l^{-1}, the average being 8.54 mg l^{-1} (n=56). Taking into account runoff volumes per experiment, calculated DOC flux ranged between 2.50 and 536.14 mg $m^{-2}h^{-1}$, with an average of 172.01 mg $m^{-2}h^{-1}$ (n=56). $\overline{SUVA}$ values measured between 14.70 and 149.50 l $g^{-1}cm^{-1}$, with an average of 48.85 l $g^{-1}cm^{-1}$.

Pearson correlation coefficients between the different numerical variables and $[\overline{DOC}]$ and $\log_{10}\overline{SUVA}$ are shown in Table 2.4. The $[\overline{DOC}]$ in runoff water was strongly positively correlated with the slope of the experimental plot and negatively correlated with variables related to the amount of water, such as rainfall intensity, total runoff, runoff intensity and runoff coefficient. Therefore, greater amounts of water led to lower $[\overline{DOC}]$ in the runoff water. A negative correlation existed between $[\overline{DOC}]$ and variables related to the initial moisture conditions of the plot, such as the cumulative rainfall 30 or 7 days before the experiments, and the initial moisture content of the topsoil. The more precipitation occurred in the period before the experiment, or the higher the initial soil moisture content, the lower the $[\overline{DOC}]$ in the runoff during the rainfall experiments. No significant correlation was found between $[\overline{DOC}]$ and the texture or SOC content of the soil. Sediment concentrations and [POC] in the runoff were positively correlated with [DOC].

Table 2.4. Pearson correlation coefficients between the different numerical variables and $[\overline{DOC}]$ and $\overline{SUVA}$ per experiment. s= measured in soil; r = measured in sediment.

Variable	Pearson correlation coefficient	
	$[\overline{DOC}]$	$\log_{10}\overline{SUVA}$
Plot properties		
Slope [1]	0.52****	NS
Clay content $_s$ [2]	NS	-0.38*
Silt content $_s$	NS	NS
Sand content $_s$	NS	NS
Bulk density$_s$ [1]	0.34 *	NS
SOC	NS	NS
C/N ratio $_s$	NS	NS
Initial moisture content [1,2]	-0.27*	0.75****
Crop cover	NS	NS
Experimental drivers		
Rainfall intensity [1]	-0.30*	NS
Rainfall $_{30\ days\ before\ experiment}$ [1,2]	-0.33*	0.80****
Rainfall $_{7\ days\ before\ experiment}$ [1,2]	-0.34**	0.84****
Experimental Outcomes		
Total runoff [1]	-0.30*	NS
Runoff intensity	-0.31*	NS
Runoff coefficient [1]	-0.32*	NS
Sediment concentration [1,2]	0.35**	-0.40*
[POC][1,2]	0.29*	-0.36*
Clay content$_r$[a]	NS	NS
Silt content $_r$[a]	NS	NS
Sand content$_r$[a]	NS	NS
C/N ratio $_r$	NS	NS

(*= p<0.05, **=p<0.01, ***=p<0.001, ****=p<0.0001, NS= not significant)

[a]Sand (0.063-2mm), silt (0.002-0.063mm), clay (< 0.002mm)

[1] Properties incorporated in the linear mixed model for $[\overline{DOC}]$ as fixed effects

[2] Properties incorporated in the linear mixed model for $\log_{10}\overline{SUVA}$ as fixed effects

$\log_{10}\overline{SUVA}$ was negatively correlated with the sediment concentration and the [POC] in the runoff. Opposite to $[\overline{DOC}]$, a positive correlation existed between $\log_{10}\overline{SUVA}$ and the cumulative rainfall 30 or 7 days before the experiment and the initial moisture content of the topsoil. The wetter the conditions before the experiment, the lower the [DOC] in the runoff, but the higher $\log_{10}\overline{SUVA}$ and thus more aromatic the DOC was. $\log_{10}\overline{SUVA}$ was also negatively correlated with the clay content of the soil.

ANOVA results for the categorical variables season, tillage technique, field and their interactions are given in Table 2.5. The field factor had a significant effect on all tested variables, reflecting variability between experimental field sites. No significant effect of tillage technique on $[\overline{DOC}]$ or $\log_{10}\overline{SUVA}$ was observed. The tillage technique did have a significant effect on other field characteristics, such as the SOC in the top 5 cm of the soil. A statistically significant effect of the interaction between field and tillage technique on $[\overline{DOC}]$ was observed, indicating a similar tillage technique can have a

different effect on [DOC] depending on field site characteristics. Season had a significant effect on $[\overline{DOC}]$, with lower DOC concentrations measured in fall. Also the C/N ratio of the soil, the initial moisture content and the sediment concentration in the runoff were significantly different between fall and spring. The effect of season on $\log_{10}\overline{SUVA}$ could not be considered, since no SUVA values were measured in the spring experiments on field site 1VA and 7VP. No significant interaction effect of season and tillage technique was found on any of the considered variables.

Table 2.5. ANOVA results for the effect of tillage technique, season, field and their interaction effects on different measured variables. P-values from type III F-test are given. Statistically significant values are indicated in bold. s = measured in soil.

	$[\overline{DOC}]$	$\log_{10}\overline{SUVA}$	SOC	C/N ratio $_s$	Initial moisture content	Sediment concentration
Tillage technique	0.6028	0.5848	**<.0001**	0.1960	0.3086	0.6765
Season [1,2]	**<.0001**	/	0.8812	**0.0007**	**0.0117**	**0.0344**
Season*tillage technique	0.8399	/	0.5631	0.5633	0.2830	0.7270
Field	**<.0001**	**0.0141**	**<.0001**	**<.0001**	**<.0001**	**<.0001**
Field*tillage technique	**0.0006**	0.1622	**0.0379**	**0.0318**	0.4676	0.8802

[1] Properties incorporated in the linear mixed model for $[\overline{DOC}]$ as fixed effects

[2] Properties incorporated in the linear mixed model for $\log_{10}\overline{SUVA}$ as fixed effects

2.3.3 Regression equation

Based on the Pearson correlation coefficients and the ANOVA results, 12 possible explaining variables for $[\overline{DOC}]$ were selected as fixed effects in the linear mixed model (Table 2.4 & Table 2.5). Based on the ANOVA results (Table 2.5) the factor field and its interaction with tillage technique were considered as random effects in the mixed procedure. Backward elimination led to a final linear mixed model (R^2=0.91), containing a fixed and a random part. The factor field was not retained in the model, so that the random part of the final model consisted only of the field-tillage technique interaction. 82 % of the variance that could not be explained by the fixed variables was due to the fact that the effect of tillage technique on $[\overline{DOC}]$ in surface runoff water differed among field sites. Figure 2.3a shows the measured DOC concentrations versus the modeled concentrations.

The fixed part of the final linear mixed regression model is given in Eq. (2.4).

$$[\overline{DOC}] = 3.4924 + 0.2483\ Slope + 0.003469\ [POC] - 1.7305\ RC + 2.7184\ Bulk\ Density - 3.6891\ Season \quad (2.4)$$

The model describes $[\overline{DOC}]$ as a function of soil bulk density, runoff coefficient (RC), slope, POC concentration in the runoff ([POC]) and season. Season is a dummy variable here that was set to 0 for spring and 1 for fall. Higher runoff coefficients led to lower DOC concentrations, while slope, bulk density and POC concentrations in the runoff had a positive effect on $[\overline{DOC}]$. Lower concentrations were predicted in fall. The R^2 of the regression model containing only the fixed effects was 0.54. Figure 2.3b shows the measured DOC concentrations versus the modeled concentrations.

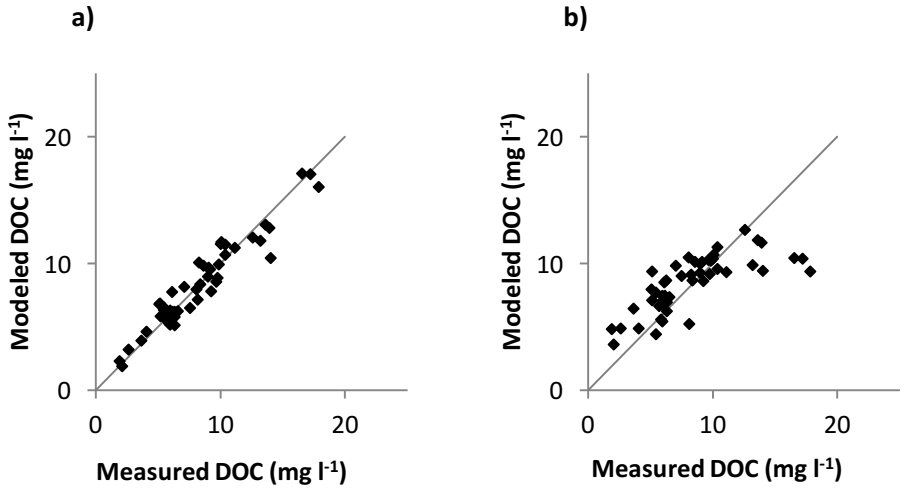

Figure 2.3. Modeled versus measured [$\overline{DOC}$] for each individual field experiment. The full line is the 1:1 line. a) model with fixed and random effects, b) model with fixed effects only.

Six possible explaining variables for $\log_{10}\overline{SUVA}$ values were selected as fixed effects for the mixed model, based on the Pearson correlation coefficients and the ANOVA results (Table 2.4 & Table 2.5). Judging the ANOVA results of the class variables (Table 2.5), only the field variable was considered as a random effect for the model. Backward elimination led to a final regression model containing both random and fixed effects (R^2=0.79). 31 % of the variance that could not be explained by the fixed variables, was explained by differences between agricultural field sites. Figure 2.4a shows the measured $\log_{10}\overline{SUVA}$ versus the modeled values for the total model. The fixed part of the linear mixed model describes $\log_{10}\overline{SUVA}$ as a function of cumulative rainfall depths during 7 days before the experiment only (Eq. 2.5).2.5

$$log_{10}\,\overline{SUVA} = 1.4021 + 0.03844\ Rainfall_{7\ days\ before\ experiment} \quad (2.5)$$

The regression model containing only fixed effects had a R^2 of 0.71 (Figure 2.4b).

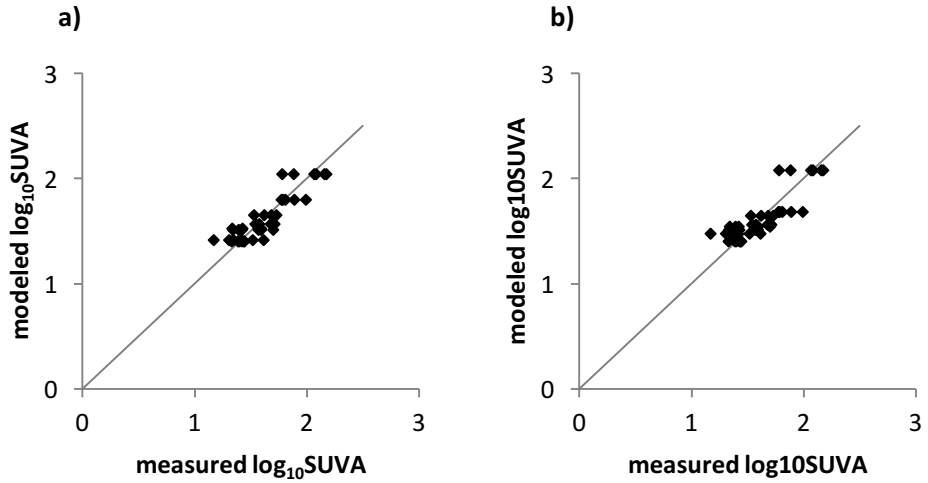

Figure 2.4. Modeled versus measured $\log_{10}\overline{SUVA}$ values for each individual field experiment. The full line is the 1:1 line. a) model with fixed and random effects, b) model with fixed effects only.

2.3.4 Laboratory rainfall simulations

Table 2.6 gives mean $[\overline{DOC}]$ and $\overline{SUVA}$ values in runoff and percolation water for all tested factors in the lab. In the control experiments $[\overline{DOC}]$ in the runoff water was on an average 1.8 mg l^{-1} whereas an average $[\overline{DOC}]$ of 7.6 mg l^{-1} was measured in the percolation water. Taking runoff and percolation fluxes of water into account, a $\overline{DOC}$ flux of 11.9 mg m^{-2} h^{-1} and 149.0 mg m^{-2} h^{-1} from the runoff and the percolation water respectively was calculated. $\overline{SUVA}$ had a mean value of 61.3 l $g^{-1}cm^{-1}$ in the runoff and 22.8 l $g^{-1}cm^{-1}$ in the percolation water. This indicates that although lower amounts of DOC were transported by surface runoff, the DOC in runoff water was more aromatic than in percolating water.

Table 2.6. $[\overline{DOC}]$ and $\overline{SUVA}$ results of the different factors tested in the laboratory experiments. For the drying-rewetting factor tested, values during the second rainfall application (after the drying period) are given. For all other factors tested mean values of the 2 replicates are given.

Factor tested	Runoff		Percolation	
	$[\overline{DOC}]$ (mg l^{-1})	$\overline{SUVA}$ (l g^{-1} cm^{-1})	$[\overline{DOC}]$ (mg l^{-1})	$\overline{SUVA}$ (l g^{-1} cm^{-1})
Control	1.8	61.3	7.6	22.8
Drop impact	1.8	52.8	9.1	23.7
Crop residues (sugar beet)	4.9	32.3	19.6	18.9
Crop residues (maize)	2.4	32.9	13.3	21.2
Drying-rewetting	1.74	31.4	4.27	25.0

Results of the first factor tested (section 2.3) showed no difference in $[\overline{DOC}]$ in the runoff between the control experiments and the experiments with reduced drop impact. In the percolating water however, the reduction of drop impact led to higher $[\overline{DOC}]$. SUVA values in the runoff water were

lower in the experiments with reduced drop impact, while SUVA values in the percolating water were not affected.

In the experiments testing the second factor, namely the addition of crop residues, significantly higher [DOC] was found in surface runoff from the experiments where crop residues were added. $[\overline{DOC}]$ in runoff water was 2.6 times higher than in the control experiments when beet residues were added and 1.5 times higher when maize residues were added to the soil. The addition of crop residues also increased DOC concentrations in the percolating water. The SUVA values were lower in the presence of crop residues than in the unamended controls in both surface and percolating waters.

The last factor tested was the effect of drying and rewetting of the soil. After 60 min of rainfall (one of the control treatments) followed by 7 days of air-drying at room temperature, rainfall was again applied for 60 min. At the start of the second rainfall simulation, right after the drying period, measured $[\overline{DOC}]$ in surface runoff water was initially significantly higher than at the end of the previous rainfall application (Figure 2.5). Concentrations then gradually decreased back to levels comparable to those in the runoff before the drying period. $\overline{SUVA}$ values in the runoff water were significantly lower during the second rainfall application and had a minimum immediately after the drying period (Figure 2.6). Likewise, higher $[\overline{DOC}]$ and lower $\overline{SUVA}$ values were measured in the percolation water at the beginning of the second rainfall application. The drying period did not bring the soil moisture content back to the initial level before the first rainfall period. The volumetric moisture content was 28.6 cm^3cm^{-3} at the start of the second rainfall period and 23.2 cm^3 cm^{-3} at the start of the first period.

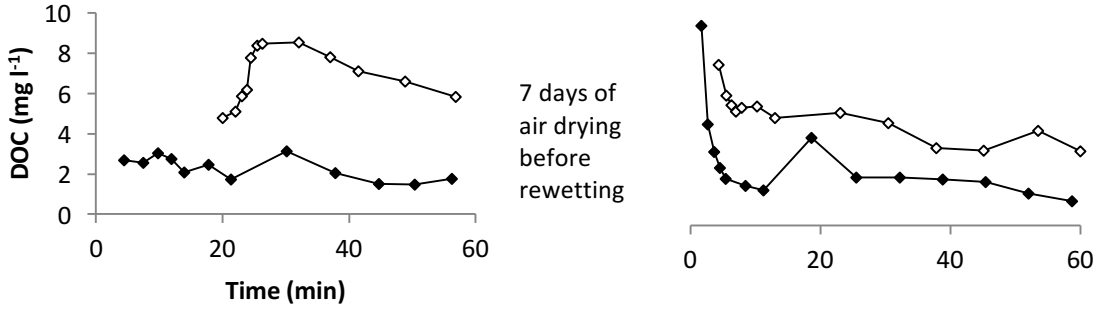

Figure 2.5. DOC concentrations versus time in surface runoff (solid diamonds) and percolation water (open diamonds) during the first (left) and second (right) rainfall application. Rainfall applications were separated by a 7 day air drying period.

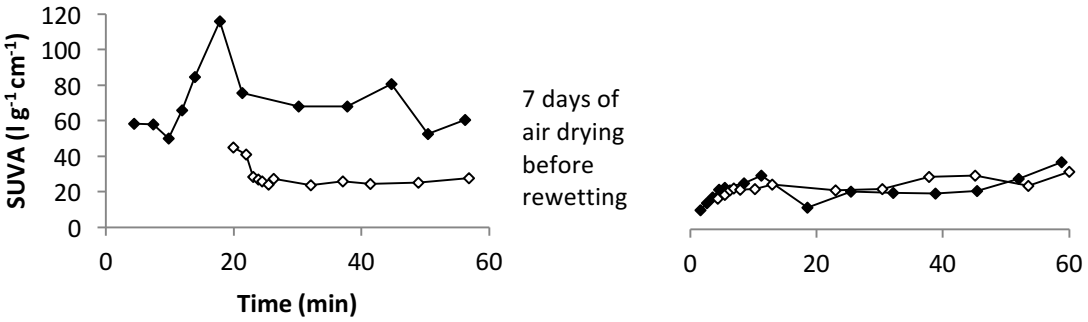

Figure 2.6. SUVA values versus time in surface runoff (solid diamonds) and percolation water (open diamonds) during the first (left) and second (right) rainfall application. Rainfall applications were separated by a 7 day air drying period.

2.4 Discussion

Dissolved organic carbon concentrations in runoff from rainfall experiments on the field were on average 8.54 mg l^{-1}. This is about 30 times smaller than the particulate carbon concentrations (Table 2.3). In surface water, this ratio is much larger, with DOC accounting for 10 to 90 % of the total organic carbon (Meybeck, 1982). This suggests that surface runoff from agricultural land is, in most cases, not the main pathway for the delivery of DOC to the river system. Nevertheless, as DOC is mobile in the soil, it can be an early indicator of changes in soil organic matter status caused by management strategies such as reduced tillage (Haynes, 2000).

We found that one of the most important controls on both DOC concentration and quality in runoff water was antecedent rainfall, which determined initial soil moisture conditions of the field site at the time of the rainfall experiment. The more precipitation occurred in the period before the experiment, or the higher the initial soil moisture content, the lower $[\overline{DOC}]$ and the higher $\overline{SUVA}$ in the runoff during the rainfall experiments. This was also reflected by the significant effect of class variable 'season' on $[\overline{DOC}]$ and $\overline{SUVA}$, whereby lower concentrations but higher aromaticity were measured in fall when soils were moist and produced more runoff. Our drying-rewetting experiment in the laboratory confirmed these trends. After a drying period of 7 days in the lab, [DOC] measured both in the runoff and percolation water showed a sharp increase, whereas SUVA values showed a marked decline. These results were very similar to the effect of soil drying on DOC concentration and quality in the soil solution (Lundquist et al., 1999; Kalbitz et al., 2000; Merckx et al., 2001; Amery et al., 2007). Drying and rewetting causes a sudden release of organic matter in the soil solution. This is attributed to an accumulation of DOC from cell lysis and decay of the biomass during dry periods, or to disruption of the soil structure and a release of organic matter trapped in small pores (Lundquist et al., 1999; Merckx et al., 2001). The DOC released by rewetting of dried soils has a low aromaticity and contains a large fraction of hydrophilic compounds (Amery et al., 2007). De Troyer (2011) showed an increase in [DOC] and drop in SUVA after a drying period in effluent water from column experiments. In our work the release of high concentrations of low aromatic DOC after a dry period was not only observed in percolating water, but also in surface runoff water. Small precipitation depths before a field experiment led to higher concentrations of low aromatic DOC in runoff water. Our data demonstrated that known processes explaining [DOC] and SUVA variations in pore water also explain variations thereof in runoff.

The drying-rewetting effect on [DOC] and SUVA also played a significant role in the typical change in [DOC] and SUVA that was observed during a rainfall event. Our results confirmed the presence of high [DOC] in both runoff and percolation water at the onset of a runoff event (Bajracharya et al., 1998). Afterwards [DOC] diminished towards a steady value at steady state runoff. A similar pattern was also observed on annual grassland and coastal sage scrub hillslopes (Fierer and Gabet, 2000). SUVA values showed an opposite pattern, with lowest values at the start of the experiment which thereafter gradually increased. This indicates that the accumulated soluble C that is released upon rewetting of the soil, causing high concentrations of low aromatic DOC, is rapidly exported from the soil. In agreement, the increasing trend in SUVA values was only found on the three field sites with the lowest recorded rainfall depths 30 days before the experiments took place, confirming that this rapidly soluble pool is formed during dry periods. Our results for mobilization of DOC via surface runoff agree well with what was reported for vertical transport of DOC, namely the presence of a steady baseline of low concentrations of highly aromatic DOC, and a small pool of readily soluble DOC that is immediately mobilized when rainfall occurs (De Troyer, 2011).

While observed temporal variations of DOC and SUVA in runoff were similar to what was observed previously in soil column effluents, a marked difference in DOC concentrations between runoff and percolated waters was observed in the laboratory experiments, with higher DOC concentrations in percolated water. Part of this difference might be due to the soil handling and sieving previous to the experiments, which can disrupt the soil structure and expose new mineral surfaces leading to increased DOC concentrations in the percolation water (Guggenberger and Kaiser, 2003). However, the limited soil disturbance in our laboratory experiments tried to mimic the disturbance that is to be expected when a soil is tilled, and artefacts of air-drying or using a fine sieve on the soil were avoided. Furthermore, lower concentrations in surface runoff are to be expected, even in undisturbed soils as pore water will almost inevitably be much longer in contact with the soil and the soil/water ratio will be much higher within the soil than on the surface. Bajracharya et al. (1998) also reported that [DOC] in percolation water was significantly higher than in runoff water, suggesting that infiltrating water picked up soluble OC as it moved through the soil.

Our laboratory experiments showed that reduced drop impact slightly but significantly increased [DOC] in the percolation water. We hypothesize that when the drop impact was reduced, crust formation was also reduced. Crust formation under simulated rainfall generally leads to lower conductivity of the soil matrix, and thus more water routing through macropores that remain connected to the soil surface. Less crust formation under reduced drop impact causes more water movement through the soil matrix and a prolonged contact time between the soil and the percolation water, allowing the water to pick up greater amounts of DOC. Our hypothesis is supported by observations by Mertens et al. (2007) who reported highest DOC concentrations in soil pore water when direct flow through macropores was limited. In the runoff water, although SUVA values were lower in experiments with reduced drop impact, we did not observe a significant effect on [DOC]. This is in contrast to what was found by Fierer and Gabet (2000). They reported that at least part of the DOC enters the runoff through turbulent mixing of the pore water and the surface water caused by raindrop impact. One may propose two possible explanations for our observations: (i) although drop impact was reduced, the drop impact was still big enough to cause turbulent mixing of the pore water and the surface water or, (ii) drop impact and turbulent mixing are not the main drivers for DOC transfer from the soil to the runoff water. We suspect the latter explanation to be valid as the reduction in drop impact was considerable. Even if some rainfall kinetic energy was

maintained, DOC concentrations are expected to be lower by eliminating the majority of the raindrop impact energy if this is the most important control on DOC release. We therefore conclude that DOC release into the surface runoff water is probably controlled by diffusion processes at the soil-water interface rather than turbulent mixing. Our hypothesis is further supported by the fact that no positive correlation was found between rainfall intensity and [DOC]. It is suggested by Fierer and Gabet (2000) that any rainfall intensity may cause sufficient turbulent mixing and that the rate limiting step is the diffusion of solutes from the soil to the pore water. We argue that no energy is necessary and that diffusion will also take place in the absence of rainfall energy, as it does within the soil profile. The negative correlation between [DOC] and rainfall intensity that we found is most likely a dilution effect, whereby greater volumes of water led to lower DOC concentrations in the runoff water. The relation of $[\overline{DOC}]$ with other variables related to the amount of water confirms this (Table 2.4). The positive correlation of slope and [DOC] was also likely the reflection of a concentration effect. Poesen (1984) and Govers (1991) showed both on the field and in the laboratory, that on rapidly crusting silty loam soils of central Belgium, the slope gradient has a negative effect on runoff generation. In our experiments this was confirmed by a negative correlation between the slope and the amount of total runoff (not shown).

We did not find a significant effect of tillage technique on $[\overline{DOC}]$ and $\log_{10}\overline{SUVA}$ in our field experiments. In addition, none of the numerical variables retained in the final regression models differed significantly between tillage techniques. However, the interaction effect of field and tillage technique did have a significant effect on $[\overline{DOC}]$ and explains a large part of the random variance in the regression model. This suggests that a tillage technique might have a different effect on DOC concentrations in runoff water on different field sites. Addition of crop residues during the laboratory experiments significantly increased the [DOC] and decreased SUVA values in the runoff. Leaving crop residues at the soil surface, as is done in reduced tillage, can thus directly deliver more DOC with lower aromaticity to the surface runoff. Also the higher SOC content found in the top 0-5 cm of reduced tilled plots is expected to affect the [DOC] in runoff water. The higher SOC content for RT than for CT (on average 12.63 versus 10.02 g $kg^{-1}_{dry\ soil}$) confirmed earlier findings where increased accumulation of SOC in the soil top layer under RT is reported (Bertol et al., 2004, 2007; Leys et al., 2007; Roper et al., 2010). However, as soil aggregates are more stable under reduced tillage, less DOC might be released from organic matter held in aggregates. Consequently, under field conditions, the net effect of reduced tillage practices remains equivocal because many soil properties, which can interact and counterbalance, are influenced at the same time (Chantigny, 2003). As a result, we expect the overall change in DOC delivery to the surface water caused by a change in tillage technique to be limited.

In the field experiments, no significant correlations were found between $[\overline{DOC}]$ and most of the soil properties such as the SOC content, the C/N ratio and the sand, clay and silt content of the soil. This might be due to the limited range of soil properties observed on the experimental field sites. All field experiments in this study were carried out on loess-derived soils in the Belgian loam belt and SOC content of the experimental soils were all between 7.33 and 17.54 g $kg^{-1}_{dry\ soil}$, which only represents a small range. On soils with a wider range in soil properties, a correlation between C content, C/N ratio or texture of the soil and the [DOC] in runoff water might still be found. After all, DOC concentrations in leaching water have been shown to be (weakly) positively correlated with the organic matter content of the soil (Currie and Aber, 1997; Tipping et al., 1999; De Troyer, 2011). On

the other hand, using soil samples collected on a large range of soil types, De Troyer et al. (2014) found that soil properties can only weakly explain DOC concentrations in the soil solution. As the current work shows that the controls on the transport of DOC in surface runoff and leaching water are similar, the effect of soil properties on the DOC concentrations in runoff water - even from a larger range of soil types - is likewise expected to be limited.

The field experiments in this work did show a positive effect of the bulk density of the soil on $[\overline{DOC}]$ in runoff water. Bulk density also came out as an important explaining variable in the final linear mixed regression model. No physical explanation for this effect could be found. However, the effect of bulk density on $[\overline{DOC}]$ might be indirect and a reflection of other variables controlling DOC concentrations in runoff water, as bulk density was significantly correlated with the initial soil moisture content, the SOC and the sand, clay and silt fractions of the soil. Bulk density also differed significantly between field sites, and might thus represent part of the variability between individual field sites. As soil bulk density was not correlated with any of the other independent variables in the regression model (slope, RC, POC concentration in the runoff and season), the addition of this variable to the regression model was not due to overfitting.

Average DOC concentrations observed in surface runoff from the rainfall experiments on the field were almost 5 times higher than average concentrations observed in surface runoff from the lab experiments. Although it might be a consequence of storing the soil without any input of fresh organic matter prior to using it in the lab experiments, none of the variables observed during the experiments in this study could explain this difference. However, it clearly illustrates the importance of field experiments to study the factors controlling the transport of DOC through surface runoff.

2.5 Conclusion

Our work evidenced that soil properties, tillage technique and field characteristics only have a limited effect on DOC concentrations and quality in runoff waters from agricultural soils located in the Belgian loam belt. The most important control on DOC concentration in runoff waters was the antecedent soil moisture condition as more DOC was released from drier soils. One of the main findings in experiments following a dry period was the release of large amounts of low aromatic DOC at the beginning of a runoff period, with a gradual shift towards lower DOC concentrations and higher DOC aromaticity. Controlled experiments indicated that even though DOC concentrations were lower in surface runoff than in percolating waters, controls on the temporal dynamics of DOC release and quality were similar.

Chapter 3. Identifying the transport pathways of dissolved organic carbon in contrasting catchments

Adapted from: Van Gaelen, N.; Verheyen, D.; Ronchi, B.; Struyf, E.; Govers, G.; Vanderborght, J. and Diels, J. 2014. Identifying the Transport Pathways of Dissolved Organic Carbon in Contrasting Catchments. Vadose Zone Journal 13,7.

3.1 Introduction

Dissolved organic carbon (DOC) plays an important role in the cycling and distribution of energy and nutrients both within and between ecosystems (Kaiser and Kalbitz, 2012). Due to its high mobility and reactivity (Neff and Asner, 2001), it is highly relevant for the global carbon cycle (Jardine et al., 2006). Because of its complexation capacity however, it affects the transport of contaminants such as heavy metals from soils to surface waters (Tipping, 1993; Kalbitz et al., 2000). In drinking water production, DOC can lead to the formation of unwanted disinfection by-products such as trihalomethanes and haloacetic acids (Liang and Singer, 2003).

During recent decades, increasing DOC concentrations have been reported in surface waters (Freeman et al., 2001; Worrall et al., 2004; Evans et al., 2005). A range of causal factors for this increase is suggested, including recovery from acidification (Evans et al., 2005), CO_2 enrichment (Freeman et al., 2004) and rising temperatures (Freeman et al., 2001; Gruau and Jardé, 2005). However, isolating controlling mechanisms based on monitoring data alone remains a challenge (Evans et al., 2005).

At the catchment scale, several authors have reported relationships between DOC concentrations measured in the stream and discharge, whereby increasing discharge leads to higher DOC concentrations (Lewis and Grant, 1979; Dawson et al., 2002, 2011; McGlynn and McDonnell, 2003). This positive relationship however might be dependent on the season (Dawson et al., 2002, 2008a). In several study catchments DOC concentrations measured in the stream show seasonal variation, with peaks in fall and minima in spring (Dawson et al., 2002, 2008a, 2011; Halliday et al., 2012). The annual flush of DOC in fall is attributed to the rewetting of the catchment after a period of high biological activity in the summer (Halliday et al., 2012) and the input of fresh organic matter caused by leaf fall and decomposition (Mulholland and Hill, 1997).

Independent of the seasonal variation, DOC concentrations measured at catchment outlets typically increase during heavy rainstorms and snowmelt compared to dry weather baseflow concentrations (McDowell and Likens, 1988; Hagedorn et al., 2000; Dawson et al., 2002; Kaiser and Guggenberger, 2005; Shanley et al., 2011; Halliday et al., 2012). Boyer et al. (2000) reported increases up to 5.3 mg l^{-1} DOC in the stream during periods of snowmelt runoff, compared to steady baseflow concentrations of 1.1 mg l^{-1}. During periods of high discharge caused by rainfall events in summer, Hagedorn et al. (2000) measured relative increments in stream DOC concentrations up to +350 %. Also properties of DOC change drastically during a rainfall event, evidenced by Hagedorn et al. (2000) who reported molar absorptivity at 285 nm, an indicator for aromaticity and molecular weight of the

DOC, to first decrease during a rainfall event, and later reach a maximum up to 450 l cm^{-1} mol^{-1} C on the descending limb of the hydrograph, compared to 340 l cm^{-1} mol^{-1} C before the start of the event. Several authors have attributed these temporal variations in DOC concentrations and properties to changes in water flow paths. Thereby high DOC concentrations are associated with near-surface hydrologic flow paths interacting with the organic carbon-rich forest floor or surficial soil layers in riparian or wetland locations (Boyer et al., 1997; Hagedorn et al., 2000; Inamdar and Mitchell, 2006). This increase in DOC concentrations in the stream caused by a rising groundwater table is often described as "flushing". Other studies also found a role for in-stream processes such as throughfall directly onto the stream from riparian branch overhang or stream channel expansion at increasing discharge (Tate and Meyer, 1983; Mulholland and Hill, 1997; Hagedorn et al., 2000). The range of possible controls often makes it challenging to define the factors controlling the transport of DOC towards the surface water at the catchment scale. Furthermore, similar solute patterns measured in the stream water catchment outlet can be produced by very different transport mechanisms, while at the same time, dissimilar solute concentration patterns might be caused by the same export mechanism (Inamdar and Mitchell, 2006).

Previously, the method of end-member mixing analysis (EMMA) as described by Christophersen and Hooper (1992), has been used to quantify the contribution of the different water flow paths to the stream runoff (Christophersen et al., 1990; Burns et al., 2001). More specifically has it been applied by Hagedorn et al. (2000), Inamdar and Mitchell (2006) and Shanley et al. (2011) to show that temporal changes in DON and DOC concentrations measured in the stream during a storm event could be largely explained by a change in flow paths. Results of the EMMA carried out by Hagedorn et al. (2000), showed that the peak in DOC concentrations on the descending limb of the hydrograph was caused by the contribution of water from the DOC rich topsoil in the later stages of the storm, while water from the subsoil dominated during baseflow.

Most research identifying the controls on DOC transport on the catchment scale have either focused on sampling at high frequency during a single or a limited number of events (Bishop et al., 2004; Kaiser and Guggenberger, 2005; Inamdar and Mitchell, 2006), or the collection of low frequency (mostly weekly) samples over a longer term (Boyer et al., 1997; Dawson et al., 2002, 2008a; Laudon et al., 2004; Hernes et al., 2008). Only few studies have combined a long record of regular baseflow sampling with high-frequency event sampling (Hagedorn et al., 2000; Shanley et al., 2011). However, by focusing on baseflow only, a major part of the DOC export is overlooked, as DOC export during rainfall events can account for a great proportion of the total DOC catchment export (Hinton et al., 1997). Event sampling only leads to a partial understanding of the controlling factors for the transport of DOC in the catchment, as regular long-term sampling is needed to account for seasonal baseflow differences (Halliday et al., 2012). Kirchner et al. (2004), Shanley et al. (2011) and Halliday et al. (2012) have already demonstrated that the combination of long-term and high-frequency monitoring provides valuable and unique insights into the hydrochemistry of a catchment.

The objective of this study was to identify the contributing pathways for the transport of DOC from the watershed to the surface water during different flow regimes in catchments differing in land use and hydrogeology. Therefore, regular stream water sampling during dry weather baseflow conditions was combined with more frequent sampling during peak flow events caused by rainfall events. We hypothesize that (1) the change in DOC concentrations and quality typically observed during periods of high discharge caused by rainfall events, can be explained by a change in the contribution of the

different transport pathways delivering DOC at the catchment outlet during a rainfall event, (2) an end-member mixing analysis combining concentrations of DOC, Si, Mg, K, Ca and S measured in the stream water with concentrations measured in throughfall/precipitation, groundwater, soil pore water and riparian zone water allows the identification of these contributing pathways for the transport of DOC to the surface water and (3) the importance of contributing transport pathways can change seasonally as the degree of saturation of the catchment soils changes.

3.2 Material and methods

3.2.1 Study area

Four headwater catchments were selected in central Belgium (Figure 3.1). The area has a temperate climate with a long-term mean annual precipitation of 820 mm and a mean temperature of 3.1 °C in January and 17.7 °C in July. Precipitation is distributed equally over the year, although intensity and duration of rainfall events vary with the season. Shorter, more intensive storms (with extremes of >80 mm of precipitation within 30 min on 18/08/2011) occur mainly in spring and summer, compared to longer, less intensive rainfall events in fall and winter. The catchments vary in size between 0.33 km² and 2.66 km². The Meerdaal and Ronquières catchment are deciduous forest catchments, with mixed beech (*Fagus sylvatica* L) and oak (*Quercus robur* L) stands. The Herve and Blégny catchments are under pasture. Regular harvesting of the grasses (*Poaceae* family) is alternated with periods of cattle grazing. All sites have a rolling topography, with slopes up to 25 %.

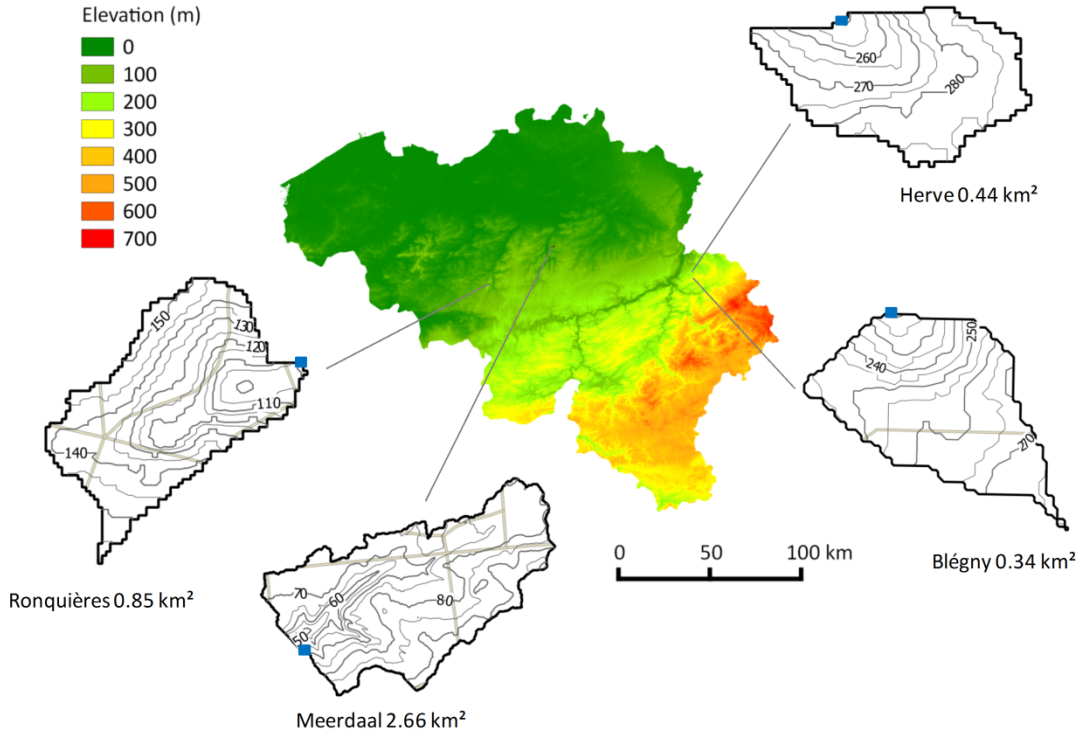

Figure 3.1. Location of the study sites on the elevation map of Belgium. For each catchment a detailed map shows the topography, roads and the position of the V-notch weir and automatic sampler (blue square).

In the Meerdaal catchment under forest, soils with a silty loam texture have developed in the Late Glacial loess covers (Deckers et al., 2009). The loess is underlain by permeable loamy sands of the Brussels Formation and the clayey Kortrijk formation (Figure 3.2). The catchment has a deep groundwater table, that is found in the Brussels Formation (Peeters, 2010). The riparian zone observed in this catchment, namely the area bordering the river which contains a thick layer of organic material and where the water table is near the surface, has a width between 1.5 m and 10 m on each river bank. In the Ronquières catchment, results of soil corings at the field suggest the hydrogeological setting is similar, with deep groundwater tables and well conductive unsaturated zones. In the Blégny pasture catchment, soils have a silty loam texture and have developed in the residual clay with chert nodules that is left after dissolution of the Gulpen chalk (Figure 3.3). Clay lenses found throughout the whole soil profile strongly limit drainage. The groundwater table follows the topography of the catchment and can be found at maximum a few meters depth (Ruthy and Dassargues, 2008). The unsaturated zone in this catchment is very thin, and becomes close to or completely saturated in winter. Seeps are found on the hill slopes at several locations throughout the catchment. At these locations the groundwater table surfaces and water flow continues towards the river at the soil surface. The (almost) saturated riparian zone spreads between 1.6 and 5.8 m on each river bank. In the Herve catchment the geology is similar, but the topography is steeper and on the highest locations groundwater tables are found deeper (Ruthy and Dassargues, 2008).

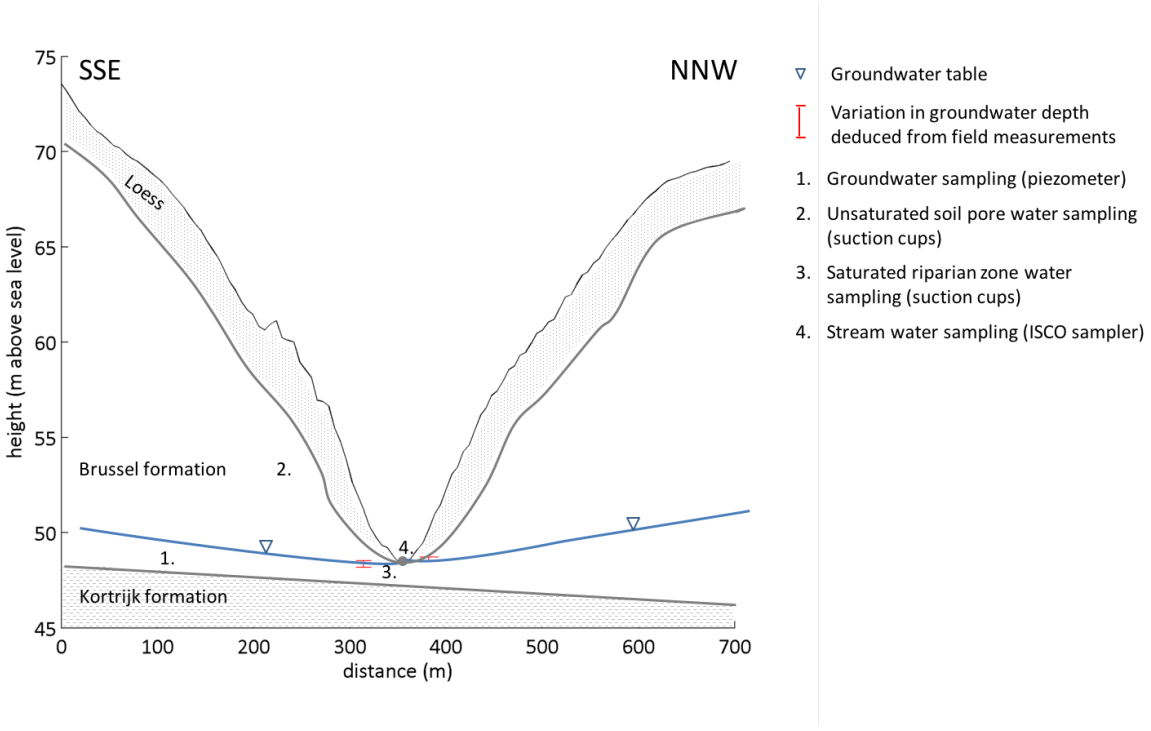

Figure 3.2. Cross-section (SSE to NNW) of the landscape in the Meerdaal catchment, with an indication of the groundwater table, deduced from the piezometer data and from field observations.

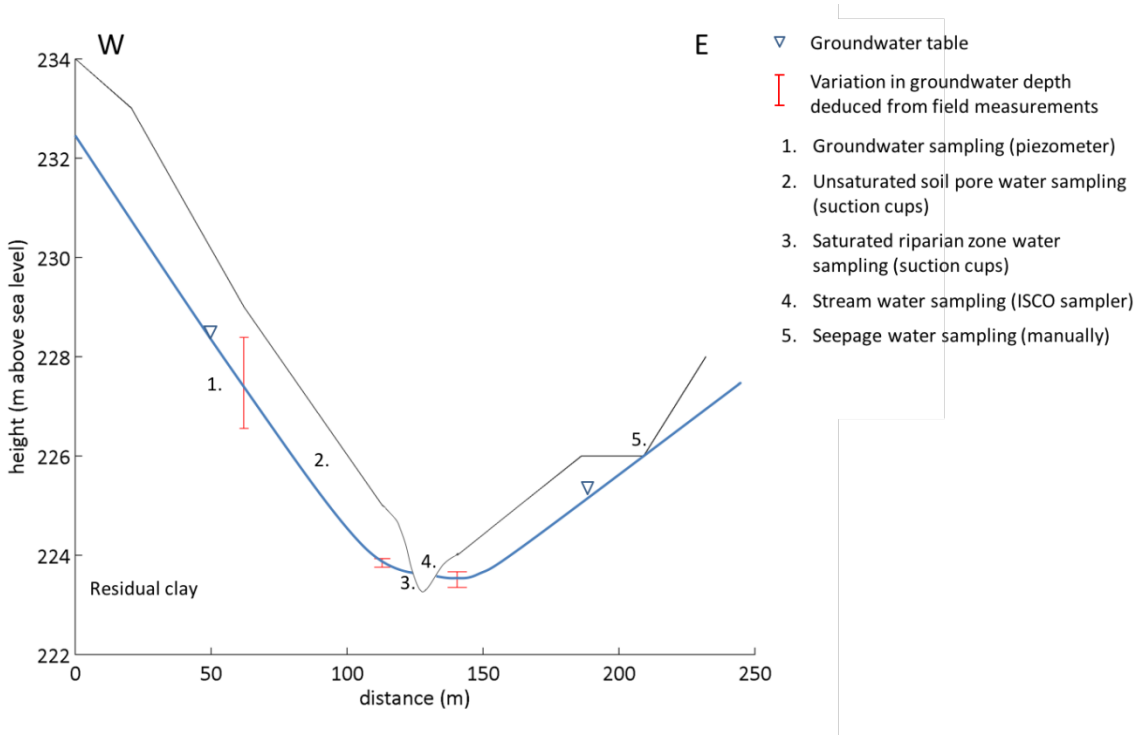

Figure 3.3. Cross-section (W to E) of the landscape in the Blégny catchment, with an indication of the groundwater table, deduced from the piezometer data and from tensiometer measurements between March 2013 and September 2013.

3.2.2 Experimental set-up

In all the catchments V-notch weirs were installed to measure discharges. Records of water height (m) were collected every 15 minutes using a flow module (ISCO 710 Ultrasone module or ISCO 720 submerged probe module, Teledyne ISCO Inc., Lincoln NE, USA) that was connected to an automatic data logger (ISCO 6712, Teledyne ISCO Inc., Lincoln NE, USA). Discharge (m^3s^{-1}) was calculated from water height measurements which were transmitted via telemetry or read out at the site location every two weeks. In the pasture catchments, a tipping bucket rain gauge present at the site yielded data of rainfall amounts and intensity. Precipitation data for the forested catchments were collected from pluviometers placed in the open field nearby the monitoring site (1.04 km distance for Meerdaal, 370 m for Ronquières).

The Meerdaal and Blégny catchments were extensively sampled starting from January 2010 and April 2010 respectively until July 2013. In Ronquières and Herve samples were only collected and analyzed for one full year (January 2010 until December 2010) (Table 3.1). Measurements of discharge and precipitation continued until May 2012. As catchment monitoring in this work focuses both on regular stream water sampling during dry weather conditions and more frequent sampling during rainfall events, the terms 'baseflow' and 'event' are used to indicate the different sampling conditions. Thereby stream flow observed during dry weather conditions is referred to as baseflow, while all stream flow observed during rainfall events is referred to as event flow.

Table 3.1. Overview of the collected samples and the analyses carried out, per catchment.

Catchment	Sample type	n †	period	Analysis
Meerdaal (forest)	Stream	191 (baseflow)	2010-2013	DOC, SUVA, Si
		398 (events)	2011-2013	cations
	Soil water	376	2010-2013	Si
			2011-2013	DOC, SUVA, cations
	Groundwater	82	2011-2013	DOC, SUVA, Si and cations
	Throughfall	29	2012-2013	DOC, SUVA, cations
			2013	Si
Blégny (pasture)	Stream	239 (baseflow)	2010-2013	DOC, SUVA, Si
		354 (events)	2011-2013	cations
	Soil water	262	2010-2013	Si
			2011-2013	DOC, SUVA and cations
	Groundwater	38	2011-2013	DOC, SUVA, Si and cations
	Seepage	159	2011-2013	DOC, SUVA, Si and cations
	Precipitation	8	2013	DOC, SUVA, Si and cations
Ronquières (forest)	Stream	153 (baseflow)	2010	DOC, SUVA
		165 (events)	2010-2012	Si
	Soil water	32	2010	Si
Herve (pasture)	Stream	174 (baseflow)	2010	DOC, SUVA
		143 (events)	2010-2012	Si
	Soil water	104	2010	Si

† number of samples collected over the monitoring period

River water baseflow samples were collected automatically by the ISCO sampler at programmed times twice a week. Peak flow event samples were collected whenever the water rose above a certain threshold water level, which was adjusted manually depending on the season and the catchment. During a rainfall event, a maximum of 15 event samples were taken by the ISCO sampler proportionally to the discharge. Samples were stored in polyethylene terephthalate (PET) bottles inside the ISCO sampler and collected as soon as the sampler was full or within maximum two weeks.

Suction cups (Soilmoisture Equipment Corp., Goleta CA, USA) were installed in every catchment along two parallel transects perpendicular to the river channel. Along each transect, three locations (spaced between 15 and 45 m) were selected, where suction cups were installed at 3 depths (30, 60 and 90 cm). Soil pore water samples were collected once a month by applying a continuous suction of ca 500 hPa one week (Meerdaal, Herve and Ronquières) or one month (Blégny) before the sample collection using a vacuum pump (Eijkelkamp, Giesbeek, The Netherlands). In Meerdaal and Blégny three piezometers were installed in 2011, in which groundwater depth was monitored every 30 minutes. Groundwater samples were collected monthly using a peristaltic pump. Information on the filter depth and the length of the filter with respect to the mean groundwater depth at the location of all piezometers is given in Table 3.2. In the scope of the work done by Ronchi (2014), in Blégny also soil water potentials were measured using tensiometers that were installed at different depths along one suction cup transect in spring 2013.

Table 3.2. Filter depth of the piezometers installed in the Meerdaal and Blégny catchment, mean groundwater depth and distance to the stream.

	Filter depth† (m)	Mean groundwater depth † (m)	Distance to the stream (m)
Meerdaal (forest)			
Piezometer 1	0.90 - 2.90	1.24	18
Piezometer 2	2.60 - 4.60	2.85	28
Piezometer 3	1.83 - 3.83	1.59	45
Blégny (pasture)			
Piezometer 1	2.00 - 3.20	0.50	8
Piezometer 2	1.00 - 3.00	1.16	19
Piezometer 3	1.00 - 2.00	0.49	31

† measured from the soil surface

As in Blégny several seeps on one of the river banks were found to deliver water to the stream year round, grab samples were taken monthly from 3 locations starting from 2011.

A precipitation/throughfall collector was installed in Meerdaal (in 2012) and Blégny (in 2013) consisting of a funnel (diameter 18 cm in Meerdaal, 14 cm in Blégny) attached to a PET bottle. A wire mesh prevented contamination from falling leafs. In Meerdaal, where it was installed under the forest canopy, it collected composite (2 week) samples of throughfall. In Blégny, composite (2 week) precipitation samples were collected in the open field.

3.2.3 Laboratory analysis

Stream water samples, both from baseflow and event conditions, soil water samples, groundwater samples and precipitation/throughfall samples were stored at 4 °C prior to analysis. One subsample was filtered upon arrival in the lab with a 0.45 µm CHROMAFIL® PET filter (Macherey-Nagel GmbH & Co., Düren, Germany) (pre-rinsed with 20 ml of demineralized water), and analyzed within 6 weeks for dissolved organic carbon concentrations ([DOC], mg l^{-1}), specific UV absorbance (SUVA, l g^{-1} cm^{-1}) and (from 2011 on) concentrations of Na, Mg, K, Ca, S, Al, Cu, Fe, Mn (mg l^{-1}). DOC was measured using a Multi N/C® 2100 (Analytik Jena AG, Jena, Germany). The absorbance at 254 nm (A_{254}) was determined with a Lambda 20 UV/VIS Spectrophotometer (PerkinElmer, Waltham MA, USA), with a path length (b) of 1 cm. SUVA (l g^{-1} cm^{-1}) was then calculated using Eq. (3.1).

$$SUVA = \frac{A_{254}\,1000}{b[DOC]} \tag{3.1}$$

where A_{254} is dimensionless, b is in cm and the DOC concentration is in mg l^{-1}. SUVA is an indicator of the aromaticity and the recalcitrant nature of the DOC, whereby higher SUVA values are measured if the DOC is more aromatic (Weishaar et al., 2003). Elemental analysis was carried out using ICP-OES (Optima 3300 DV, PerkinElmer Waltham MA, USA). Therefore the subsamples were acidified to pH 1 using a 5M HNO_3 solution prior to analysis.

In the scope of the work by Clymans (2012), Clymans et al. (2013) and Ronchi (2014), another subsample was taken to determine the dissolved silica (Si) concentration. This was done

colorimetrically using the molybdenum blue method, after filtration using a CHROMAFIL® MV filter (Macherey-Nagel GmbH & Co., Düren, Germany) with a pore size of 0.45 µm upon arrival in the lab.

3.2.4 Statistical analysis

An ANOVA analysis was carried out for the Meerdaal (forest) and Blégny (pasture) catchment to statistically test whether DOC concentrations and SUVA values differed significantly between the seasons. Therefore, DOC concentrations and SUVA values measured during baseflow conditions were grouped according to the season: spring (21 March-20 June), summer (21 June-20 September), fall (21 September-20 December) and winter (21 December-20 March). As in the Herve and Ronquières catchment a limited number of samples were analyzed for DOC concentrations and SUVA values (Table 3.1), this analysis was not carried out for these catchments.

3.2.5 End-member mixing analysis

An end-member mixing analysis (EMMA) (Christophersen and Hooper, 1992) was carried out for Meerdaal (forest) and Blégny (pasture) in order to identify the contribution of different sources (end-members) to the streamflow and thus DOC concentrations in the stream. Potential source water end-members considered were soil pore water collected from the suction cups sampling the unsaturated soil zone, groundwater, throughfall or precipitation water and seepage water (in Blégny only). In both catchments samples collected in the suction cups located closest to the stream channel were considered to represent water from the year-round (almost) saturated riparian zone, a fifth possible end-member.

In order to be used successfully in an end-member analysis, the solute concentrations of the end-members must (1) be constant in time and space, (2) differ significantly between end-members and (3) mix conservatively (Christophersen et al., 1990). In our case, the solutes used in the end-member mixing analysis were DOC, Si, Mg, K, Ca and S. Other measured solutes were not included in the analysis, as concentrations were not always above the detection limit, or were prone to contamination during analysis. Although we recognize the non-conservative nature of DOC, it was included in the analysis because DOC typically accumulates in surficial soil layers and is thus a good proxy of near-surface runoff transport pathways. DOC has previously been used successfully to identify flow paths and geographic sources of runoff (McGlynn and McDonnell, 2003; Inamdar and Mitchell, 2006).

Concentrations of DOC, Si, Mg, K, Ca and S measured in the stream water samples were used first in a principal component analysis (PCA). Therefore, following Christophersen and Hooper (1992) and Hooper (2003) all solute concentrations were standardized to zero mean and unit standard deviation (Eq. 3.2) so that all solutes have equal weight in the analysis.

$$C_j^* = \frac{C_j - \mu}{\sigma} \qquad (3.2)$$

where C_j and C_j^* are respectively the original and the standardized concentration of solute j, μ is the mean concentration of solute j in the stream water and σ is the standard deviation of solute j in the stream water. The PCA analysis allowed the identification of the number of end-members defining the system, which equals the number of principal components needed to explain a sufficient amount of variance in the stream water data plus one. By multiplying the mean and ranges (mean +/- standard deviation) of concentrations of the potential source water end-members (standardized with

respect to the mean and standard deviation of the stream water concentrations) with the loadings of the principal components, the scores of the potential end-members were projected into the principal component space. Following Christophersen and Hooper (1992), the end-members whose projections best enclose the scores of the stream water samples in the principal component space were selected as sources contributing to the stream water.

The end-member mixing analysis was then carried out using the mean solute concentrations of the selected end-members. The mean concentrations were used in a constrained nonlinear optimization to calculate the discharge volume fractions of the different source end-members contributing to the stream at each sampling time during the entire research period. Therefore, the mixing equation given by Eq. 3.3 was solved under the condition of Eq. 3.4.

$$Ctot_{ij} = \sum_{k} v_{ki} C_{kj} \tag{3.3}$$

$$\sum_{k} v_{ki} = 1 \tag{3.4}$$

where $Ctot_{ij}$ represents the concentration of solute j in the stream at time i, C_{kj} the mean concentration of solute j in the k^{th} end-member and v_{ki} is the discharge volume fraction of the k^{th} end-member at time i. At each sampling time, concentrations of DOC, Si, Mg, K, Ca and S were considered, leading to a set of 6*i equations. All event and baseflow samples for which all 6 solute concentrations were available, were used. Constraints were formulated so that all discharge volume fractions were between 0 and 1.

The fmincon solver in matlab (Matlab®, version 7.6.0.324 R2008a, The MathWorks, Inc.) then solved for v_{ki} by minimizing the sum of squared deviations f (Eq. 3.5).

$$f = \sum_{i,j} \left(Ctot_{ij} - Ctot_{ij,measured} \right)^2 \tag{3.5}$$

where $Ctot_{ij,\ measured}$ are the measured concentrations of the different solutes in the river water samples.

The fractions of the contributing end-members as determined by the EMMA at each sampling time were used to calculate discharge weighted mean fractions. This was done separately for baseflow samples and for each individual rainfall event. For each event the timing of the peak of the end-member fractions was compared to the timing of maximum discharge. In this way the importance of the contribution from the different end-members could be assessed both seasonally and during different hydrological regimes.

The performance of the EMMA solution was evaluated by calculating the coefficient of determination (R^2), which provides information about the goodness-of-fit of the regression and is given in Eq. 3.6 (Kvalseth, 1985). The Pearson's linear correlation coefficient (P_{corr}) (Eq. 3.7) gives the degree of correlation between the measured and the modeled values.

$$R^2 = 1 - \frac{\sum (x_i - y_i)^2}{\sum (x_i - \bar{x})^2} \tag{3.6}$$

$$P_{corr} = \frac{\sum (x_i - \bar{x})(y_i - \bar{y})}{\sqrt{\sum (x_i - \bar{x})^2 \sum (y_i - \bar{y})^2}} \quad (3.7)$$

where x_i and y_i are respectively the measured and the modeled values, and $\bar{x}$ and $\bar{y}$ are the mean of the measured and the modeled values. For the evaluation of SUVA values, predicted SUVA values were calculated by weighing SUVA in the different end-members by the end-member DOC concentration.

3.2.6 Load and flux calculations

Using the discharge weighted mean fractions of the different contributing end-members, the importance of the different pathways for the total annual export of DOC was determined. Therefore, the series of observed discharge data in the Meerdaal and the Blégny catchment were first split into periods of baseflow and periods of event flow by applying a threshold water level. Whenever the water level rose above this threshold level, event conditions were assumed. For Meerdaal, a fixed threshold of 0.0002 m^3 s^{-1} was used. For Blégny the threshold was adjusted manually according to the season. Discharge weighted mean fractions of the contributing end-members, calculated as described in 3.2.5, were then used to determine the water fluxes originating from each end-member during dry weather baseflow conditions on the one hand and during times when discharge was elevated in response to rainfall events on the other hand. Annual DOC fluxes for each transport pathway were calculated by combining these water fluxes with the mean DOC concentrations measured in in the end-members.

For the Meerdaal catchment, Clymans (2012) has previously addressed the uncertainty of the groundwater contributing area. He has estimated the groundwater contributing area to be 0.018 km^2, and thus much smaller than the surface contributing area. Therefore, for the Meerdaal catchment total DOC loads were calculated, rather than fluxes that require accurate knowledge on the total contributing area. The comparison of DOC loads reaching the catchment outlet via each transport pathway also allowed to judge the importance of the contributions for the total annual DOC export.

3.3 Results

3.3.1 Hydrology

In the forested Meerdaal catchment (Figure 3.4), average dry weather baseflow discharge during the years of monitoring was $1.2*10^{-4}$ m^3s^{-1} (n=191). Only small seasonal variation in baseflow discharge was observed (between $1*10^{-5}$ and $5*10^{-4}$ m^3s^{-1}) with lowest discharge between May and August and highest discharge around December. Discharge changed dramatically during rainfall events, rising up to several hundred times the baseflow discharge during the largest events (Figure 3.4), but returning rapidly to pre-event baseflow discharge after a rain event (Figure 3.5). Groundwater level data showed small seasonal variation, with only a 30 cm difference between the highest and lowest groundwater levels. Groundwater level reactions to rainfall events were smaller and less flashy than the reactions in stream discharge (Figure 3.4). The hydrology in Ronquières, the other forested catchment, was similar, with an average baseflow discharge of $2.3*10^{-3}m^3s^{-1}$ and small seasonal variations (data not shown). Lowest baseflow discharges were recorded between July and September

and greatest baseflow discharges between December and February. Rainfall events caused flashy discharge responses with peak event discharges up to 10 or even 100 fold larger than baseflow discharge.

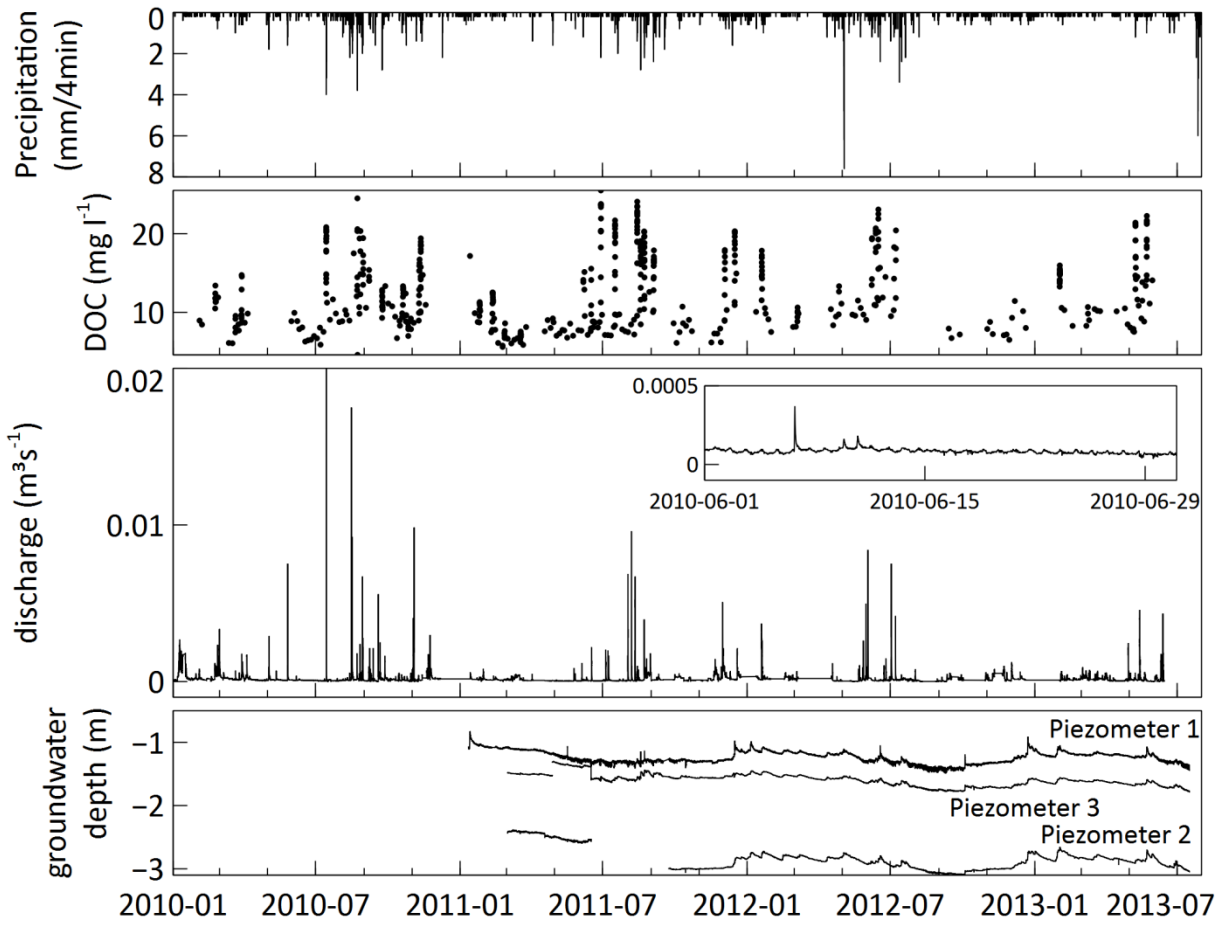

Figure 3.4. Hydrology and DOC concentrations in the stream at the outlet of the Meerdaal catchment (January 2010 - July 2013). The inset shows an enlargement of the baseflow discharge during one month (July 2010). The bottom graph shows groundwater depth measured in 3 piezometers. Discharge was not measured during the large rainfall event on 03/05/2012 due to malfunctioning of the equipment.

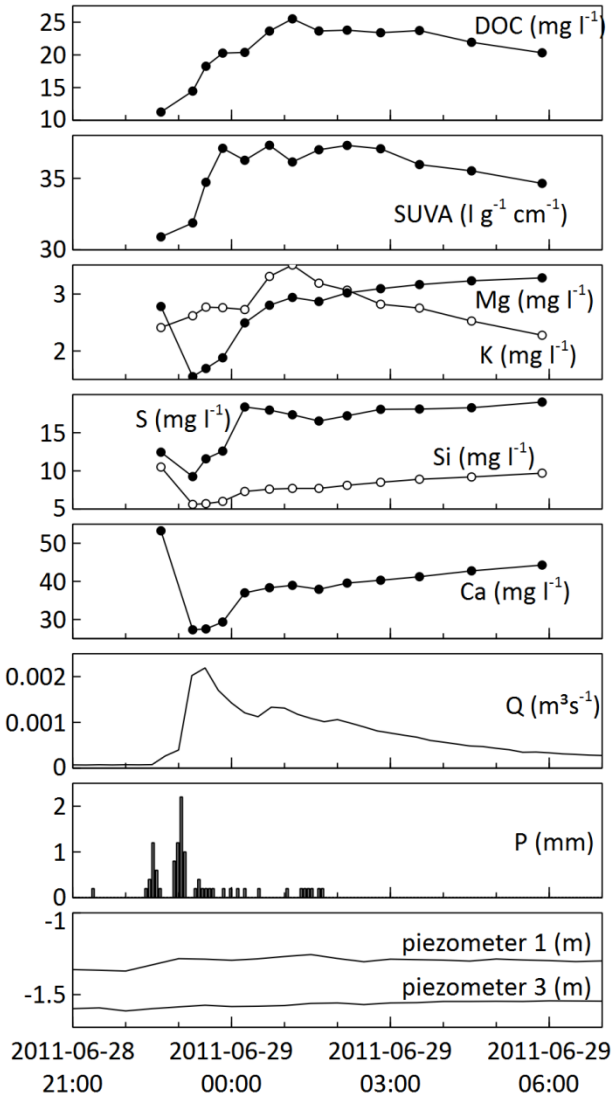

Figure 3.5. General representation of discharge, precipitation and solute concentrations measured in the stream outlet of the Meerdaal catchment during a rainfall event (29/06/2011).

In the pasture catchments, dry weather baseflow discharge varied greatly according to the season. In Blégny (Figure 3.6), during the 3 years of monitoring, baseflow discharge yearly reached its lowest values around November. In December, baseflow discharge rose and reached a maximum in January-February after which it gradually decreased again. Independent of the general pattern in baseflow, rainfall events caused discharge numbers to peak up to 5-times the baseflow discharge, with sometimes slow returns back to baseflow levels. As the groundwater table follows the topography and is found at few meters depth throughout the whole catchment (Figure 3.3), groundwater response to rainfall events was more pronounced than in the forest catchments, with groundwater levels remaining elevated for several days before returning to pre-event values. The hydrology of the Herve catchment was very similar to that of Blégny, with baseflow discharge changing with the seasons, and additional rises in discharge as a response to rainfall events (data not shown). Discharge reactions to rainfall events in both pasture catchments were less flashy than in the forested catchments.

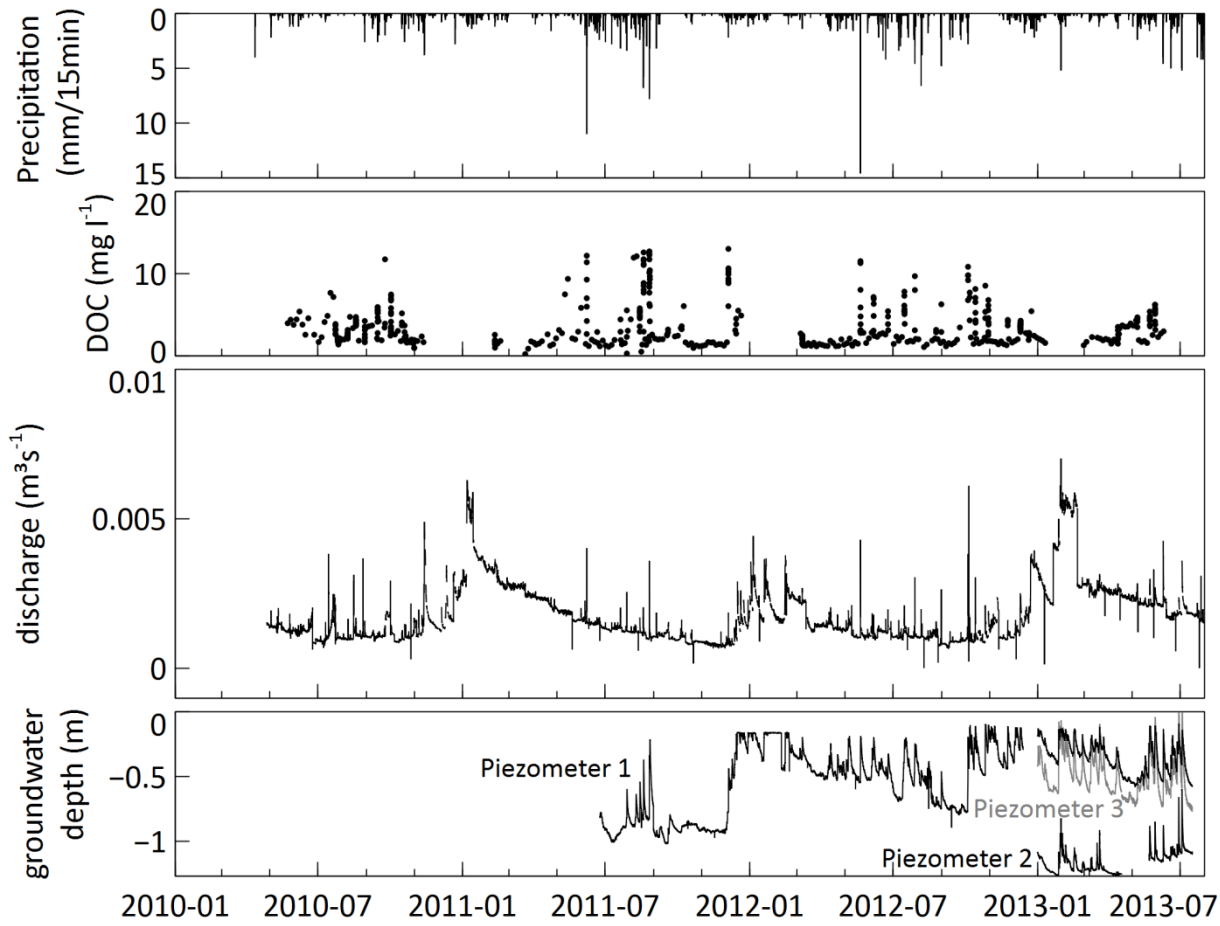

Figure 3.6. Hydrology and DOC concentrations in the stream outlet of the Blégny catchment (January 2010 - July 2013). The bottom graph shows groundwater depth measured in 3 piezometers.

3.3.2 Solute concentrations

Concentrations of DOC during baseflow conditions were highest in the forest catchments (Table 3.3). Average DOC concentrations of 9.1, 5.7, 2.4 and 2.9 mg l^{-1} were measured for Meerdaal, Ronquières, Blégny and Herve, respectively. Also SUVA values measured in the forest catchments during baseflow conditions were higher than values measured in the pasture catchment (Table 3.3). DOC concentrations measured during baseflow in the Meerdaal and Blégny catchments did not differ significantly between the seasons (data not shown). SUVA values during baseflow did differ significantly ($p<0.05$ for Blégny, $p<0.001$ for Meerdaal) between the seasons, with higher SUVA values measured in summer and fall. Great variation was observed in DOC concentrations, SUVA values and cation concentrations in the stream as a response to rainfall events. The evolution of DOC concentrations and SUVA values were similar in all rain events in both catchments. For the Meerdaal catchment, also the evolution of the cation and Si concentrations was similar for different rain events whereas for the Blégny catchment, concentrations reacted differently during two distinct periods of the year: between half March and half October and between half October and half March. Therefore, one and two exemplary time series of concentrations and SUVA values during a discharge event are shown in Figure 3.5 and Figure 3.7 for the Meerdaal and Blégny catchments, respectively. During a discharge event both DOC concentrations and SUVA values increased with discharge, reached a maximum and decreased again as discharge returned to pre-event baseflow values. In Blégny, DOC

concentrations and SUVA values were highest exactly at peak discharge (Figure 3.7). In Meerdaal, the peak in discharge preceded the peak in DOC concentrations and SUVA values (Figure 3.5). This delayed response in DOC was observed for most events sampled in the Meerdaal catchment.

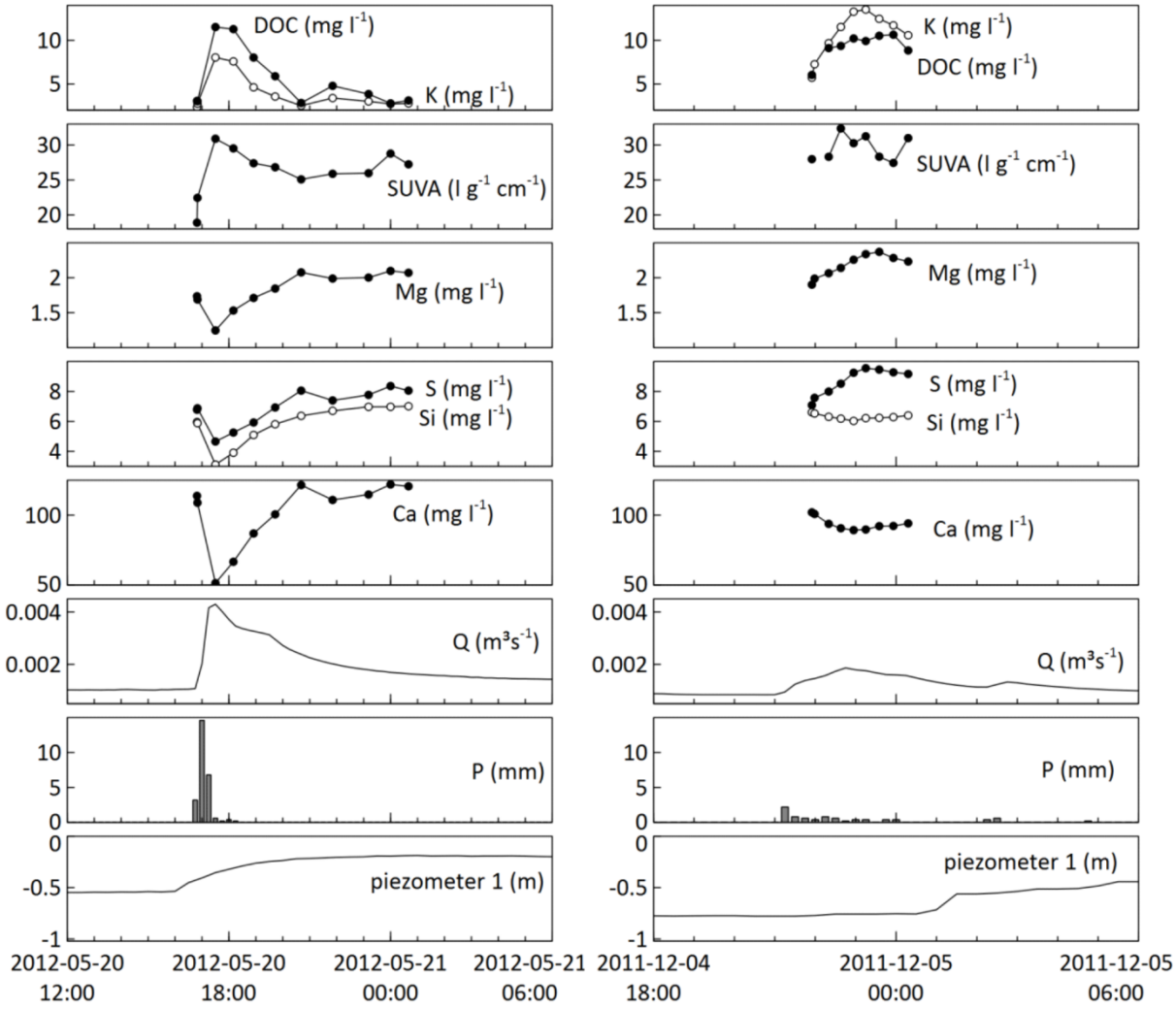

Figure 3.7. General representation of discharge, precipitation and solute concentrations measured in the stream outlet of the Blégny catchment during the spring-summer period (20/05/2012, left) and the fall-winter period (05/12/2012, right).

In the forested Meerdaal catchment, as discharge rose, concentrations of Si, Mg, Ca and S dropped and reached a minimum when discharge was at its highest point. Potassium concentrations on the other hand increased as discharge increased and concentrations peaked after the discharge peak, similar to the DOC concentrations (Figure 3.5). In Blégny, during a discharge event in the spring-summer periods (half March - half October), cation concentrations changed in the same way as in the Meerdaal catchment, with rising DOC and K concentrations and descending concentrations of Si, Mg, Ca and S. In the fall-winter periods (half October - half March), most variables reacted in the same way to rising discharge, but Mg and S showed an opposite reaction, by increasing during a rainfall event. In Blégny, minimum and maximum peak concentrations of the different solutes were reached simultaneously.

Table 3.3. Mean values and standard deviations of DOC, Si and cation concentrations measured in the stream water baseflow, soil pore water, groundwater, riparian water, seeps (Blégny only) and throughfall/precipitation samples. For stream water event samples minimum and maximum are given.

Sample	DOC (mg l^{-1})	SUVA (l g^{-1} cm^{-1})	Si (mg l^{-1})	Mg (mg l^{-1})	K (mg l^{-1})	Ca (mg l^{-1})	S (mg l^{-1})
Meerdaal (forest)							
Stream - baseflow	9.1 (2.1)	31.99 (3.01)	10.89 (1.95)	3.41 (0.39)	1.86 (0.53)	58.27 (11.06)	19.94 (5.50)
Stream - event minimum	6.2	23.75	0.19	0.74	0.88	11.75	3.59
Stream - event maximum	25.5	46.07	13.02	4.90	5.76	93.58	33.37
Soil water†	54.6 (27.7)	10.13 (7.04)	9.63 (3.27)	2.63 (2.26)	0.85 (1.81)	5.00 (5.99)	17.53 (15.43)
Groundwater -piezometer 3	3.2 (2.4)	18.18 (5.11)	12.49 (2.87)	5.59 (1.89)	0.53 (0.49)	49.43 (20.88)	16.81 (12.26)
Riparian water†	32.6 (16.4)	9.01 (6.47)	9.46 (2.39)	5.84 (2.75)	2.22 (1.72)	35.41 (15.32)	32.38 (19.20)
Throughfall	15.2 (6.5)	28.86 (8.23)	0.13 (0.10)	0.68 (0.32)	5.64 (5.30)	2.80 (1.53)	1.72 (0.88)
Blégny (pasture)							
Stream - baseflow	2.2 (1.3)	21.64 (12.16)	7.54 (0.66)	1.89 (0.14)	1.64 (0.92)	111.69 (16.72)	7.17 (1.11)
Stream - event minimum	0.9	8.04	3.11	1.15	0.77	13.41	2.57
Stream - event maximum	13.0	85.62	8.74	2.37	13.52	144.58	11.30
Soil water†	25.9 (17.9)	19.13 (8.12)	7.78 (3.77)	2.65 (2.39)	1.19 (1.83)	38.63 (28.20)	14.37 (8.88)
Groundwater‡	8.3 (7.1)	25.74 (13.43)	9.45 (2.46)	1.55 (0.28)	1.50 (1.62)	102.27 (21.82)	16.76 (7.03)
Riparian water†	28.6 (10.4)	35.10 (7.81)	7.34 (2.07)	2.66 (0.54)	9.32 (2.94)	62.23 (25.44)	17.32 (8.40)
Seepage	1.9 (1.2)	18.39 (9.28)	7.81 (1.39)	1.73 (0.14)	1.34 (0.53)	124.85 (12.46)	7.43 (1.06)
Precipitation	3.9 (0.7)	14.68 (6.45)	0.05 (0.02)	0.23 (0.11)	0.72 (0.41)	2.23 (1.28)	1.55 (1.21)
Ronquières (forest)							
Stream - baseflow	5.7 (1.8)	33.79 (15.68)	10.05 (1.02)	-	-	-	-
Stream - event minimum	5.3	15.06	0.27	-	-	-	-
Stream - event maximum	17.7	50.54	12.55				
Soil water†	-	-	11.33 (2.97)	-	-	-	-
Herve (pasture)							
Stream - baseflow	2.9 (2.4)	16.95 (6.71)	5.28 (0.54)	-	-	-	-
Stream - event minimum	0.9	5.20	1.61	-	-	-	-
Stream - event maximum	16.0	48.74	5.91				
Soil water†	-	-	3.32 (2.02)	-	-	-	-

† Mean values and standard deviations of the soil pore water and the riparian water were calculated using suction cup samples from all depths.

‡ Mean values and standard deviation of the groundwater in Blégny were calculated using samples from all 3 piezometers.

3.3.3 End-member mixing analysis

PCA analysis of DOC, Si, Mg, K, Ca and S concentrations of stream water samples in Meerdaal showed the first principal component was able to explain 72 % of the variation in the data (Table 3.4). While the stream water concentrations could thus be considered to be largely determined by just 2 end-members, we suspect a third end-member plays a vital role in understanding the transport of DOC to the surface water. As Figure 3.5 already indicated, K and DOC concentrations during an event in Meerdaal peaked simultaneously, but always a little later than the moment that the minimum was reached in other solute concentrations. This difference in timing of the solute peak concentrations cannot be explained by the mixing of just two end-members, suggesting that a third end-member contributed to the stream during an event. The fact that the second principal component (indicating a third end-member, Section 3.2.5) is mainly determined by the DOC and K concentrations (not shown) strengthens this theory. Furthermore, Clymans (2012) has put forward that for the transport of dissolved silica concentrations towards the surface water in this catchment, all 3 sources: groundwater, precipitation water and soil pore water play a role. Figure 3.8 projects the scores of baseflow and event samples of the Meerdaal catchment in their principal component space, together with the mean and standard deviation of the potential end-members at the site (Table 3.3). Concentrations in the samples from the suction cups located closest to the stream were considered to represent the riparian zone water end-member (as explained in Section 3.2.5) as concentrations of several elements measured in these suction cups differed significantly ($p<0.0001$, $\alpha=0.05$) from the concentrations measured in the other suction cups or in the groundwater. Therefore, in Figure 3.8, the riparian zone end-member was indicated separately from the soil water end-member. Concentrations in samples from piezometer 1 closely resembled those of the riparian zone water, which could be explained by the fact that this piezometer was located close to the river and had a shallow filter and groundwater table. As the suction cups close to the river also sampled at shallower depth than this piezometer, we chose to have the suction sup samples represent the riparian zone water and not to consider samples from piezometer 1 in the end-member mixing analysis. Piezometer 3 represents the groundwater end-member. Water from piezometer 2 was not considered as a potential end-member, since the groundwater level in piezometer 2 and the area around it was below the river water level. The throughfall end-member showed considerable variation in observed solute concentrations, which also came forward in the principal component scores plotted in Figure 3.8. As the observed variation in solute concentrations however was not the effect of seasonal trends, the throughfall end-member was not split into two (or more) seasonally determined throughfall end-members. Stream water samples during baseflow were mainly determined by the groundwater end-member. Event samples were spanned by the end-members groundwater, throughfall and riparian zone water. As the soil pore water end-member also plots within the space defined by the groundwater, throughfall and riparian zone water end-members, the possible contribution of this end-member to the stream water could not be determined.

Table 3.4. Percentage of variance explained by principal components.

	Meerdaal (forest)	Blégny (pasture)
PC1	72.06	45.70
PC2	15.37	26.14
PC3	5.31	12.50
PC4	4.28	8.86
PC5	2.00	4.30
PC6	0.98	2.50

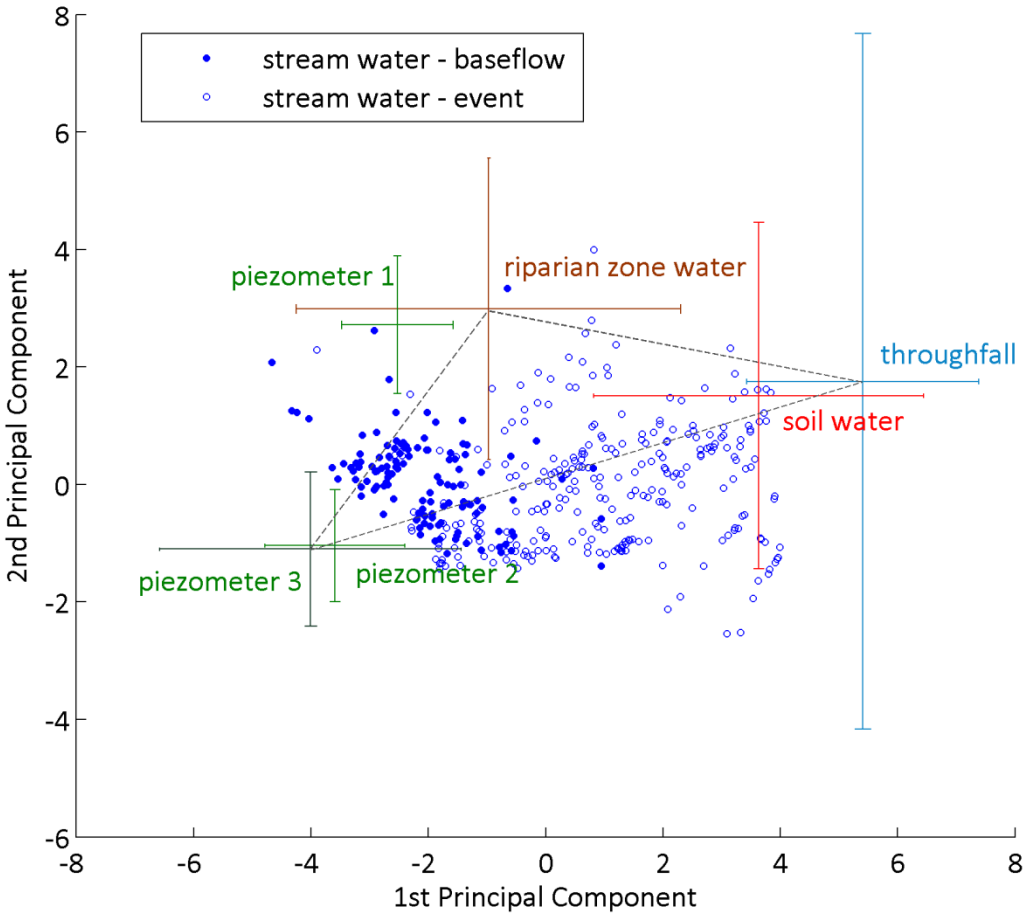

Figure 3.8. PCA results for the Meerdaal catchment. Baseflow and event stream water samples are shown with mean values and standard deviations of potential end-members.

In Blégny, two principal components were needed to explain 72 % of the variation in the stream water sample data (Table 3.4). At least 3 end-members thus determine concentrations measured in the stream. Figure 3.9 shows the baseflow and event sample scores projected in their principal component space, together with the mean and standard deviation of the potential end-members (Table 3.3). In Blégny, potential end-members were groundwater from 3 different piezometers (depicted separately), soil pore water, riparian zone water, seepage water and precipitation. Although solute concentrations measured in seepage water closely resemble concentrations measured in the stream water during baseflow conditions, the seeps were found on distinct locations high up on the hill slopes, where the groundwater table surfaces. This aided the decision to consider the seepage water as an end-member contributing to the stream water, rather than it representing secondary sampling of the stream water. During baseflow conditions, stream water samples in Blégny were mainly determined by the seepage water end-member. Event samples were determined by a mixture of seepage water, riparian zone water and precipitation.

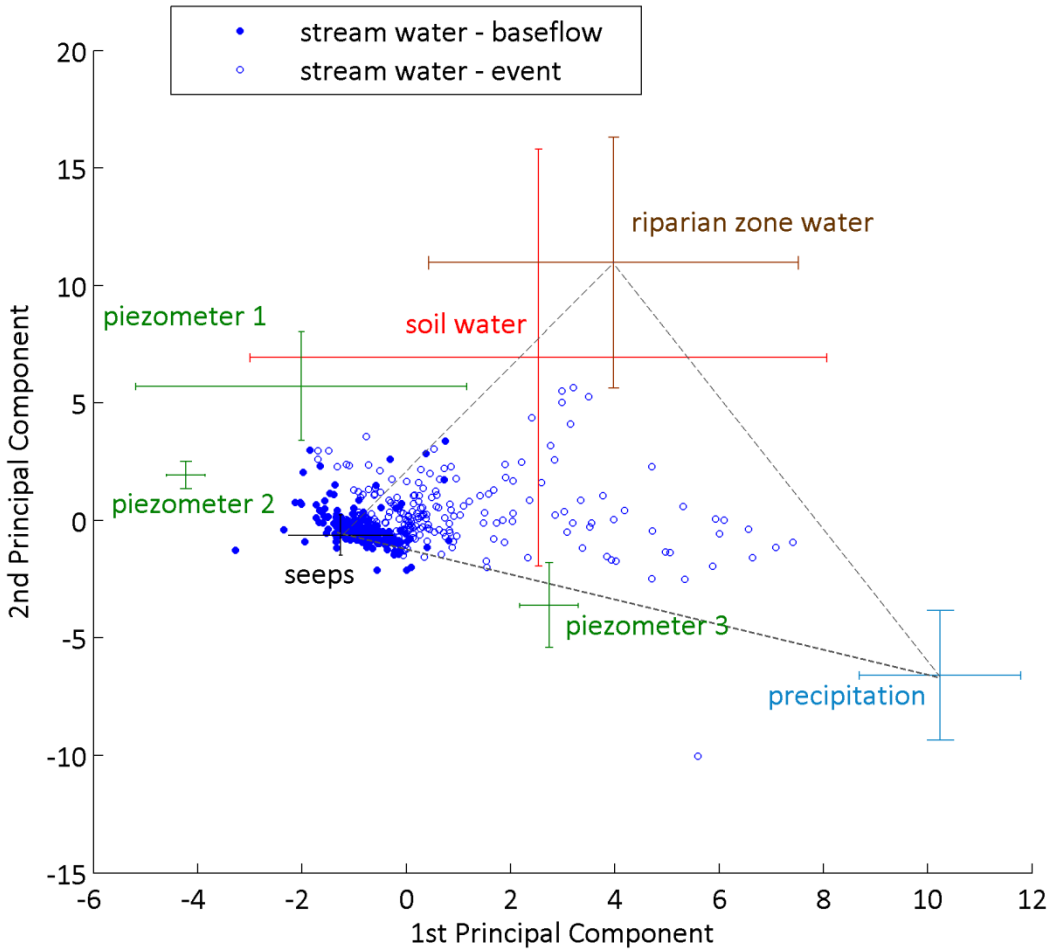

Figure 3.9. PCA results for the Blégny catchment. Baseflow and event stream water samples are shown with mean values and standard deviations of potential end-members.

Based on the results of the PCA analysis, 3 end-members that are assumed to define concentrations measured at the stream outlet were selected for each catchment. For the Meerdaal catchment, these were groundwater, riparian zone water, and throughfall. For the Blégny catchment, the seepage water, riparian zone water, and precipitation were selected. Mean concentrations of these selected end-members were used in the constrained nonlinear optimization EMMA analysis as described in Section 3.2.5, to determine the fraction in the discharge of each end-member. Table 3.5 gives the calculated discharge weighted mean fractions and their standard deviations for both the Meerdaal and the Blégny catchment. General discharge weighted mean fraction values of the contributing end-members were calculated for baseflow. For the events, discharge weighted mean fractions were calculated for each event individually. The values in Table 3.5 then are the average and standard deviation of these separate events. For the Blégny catchment, as solute patterns were different in the spring-summer periods compared to the fall-winter periods, values were calculated for each period separately.

Table 3.5. Discharge weighted mean fractions and standard deviations of contributing end-members in the Meerdaal and Blégny catchments as calculated by the EMMA. For the events, the mean and standard deviation of the discharge weighted mean values calculated per event are given.

	Discharge weighted mean fractions		
Meerdaal (forest)	Groundwater	Throughfall	Riparian zone water
Baseflow	0.63 (0.54)	0.27 (0.42)	0.10 (0.16)
Events	0.35 (0.22)	0.50 (0.18)	0.15 (0.02)
Blégny (pasture)	Seepage water	Precipitation	Riparian zone water
Baseflow	0.92 (0.39)	0.03 (0.05)	0.04 (0.06)
Spring-summer events	0.74 (0.16)	0.14 (0.10)	0.12 (0.07)
Fall-winter events	0.81 (0.16)	0.06 (0.05)	0.13 (0.12)

In the Meerdaal catchment, the groundwater was the main contributor during baseflow, delivering almost 65 % of the water to the stream (Table 3.5). The estimated contributions of the other end-members during baseflow were most likely the effect of over-fitting due to the variance in the end-member concentrations. During an average rainfall event, the fraction of the groundwater end-member diminished compared to baseflow conditions. As the largest contribution of water to the stream originated from the throughfall end-member, the timing of the maximum contribution of this end-member coincided with the maximum in peak discharge. The fraction of water originating from the riparian zone during an average event was only 15 %. In more than 85 % of the events, the maximum contribution of the riparian zone water occurred only after the peak in discharge. No difference in importance of contributing end-members was observed over the seasons.

In the Blégny catchment, water originating from the seeps located on the hillslope was year round the dominant source of water delivered to the stream water. During baseflow conditions, up to 100 % of the water came from this end-member. During rainfall events, the fraction of water from the seeps diminished, however it remained the main contributor of water to the stream, with 74 % and 81 % during an average spring-summer and fall-winter event, respectively. In the spring-summer period, almost equal fractions came from the precipitation water and the riparian zone water end-member during an event. During a fall-winter event however, riparian zone soil water contributed on average double as much water to the stream as the precipitation. No difference in time was observed between the peak in the different end-member fractions and the peak in discharge during the individual events. The contribution of water originating from the different end-members, is shown in Figure 3.10 and Figure 3.11 for the same representative rainfall events as discussed earlier in Meerdaal and Blégny.

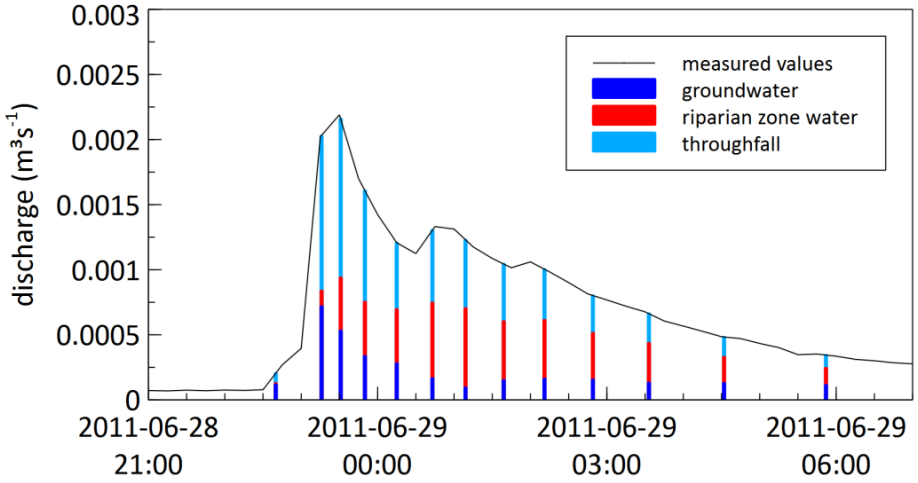

Figure 3.10. Estimated contributions based on the EMMA of the different end-members at sample time during the event on 29/06/2011 in the Meerdaal catchment. The full line shows the measured discharge data (recorded every 15 minutes). Estimated fractions were multiplied with the measured discharge to be able to show them on the discharge axis.

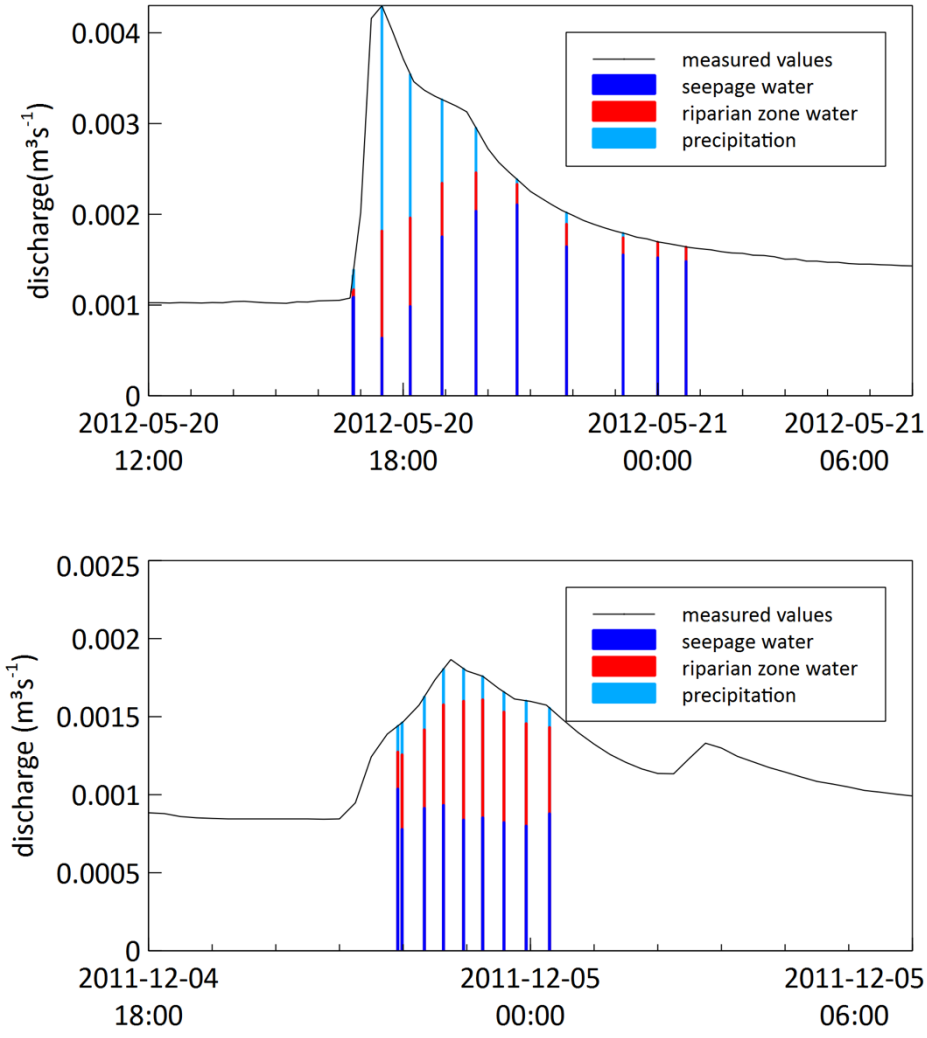

Figure 3.11. Estimated contributions based on the EMMA of the different end-members at sample time during the events on 20/05/2012 (top) and 05/12/2012 (bottom) in the Blégny catchment. The full line shows the measured discharge data

(recorded every 15 minutes). Estimated fractions were multiplied with the measured discharge to be able to show them on the discharge axis.

The coefficients of determination (R^2) and Pearson's linear correlation coefficients of measured concentrations in the stream and concentrations predicted by the EMMA are given in Table 3.6. For the Meerdaal catchment, concentrations of Si, DOC and S were predicted well. Concentrations of Mg and K were consistently overestimated, while predicted concentrations of Ca were consistently lower than measured concentrations. The Pearson linear correlation coefficient values however were high for all solutes. SUVA values could not be predicted well. For the Blégny catchment, concentrations of Si, DOC and Ca were predicted very well, while R^2 for SUVA, Mg, K and S were somewhat lower. High Pearson correlation coefficients were found for all solutes in the Blégny catchment.

Table 3.6. Coefficients of determination (R^2) and Pearson correlation coefficient (P_{corr}) of measured and predicted concentrations based on the EMMA.

	Meerdaal (forest) (n†=400)		Blégny (pasture) (n†=421)	
	R^2	P_{corr}	R^2	P_{corr}
DOC	0.82	0.95 ***	0.70	0.85 ***
SUVA	-7.72	-0.35 ***	0.27	0.55 ***
Si	0.67	0.88 ***	0.54	0.77 ***
Mg	-0.75	0.94 ***	0.20	0.89 ***
K	-0.24	0.68 ***	0.33	0.87 ***
Ca	0.16	0.91 ***	0.57	0.76 ***
S	0.43	0.86 ***	0.19	0.68 ***

† number of samples used in the analysis

***significant at the 0.001 level

3.3.4 DOC loads and fluxes

Combining the discharge weighted mean fractions of the contributing end-members in the Meerdaal and the Blégny catchment as calculated by the end-member mixing analysis (Table 3.5) with observed DOC values in the field (Table 3.3), annual loads and fluxes of DOC reaching the stream via the different transport pathways during dry weather conditions and during peak discharges were calculated (Table 3.7 and Table 3.8). The total annual load of DOC in the forested Meerdaal catchment was 68.95 kg $year^{-1}$. Thereof, 30 % reached the catchment outlet during baseflow conditions, whereas 70 % was transported during times that discharge was elevated in response to a rainfall event. Overall, 12 %, 52 % and 36 % of the total annual DOC originated from the groundwater, the throughfall and the riparian zone water pathways respectively.

Table 3.7. Annual DOC loads reaching the stream of the Meerdaal (forest) catchment via the different transport pathways during dry weather baseflow conditions and during peak event conditions.

	Annual DOC loads (kg $year^{-1}$)			
	Groundwater	Throughfall	Riparian zone water	Total
Baseflow	4.50	9.16	7.28	20.93
Events	3.95	26.81	17.25	48.02

Total	8.45	35.97	24.53	**68.95**

In the Blégny catchment, total annual DOC flux was calculated to be 6.79 kg ha^{-1} $year^{-1}$. In this grassland catchment, 28 % of the annual DOC flux was transported during dry weather baseflow conditions and 38 % and 34 % of the annual DOC flux was transported during spring-summer peak event conditions and fall-winter event conditions respectively. Annually, 36 % of the DOC flux originated from the seepage water, 6 % from the precipitation water and 58 % from the riparian zone water.

Table 3.8. Annual DOC fluxes reaching the stream of the Blégny (grassland) catchment via the different transport pathways during dry weather baseflow conditions and during peak event conditions.

	Annual DOC fluxes (kg ha^{-1} $year^{-1}$)			
	Seepage water	Precipitation	Riparian zone water	Total
Baseflow	1.11	0.07	0.73	1.91
Spring-summer events	0.67	0.26	1.63	2.56
Fall-winter events	9.80	0.09	1.57	2.32
Total	2.42	0.43	3.93	**6.79**

3.4 Discussion

In agreement with Grieve (1991b), average DOC concentrations observed in the streams draining our study catchments were higher in forest catchments than in grassland catchments. The greatest part (70 % in Meerdaal and 72 % in Blégny) of the total annual DOC export occurred during periods of elevated discharge caused by rainfall events. This is in agreement with Hinton et al. (1997), who found that 57-68 % of the DOC export in autumn was transported during storms and Boyer et al. (1996) who described that rain events can account for a great proportion of the total annual DOC export from soils to rivers and streams.

No seasonal variation in DOC concentrations was observed in any of our catchments. This is in contrast to what was found by McDowell and Likens (1988), Dawson et al. (2002, 2008a, 2011) and Halliday et al. (2012), but in agreement with the results of Benning et al. (2012). As was the case for the latter, DOC concentrations in our catchments appeared to be controlled by discharge dynamics rather than seasonally changing sources and production mechanisms.

Although there was a lack in seasonal variations, clear temporal changes in both DOC concentrations and quality was observed during rainfall events, which gave a first indication of the transport mechanisms of DOC present in our catchments. The peak in DOC concentration observed during peak discharge events in our four catchment is in agreement with what was reported earlier by other authors (McDowell and Likens, 1988; Hagedorn et al., 2000; Dawson et al., 2002; Kaiser and Guggenberger, 2005; Shanley et al., 2011; Halliday et al., 2012), e.g. rises in DOC concentrations during discharge events up to +350 % (Hagedorn et al., 2000) or +450 % (Boyer et al., 2000). The accompanying peak in specific UV absorbance during a rainfall event, indicating that the increase in

DOC goes along with a change in the composition of the organic matter and also reported by Hagedorn et al. (2000), gives an indication on the transport mechanisms present in the catchments. Rapid water flow through macropores during an event would likely deliver 'fresh' dissolved organic matter with lower SUVA values to the stream outlet than during matrix flow (Kaiser and Guggenberger, 2005). It is therefore unlikely that water flow through macropores is a transport mechanism playing an important role in our catchments. The elevated SUVA values in the stream at higher discharges are more probably an indication of a transport pathway intersecting a surficial layer of the soil, as SUVA values are typically high in the litter layer but decline with increasing soil depth (Jaffrain et al., 2007).

The changes in concentrations of DOC and other solutes such as Si and major cations during a rain event can be subscribed to a switch in transport pathways of water to the stream. Several authors have shown changes in solute concentrations similar to our results, with elevated DOC and K concentrations during stormflow, and decreasing concentrations of Si and cations such as Ca, Mg and Na (Holloway and Dahlgren, 2001; Shanley et al., 2011; Halliday et al., 2012). Elevated concentrations of Ca and Si during baseflow indicate the dominance of shallow groundwater (Halliday et al., 2012), while at peak storm flow, these cations and silicon concentrations typically decrease due to dilution by water originating from other pathways. High concentrations of DOC and K during a rain event likely originate from a flow pathway intersecting the upper soil layers where these solutes are concentrated by nutrient cycling (Boyer et al., 1997; Hagedorn et al., 2000; Holloway and Dahlgren, 2001; Inamdar and Mitchell, 2006). In the Blégny catchment contrasting behavior in Mg and S concentrations was found in different periods over the year, with Mg and S decreasing and reaching a minimum during spring-summer events, but increasing to a maximum during fall-winter events. The seasonal differences in these solutes behavior has to our knowledge never been reported before, but can also be explained by a difference in importance of contributing transport pathways of DOC during different periods in the year. We found that during events in the fall-winter periods, contributions of water from the riparian zone with higher Mg and S concentrations than precipitation and seepage water, were more important than during events in the spring-summer periods.

As the different transport pathways deliver water to the streams with different solute concentrations, the timing of the solutes peak during a rainfall event is linked to the importance of contributions of different transport pathways at different stages during the peak event. The peak in DOC concentrations and quality on the descending limb of the hydrograph observed in the Meerdaal catchment is in agreement with the observations by Hagedorn et al. (2000) and Inamdar and Mitchell (2006). Hagedorn et al. (2000) attributed this DOC peak only after the peak in discharge to contributions of water from DOC rich top soil layers in later stages of the storm. Similarly, during rainfall events in the Meerdaal catchment, we found the highest contribution of riparian zone water rich in DOC to occur after the peak in discharge. As in the Blégny catchment the peak in DOC concentrations and quality during a rainfall event coincided with the discharge peak, the finding of Inamdar and Mitchell (2006), namely that the DOC peak is more delayed after maximum discharge in bigger than in smaller catchments, is supported. They attributed this to a greater number of discrete saturated areas as the catchment area increases, which form untapped 'reserves' of DOC that become mobilized as moisture conditions increase during a rainfall event.

An EMMA analysis allowed the identification of the end-members contributing DOC to the stream water and the quantification of their contribution during rainfall events. In agreement with results

from EMMA carried out in other catchments using electrical conductivity (EC), Ca^{2+}, SO_4^{2+} and Cl^- (Hagedorn et al., 2000) or Mg^{2+}, Si, and DOC (Inamdar and Mitchell, 2006), the greatest contributions of water to the stream during baseflow conditions in the Blégny and the Meerdaal catchment came from the groundwater or shallow groundwater discharged at seeps. Contributions of the throughfall end-member caused dilution of Si and cation concentrations in the stream especially in the early part of the event, which supports the findings by Hagedorn et al. (2000) and Inamdar and Mitchell (2006). Rather than only accounting for the throughfall directly intercepted by the river, this end-member here likely represents a transport pathway through the organic rich top soil layers that we did not sample in the field, as was the case in the work of Shanley et al. (2011). It delivers water to the stream that has had only limited contact with the soil, and thus is poor in cation concentrations. In agreement with Boyer et al. (1997) and Hagedorn et al. (2000), the peak in DOC and K concentrations observed during rainfall event in our catchments, was mainly caused by water flow from the riparian zones, rich in organic matter.

This study additionally shows that the importance of contributions from the riparian zone can differ seasonally. In the fall-winter period in Blégny, as groundwater tables are high and soils are (almost) completely saturated, water originating from the riparian zone was the main cause of changing solute concentrations during peak events, which is in contrast with the more equal contributions of throughfall and riparian or subsoil water reported by others (Hagedorn et al., 2000; Inamdar and Mitchell, 2006), and observed during spring-summer periods. We attribute the larger contributions of riparian zone water to increased volumes of water stored in the soil around the river, and thus a larger saturated riparian zone. However, although different end-members were thus responsible for the delivery of DOC to the stream in the different seasons, the DOC concentration pattern observed during peak flow was identical.

Due to the large variation in concentrations of some of the end-members in our catchment, the end-member analysis was not able to predict the exact concentrations of all solutes well, although we were able to predict the rising or decreasing patterns observed during the rain events, as well as the timing of minimum/maximum concentrations of all solutes. The high Pearson correlation coefficients reported for all solutes in our catchments, indicate the dynamics of all solutes concentrations were predicted well and the contributing source end-members in our catchment were selected correctly. The low coefficient of determination for some of the solutes in our catchments is likely due the large variation in concentrations of some of the end-members. However, not even the highest end-member concentrations measured were able to predict the high Ca concentrations measured in the stream of the Meerdaal catchment during rainfall events. This likely indicates that the Ca concentration of at least one of the sampled end-members we selected in Meerdaal was underestimated. Neither SUVA values at the Meerdaal catchment outlet could be predicted as a weighted combination of SUVA values from the different end-members, which could be due to in-stream processes such as stream channel expansion at increasing discharge or throughfall directly onto the stream. Verheyen et al. (2015) also suggested that the microbial breakdown of vegetative material falling into the stream might contribute to solute concentrations measured in the stream of the Meerdaal catchment.

The greatest part (52 %) of the total annual export of DOC from the Meerdaal catchment originated from the throughfall end-member that represents a transport pathway through the organic rich top soil layers. This pathway delivers the greatest contributions of water to the stream during rainfall

events. 36 % of the total DOC export in the Meerdaal catchment originated from the riparian zone, whereas only 12 % was transported to the stream via groundwater flow. This shows that although groundwater flow year round delivers vast quantities of water to the catchment outlet, in terms of DOC loads it contributes the least to the annual DOC export in the Meerdaal catchment. In the Blégny grassland catchment, although water originating from the seeps on the hillslope was year round the dominant source of water delivered to the stream, this pathway only accounts for 36 % of the total annual DOC flux. Not more than 6 % of the total annual flux was transported via precipitation water. The main contributions (58 %) to the total annual DOC flux originated from the riparian zone that only delivers 4 % of the water to the catchment outlet during baseflow conditions, and 12 to 13 % during event conditions. Overall, this indicates that at the catchment scale, a transport pathway that has only limited contributions to the total annual water flux, can be responsible for the greatest part of the total annual DOC flux.

3.5 Conclusion

Using an end-member mixing analysis we were able to identify the contributing pathways for the transport of DOC from the soil to the surface water during different flow regimes in catchments differing both in land use. During baseflow conditions, the greatest contributions of water to the stream in the Blégny and the Meerdaal catchment came from the groundwater or shallow groundwater discharged at seeps. The rise in DOC concentrations measured in the streams during rainfall events, that was accompanied by a rise in SUVA values, could be accounted for by additional contributions of water from the riparian zone and from the precipitation/throughfall end-member that represents a transport pathway through the organic rich top soil layer. Our study showed that the importance of the contributing transport pathways for the transport of DOC from the watershed to the surface water is dependent on the hydrogeological setting of the catchment. In a grassland catchment with shallow groundwater tables (Blégny) we proved that the importance of contributing transport pathways can change seasonally. In fall and winter, when increased volumes of water are stored in the soil around the river, contributions of the riparian zone water to the stream are greater than in spring and summer.

Chapter 4. Modeling the export of dissolved organic carbon from a pasture catchment

4.1 Introduction

Dissolved organic carbon (DOC) present in stream waters is an important agent in the aquatic system, as it provides energy and nutrients to biota. Due to its high mobility and reactivity (Neff and Asner, 2001), it plays a role in the cycling and distribution of carbon both within and between ecosystems (Kaiser and Kalbitz, 2012) and is thus highly relevant for the global carbon cycle (Jardine et al., 2006). DOC has an effect on stream water pH and light penetration (Morris et al., 1995), and due to its complexation capacity, it can affect the solubility, toxicity and transport properties of heavy metals and organic contaminants (Tipping, 1993; Kalbitz et al., 2000). Surface water DOC also has implications for drinking water production, as it can lead to the formation of carcinogenic disinfection by-products such as trihalomethanes and haloacetic acids (Liang and Singer, 2003).

DOC concentrations measured in the stream water of headwater catchments have been reported to show considerable temporal variation, on multiple time scales. Across dry weather baseflow conditions, seasonal variation in DOC concentrations has been observed, typically with minima in spring and peaks in fall (Dawson et al., 2002, 2008a, 2011; Halliday et al., 2012) which can be attributed to rewetting of the catchment after a period of high biological activity in the summer (Halliday et al., 2012). Greater variation in DOC concentration occurs during periods of elevated discharge caused by rain events or snowmelt. DOC concentrations increase and reach a maximum during peak events compared to baseflow concentrations (Mcdowell and Likens, 1988; Boyer et al., 2000; Hagedorn et al., 2000; Dawson et al., 2002; Kaiser and Guggenberger, 2005; Shanley et al., 2011; Halliday et al., 2012; Chapter 3). Likewise, quality measures of DOC such as UV absorptivity vary considerably during rain events (Hagedorn et al., 2000).

Several authors have linked the varying DOC concentrations to stream discharge, reporting a positive relationship between DOC concentrations measured in the stream and discharge (Lewis and Grant, 1979; Dawson et al., 2002, 2011; McGlynn and McDonnell, 2003), although the relationships might differ seasonally (Dawson et al., 2002, 2008a). Moreover, it has been shown that the temporal variation in DOC concentration and quality measured at the catchment outlet during periods of elevated discharge can be explained by changes in hydrologic flow paths (Boyer et al., 1997; Hagedorn et al., 2000; Inamdar and Mitchell, 2006; Chapter 3). Low, relatively constant DOC concentrations measured during baseflow conditions typically indicate the dominance of groundwater flow (Hornberger et al., 1994). The high DOC concentrations measured in the stream during peak events can be attributed to increased contributions of near-surface pathways interacting with organic carbon-rich surficial soil layers, which is often described as “flushing” (Boyer et al., 1997; Hagedorn et al., 2000; Inamdar and Mitchell, 2006).

The coupling between discharge and stream DOC concentrations has previously been formalized into mathematical expressions (Grieve, 1991a; Hornberger et al., 1994; Boyer et al., 1996; Futter et al., 2007; Xu et al., 2012) although attempts to model the DOC export at the watershed scale remain rather scarce. Moreover, few of these modeling attempts have been tested against data collected

during event conditions. The INCA-C model of Ledesma et al. (2012) and the landscape model of Futter et al. (2007) proved capable of reproducing seasonal and interannual variations in DOC concentrations, but did not consider (Ledesma et al., 2012) or highly underestimated (Futter et al., 2007) stream DOC concentrations during peak discharges. Boyer et al. (1996) obtained a good agreement between modeled and measured weekly DOC concentrations during springmelt, by first simulating the hydrological response of a catchment using TOPMODEL, and afterwards routing the predicted flows through a simple DOC model. More recently, Xu et al. (2012) presented a model capable of reproducing hourly variations of stream DOC concentrations in a forested catchment. This was achieved by linking parametrically simple soil water carbon formulations to temporal changes in catchment water storage obtained from a rainfall-runoff formulation based on the catchment model of Kirchner (2009).

In this study, we investigated whether the hydrological modeling of the discharge in a catchment, yielding fluxes of water reaching the catchment outlet via different transport pathways, can lead to an adequate description of the DOC concentrations measured at the catchment outlet during different flow regimes. Two different hydrological modeling approaches were followed, whereby the first consisted of a hydrological model that splits discharge into different flow components based on the water stored in different conceptual compartments of the hydrological catchment. The parameters of this conceptual model were derived in a calibration procedure using observed discharge data. As the simulation of discharge using this conceptual hydrological model proved to be unsatisfactory, a second hydrological modeling approach was followed, whereby total flow was split into different flow components based on a time series analysis of the observed discharge. We hypothesized that the combination of (1) modeled fluxes of water reaching the catchment outlet via different transport pathways and (2) mean DOC concentrations measured in the different transport pathways, allows the prediction of DOC concentrations both during baseflow and peak event conditions.

4.2 Materials and methods

4.2.1 Study area

The Blégny catchment is located in central east Belgium (50° 40' 22.3386" N, 5° 45' 52.2576" E) and has a mean elevation of 254 m above sea level. Based on a digital terrain model analysis the area of the catchment was determined to be 0.339 km^2 (Figure 4.1). The catchment is under pasture, and regular harvesting of the grasses (*Poaceae* family) is alternated with periods of cattle grazing. The area has a temperate climate with a long-term mean annual precipitation of 820 mm and a mean temperature of 3.1 °C in January and 17.7 °C in July. Precipitation is distributed equally over the year, although intensity and duration of rainfall events vary with the season. Shorter, more intensive storms occur mainly in spring and summer, whereas longer, less intensive rainfall events occur in fall and winter.

The study catchment has a rolling topography, with slopes up to 25 %. Soils have a silty loam texture and have developed in the residual clay with chert nodules that is left after dissolution of the Gulpen chalk. Clay lenses that are found throughout the whole soil profile strongly limit the drainage in the

catchment. The groundwater table follows the topography of the catchment and can be found at maximum a few meters depth (Ruthy and Dassargues, 2008). The unsaturated zone in the catchment is very thin, and in winter becomes close to or completely saturated. Seeps are found at several locations where the groundwater table intersects the soil surface (Figure 4.1).

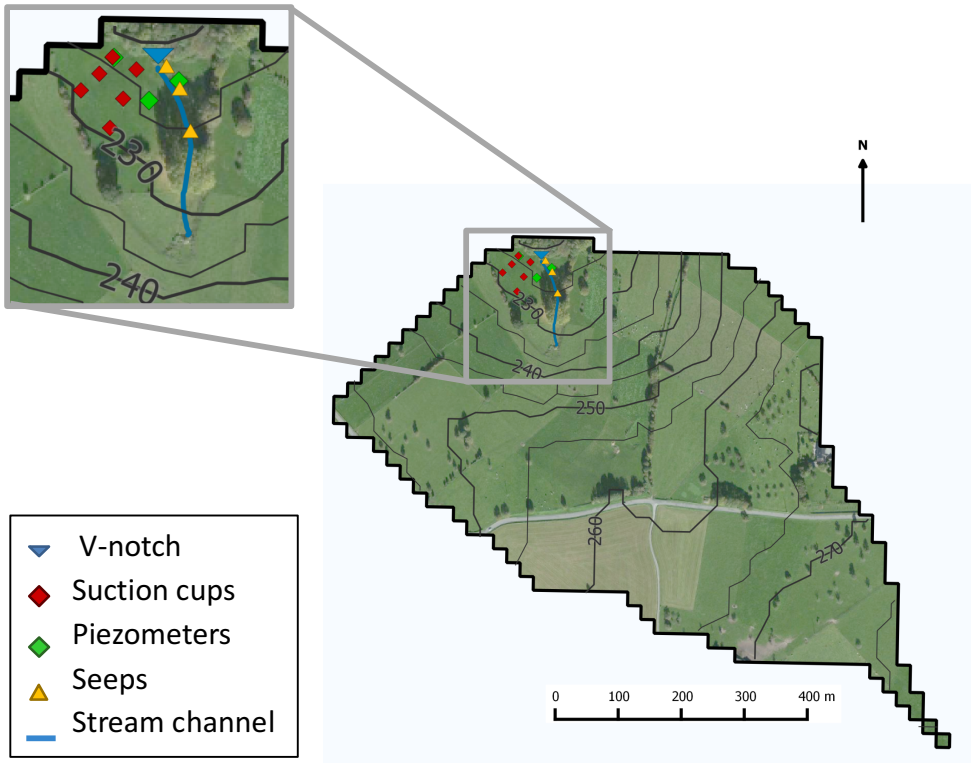

Figure 4.1. The Blégny catchment with indication of the position of the V-notch, suction cups transects, piezometers and seeps, and elevation contour lines (m above sea level).

4.2.2 Experimental set-up

The Blégny catchment was monitored starting from April 2010 until December 2013. A V-notch weir with an angle of 45° was installed at the catchment outlet. Records of water height (m) were collected every 15 minutes using a flow module (ISCO 720 submerged probe module, Teledyne ISCO Inc., Lincoln NE, USA) that was connected to an automatic data logger (ISCO 6712, Teledyne ISCO Inc., Lincoln NE, USA). Discharge (m^3s^{-1}) was calculated from the water height measurements which were transmitted via telemetry or read out at the site location every two weeks. A tipping bucket rain gauge present at the site yielded rainfall amount data at 15 minute time intervals.

Potential evapotranspiration (FAO Penman-Monteith) and temperature data at 15 minute intervals for the period between April 2008 and December 2013 were collected from the meteorological station of the Flanders Environment Agency (VMM) in Niel-bij-Sint-Truiden, which is located 45km from the study catchment. This station also provided precipitation data between April 2008 and April 2010. The first two years of available meteorological data (April 2008 - April 2010), when discharge in the Blégny catchment was not yet monitored, were used as a warming-up period for the hydrological model.

4.2.3 Sample collection and analysis

Samples of river water during dry weather conditions were collected automatically at regular intervals (twice a week) by the ISCO sampler. Additionally, whenever the water level rose above a set threshold, a maximum of 15 event river water samples was collected proportionally to the discharge. This event threshold level was adjusted manually depending on the season. To distinguish the different sampling conditions the terms 'baseflow' and 'event' are used throughout this chapter. Thereby stream flow observed during dry weather conditions is referred to as baseflow, while all stream flow observed during rainfall events is referred to as event flow. Samples were stored in polyethylene terephthalate (PET) bottles inside the ISCO sampler and collected as soon as the sampler was full or within maximum two weeks.

For the collection of soil pore water, suction cups (polyamide, Soilmoisture Equipment Corp., Goleta CA, USA) were installed along two parallel transects perpendicular to the river channel. Along each transect, suction cups were placed at different depths (30, 60 and 90 cm) at three locations (Figure 4.1). The suction cups were allowed to equilibrate with the environment for several months before sample collection started. Samples were taken once a month by applying a continuous suction of ca. 500hPa one month before the sample collection using a vacuum pump (Eijkelkamp, Giesbeek, The Netherland). Samples collected in the suction cups located closest to the river (<10 m) were considered to represent the riparian zone soil pore water.

Three piezometers (Figure 4.1) were installed in the catchment, in which groundwater depth was monitored every 30 minutes starting from 2011. Groundwater samples were collected monthly using a peristaltic pump.

Several seeps on one of the river banks (Figure 4.1) were found to deliver water to the stream year round. Therefore, also monthly grab samples were collected from three locations starting from 2011.

In 2013, a precipitation collector was installed for the collection of composite (2 week) precipitation samples. It consisted of a funnel (diameter 14 cm) attached to a PET bottle. A wire mesh on top of the funnel prevented contamination.

All samples of river water, suction cup water, groundwater, seepage water and precipitation water were stored at 4 °C prior to analysis. Subsamples were filtered upon arrival in the lab with a 0.45 µm CHROMAFIL® PET filter (Macherey-Nagel GmbH & Co., Düren, Germany) (pre-rinsed with 20 ml of demineralized water). They were analyzed within 6 weeks for dissolved organic carbon concentrations ([DOC], mg l^{-1}) using a Multi N/C® 2100 (Analytik Jena AG, Jena, Germany).

4.2.4 Modeling of catchment hydrology

4.2.4.1 FLEX hydrological model

The hydrological model used to simulate discharge at the Blégny catchment outlet was the FLEX (Flux Exchange) model, described by Fenicia et al. (2006) and further expanded and tested by Fenicia et al. (2008, 2011) and Kavetski and Fenicia (2011). It is a lumped conceptual model that requires input time series of precipitation, potential evapotranspiration and temperature for the simulation of streamflow discharge. The Flux Exchange model has a flexible model structure, allowing the optimal model configuration to be derived iteratively during the calibration process (Fenicia et al., 2006). For the Blégny catchment, the model configuration was initially based on the catchment functioning as

observed in Chapter 3. The optimal model configuration was then derived during a preliminary calibration run using only the first three years of collected data. The optimal model configuration for the study catchment is composed of several interconnected boxes that represent different zones of catchment response (Figure 4.2): a riparian zone reservoir which conceptualizes the contribution of the zone close to the stream with little storage capacity, an unsaturated soil reservoir which represents the storage capacity of the soil, a fast reacting reservoir accounting for the formation of fast runoff components and a slow reacting reservoir representing the slow runoff components such as groundwater flow. The modeled streamflow consequently is a combination of water from the fast flow component, the slow flow component and the riparian component. For other catchments, different configurations of the FLEX model might prove to be more suitable, including less or more reservoirs (e.g. an interception reservoir) (Fenicia et al., 2006, 2008 and Kavetski and Fenicia, 2011). The state and flux equations of the FLEX model configuration used for the Blégny catchment and the definition of the 9 different model parameters are given in Table 4.1 and Table 4.2. Parameter ranges were defined prior to the calibration (Table 4.2). The differential equations of the FLEX model were solved using a fixed time step (1h) implicit Euler scheme.

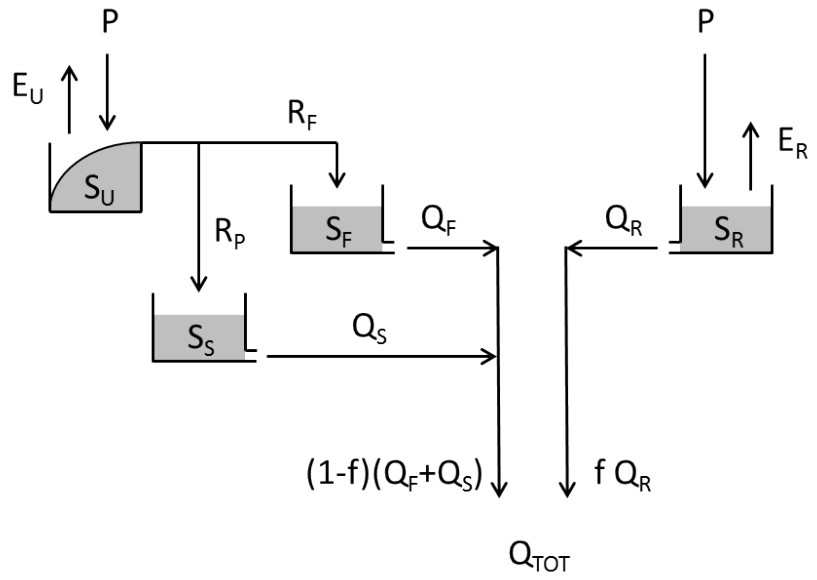

Figure 4.2. Structure of the hydrological model. Symbols are explained in detail in Table 4.2.

Table 4.1. State and flux equations of the FLEX hydrological model.

Process	Water balance	Constitutive relationships
Unsaturated zone	$\frac{dS_U}{dt} = P - E_U - R_F - R_P$	$E_U = E_p \min\left(1, \frac{S_U}{S_{U\max}} \frac{1}{L_P}\right)$ $R_F = C_R(1-D)P$ $R_P = C_R DP$ $C_R = \frac{1}{\left(1+\exp\left(\frac{-S_U/S_{U\max}+\lambda}{\beta}\right)\right)}$
Fast reservoir	$\frac{dS_F}{dt} = R_F - Q_F$	$Q_F = k_F S_F$
Slow reservoir	$\frac{dS_S}{dt} = R_P - Q_S$	$Q_S = k_S S_S$
Riparian reservoir	$\frac{dS_R}{dt} = P - Q_R - E_R$	$Q_R = k_R S_R$ $E_R = \min\left(E_p, \frac{S_R}{\Delta t}\right)$
Total flow		$Q_{tot} = (1-f)(Q_F + Q_S) + fQ_R$ $E_{tot} = (1-f)E_U + fE_R$

Table 4.2. States, fluxes and model parameters of the FLEX hydrological model. For the model parameters, calibration ranges are indicated.

Symbol	Unit	Definition	Calibration ranges
States			
S_U	mm	Storage in unsaturated reservoir at time t	
S_F	mm	Storage in fast responding component at time t	
S_S	mm	Storage in slow responding component at time t	
S_R	mm	Storage in riparian/wetland component at time t	
Fluxes			
P	mm	Precipitation at time t	
E_p	mm	Potential evapotranspiration at time t	
E_U	mm	Actual evapotranspiration from S_U at time t	
E_R	mm	Actual evapotranspiration from S_R at time t	
R_F	mm	Recharge to fast responding reservoir at time t	
R_P	mm	Recharge to slow responding reservoir at time t	
C_R	-	Runoff coefficient, i.e. proportion of water that cannot be stored in S_U and that recharges S_F and S_S at time t	
Q_F	mm	Flow from S_F at time t	
Q_S	mm	Flow from S_S at time t	
Q_R	mm	Flow from S_R at time t	
Q_{tot}	mm	Total runoff at time t	
E_{tot}	mm	Total actual evapotranspiration at time t	
Model parameters			
S_{Umax}	mm	Maximum storage capacity in unsaturated zone (root zone)	10 - 800
L_P	-	Relative soil moisture below which evapotranspiration is moisture constrained	10^{-10} - 0.75
D	-	Proportion of water that recharges S_S	0.3 - 1
λ	-	Shape parameter	0 - 1
β	-	Shape parameter	10^{-10} - 65
k_F	h^{-1}	Storage coefficient of S_F	0.001 - 0.025
k_S	h^{-1}	Storage coefficient of S_S	0.0001 - 0.004
k_R	h^{-1}	Storage coefficient of S_R	0.01 - 0.25
f	-	Proportion of catchment covered by riparian zone/wetland	0 - 0.1

For the calibration of the hydrological model, the 15 min meteorological and stream discharge data were aggregated to hourly sums. The first two years of available meteorological data (April 2008 - April 2010), for which no discharge data were available, were used as a warming-up period for the hydrological model to reduce sensitivity to predefined initial storage values. The data between April 2010 and November 2011 were used in a calibration procedure for the estimation of the posterior parameter distribution. Within the calibration period, discharge data corresponding to water levels above 15 cm were omitted, as these represent stream water flow above the maximum height of the V-notch. In the last two years of the observation period (December 2011 – December 2013), considerable amounts of snowfall were observed in the Blégny catchment. As snowfall and subsequent snowmelt can highly alter the hydrological response of the catchment in winter and spring and these processes were not included in the model configuration, the discharge data measured during this period were not used for the calibration of the hydrological model.

The calibration of the model parameter values was done using the Differential Evolution Adaptive Metropolis (DREAM) algorithm (Vrugt et al., 2008a). The DREAM approach is an adaptation of the Shuffled Complex Evolution Metropolis global optimization algorithm (Vrugt et al., 2003) and uses a Markov Chain Monte Carlo (MCMC) sampling scheme to estimate the posterior probability density function of the model parameters. It has the advantage of maintaining detailed balance and ergodicity while showing good efficiency in complex, high-dimension sampling problems (Vrugt et al., 2008b, 2009). The objective function that was minimized to infer the model parameter set with the highest likelihood and the posterior probability density function of the model parameters, was the sum of squared residuals (Eq. 4.1):

$$SSR = \sum \left(Q_{obs} - Q_{mod}\right)^2 \tag{4.1}$$

whereby Q_{obs} and Q_{mod} are the observed and modeled discharge data respectively. The sum of squared residuals gives the same weight to the error on different portions of the hydrograph. However, as errors related to high flows tend to be larger than errors related to low flows, using the sum of squared residuals as the objective function emphasizes the simulation of high flows.

The Gelman-Rubin convergence statistic (Gelman and Rubin, 2007), which compares the variance within and between the parameter chains, was monitored to check whether the DREAM algorithm converged to the stationary posterior parameter distribution.

To assess the match between measured discharge data and discharge data modeled using the parameter set with the highest likelihood, the coefficient of determination (R^2) (Eq. 4.2) and the Pearson's linear correlation coefficient (P_{corr}) (Eq. 4.3) were calculated. The former provides information about the goodness-of-fit of the regression. The latter gives the degree of correlation between the measured and the modeled values.

$$R^2 = 1 - \frac{\sum \left(x_i - y_i\right)^2}{\sum \left(x_i - \bar{x}\right)^2} \tag{4.2}$$

$$P_{corr} = \frac{\sum \left(x_i - \bar{x}\right)\left(y_i - \bar{y}\right)}{\sqrt{\sum \left(x_i - \bar{x}\right)^2 \sum \left(y_i - \bar{y}\right)^2}} \tag{4.3}$$

where x_i and y_i are respectively the measured and the modeled values, and $\bar{x}$ and $\bar{y}$ are the mean of the measured and the modeled values.

To calculate the uncertainty bounds of the model simulation due to parameter uncertainty, 2000 discharge time series were obtained by running the model with 2000 parameter sets drawn from the posterior parameter distribution. The 95 % confidence intervals due to parameter uncertainty were then estimated by sorting those discharge samples at each time step.

4.2.4.2 WETSPRO hydrological model

The river discharge series measured at the Blégny catchment outlet was additionally separated into its hydrological components using the WETSPRO tool (Water Engineering Time Series PROcessing tool) following the method described by Willems (2009). The WETSPRO tool is a Microsoft Excel-based filter that splits a measured river flow series into quick flow and slow flow components, after

which the quick flow component might be further split up in a quickest flow component (most often related to surface runoff processes) and an interflow component (drainage flow, subsurface flow, macropore flow, seepage flow). The slow flow component in most cases consists of the groundwater runoff.

For each subflow component (slow flow, interflow, quick flow), the WETSPRO tool calibrates two parameters based on visual inspection of the discharge time series: a recession constant k and a parameter w that represents the average fraction of the subflow volume over the total flow volumes. The separation of total flow into the different subflows is carried out in a step-wise way. The slow flow component is first split from the total flow. In a second step the interflow is separated from the remaining flow, after which the rest fraction represents the quickest flow component. The recession constant or recession time k for each subflow can be quantified as the average value of the inverse of the slope of the linear path in the subflow recession periods of a ln(q) – time graph. By visually inspecting this slope for a number of recession periods, an average value for the recession constant can be estimated. Next, the parameter w can be calibrated by optimizing the height of the subflow during the recession periods (Willems, 2009).

4.2.5 Modeling of DOC concentrations

Both the FLEX hydrological model and the WETSPRO subflow filter split up total flow into several subflow components. The modeled flows from these different components were in turn used to predict the stream water DOC concentration at the catchment outlet as a simple mixture of DOC in waters from the different components (Eq. 4.4):

$$[DOC]_{tot} = \frac{Q_1[DOC]_1 + Q_2[DOC]_2 + Q_3[DOC]_3}{Q_{tot}} \quad (4.4)$$

whereby Q_{TOT} is the total predicted discharge and Q_1, Q_2 and Q_3 are the predicted discharges from the different components. For the results of the FLEX model, these are the slow responding component, the fast responding component and the riparian component. For the results of the WETSPRO model, these are the slow flow, the interflow and the quick flow. $[DOC]_{TOT}$ is the total modeled stream DOC concentration at the catchment outlet and $[DOC]_1$, $[DOC]_2$ and $[DOC]_3$ are the DOC concentrations in the water from the respective hydrological components. Taking the results of Chapter 3 into account, DOC concentrations of the different hydrological components were based on the average concentrations measured in the seeps, the riparian zone samples and the precipitation samples collected at the field. For the simple mixing equation to be applicable, DOC concentrations in the different components were assumed (1) to be constant in time and space, and (2) to mix conservatively. Although we recognize the non-conservative nature of DOC, DOC has previously successfully been used in similar mixing analyses to distinguish flow pathways (McGlynn and McDonnell, 2003; Inamdar and Mitchell, 2006; Chapter 3).

As discharge contributions from the different components were simulated at hourly time steps, DOC concentrations were predicted hourly. Modeled DOC concentrations at hourly time steps were then linearly interpolated to obtain values at the exact measuring times.

4.3 Results

4.3.1 Rainfall-runoff characteristics

During the monitoring period (April 2010 – December 2013), the Blégny catchment received a total precipitation of 2418 mm. Total potential evapotranspiration calculated based on data from the nearby meteorological station was 2106 mm and the total discharge monitored at the catchment outlet equaled 512 mm.

During the years of monitoring, dry weather baseflow discharge varied greatly over the seasons (Figure 4.3). Baseflow yearly reached a minimum as low as $6*10^{-4}$ m^3s^{-1} around November, after which it increased in December and reached maximum values greater than $4*10^{-3}$ m^3s^{-1} in January-February. Over the next months the baseflow discharge decreased again, until a minimum was reached in November and the cycle was repeated. For the entire monitoring period, the runoff coefficient (the ratio of runoff to rainfall) was 0.23. Besides the seasonal baseflow variation, discharge reacted rapidly to rainfall, with discharge peaks up to 5-times the baseflow discharge in response to rainfall events. After rainfall ceased, discharge returned to baseflow levels within the next day. In Chapter 3, we have previously shown that also the groundwater levels had a pronounced response to rain events, with groundwater levels only returning to pre-event values after several days (Figure 3.6).

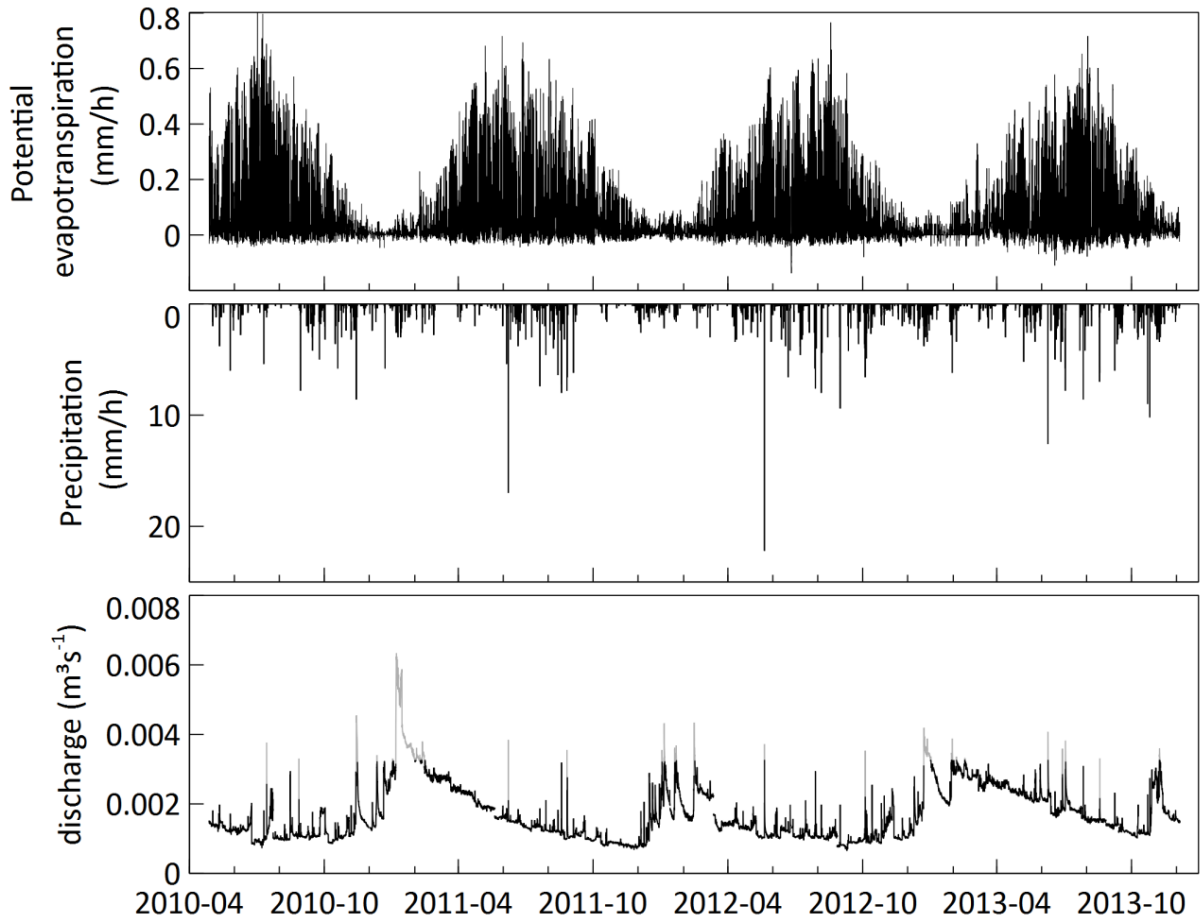

Figure 4.3. Discharge and precipitation measured at the site between April 2010 and December 2013 aggregated over intervals of 1 hour. Hourly potential evapotranspiration from a station nearby. Discharge data corresponding to a level of >15cm are indicated in grey, and are not included for the calibration of the hydrological model.

4.3.2 DOC dynamics

During the monitoring period, the average baseflow stream water DOC concentration was 2.2 mg l^{-1}. No significant seasonal variation in baseflow concentrations was observed. As a response to rainfall events however, DOC concentrations measured in the stream changed drastically (Figure 4.4). As discharge rose, concentrations increased and reached a maximum up to 13 mg l^{-1} at peak discharge. As discharge returned to pre-event discharge values when rainfall ceased, DOC decreased again to baseflow concentrations. The temporal variation in concentrations of DOC as well as other solutes such as DSi, Mg, K, Ca and S in the stream water of the Blégny catchment have been described in more detail in Chapter 3 (Figure 3.7).

Average DOC concentrations measured in the samples collected at the field were typically lowest in the shallow groundwater originating at seeps and in the precipitation water (Table 4.3). High average DOC concentrations were measured in soil pore water and riparian water.

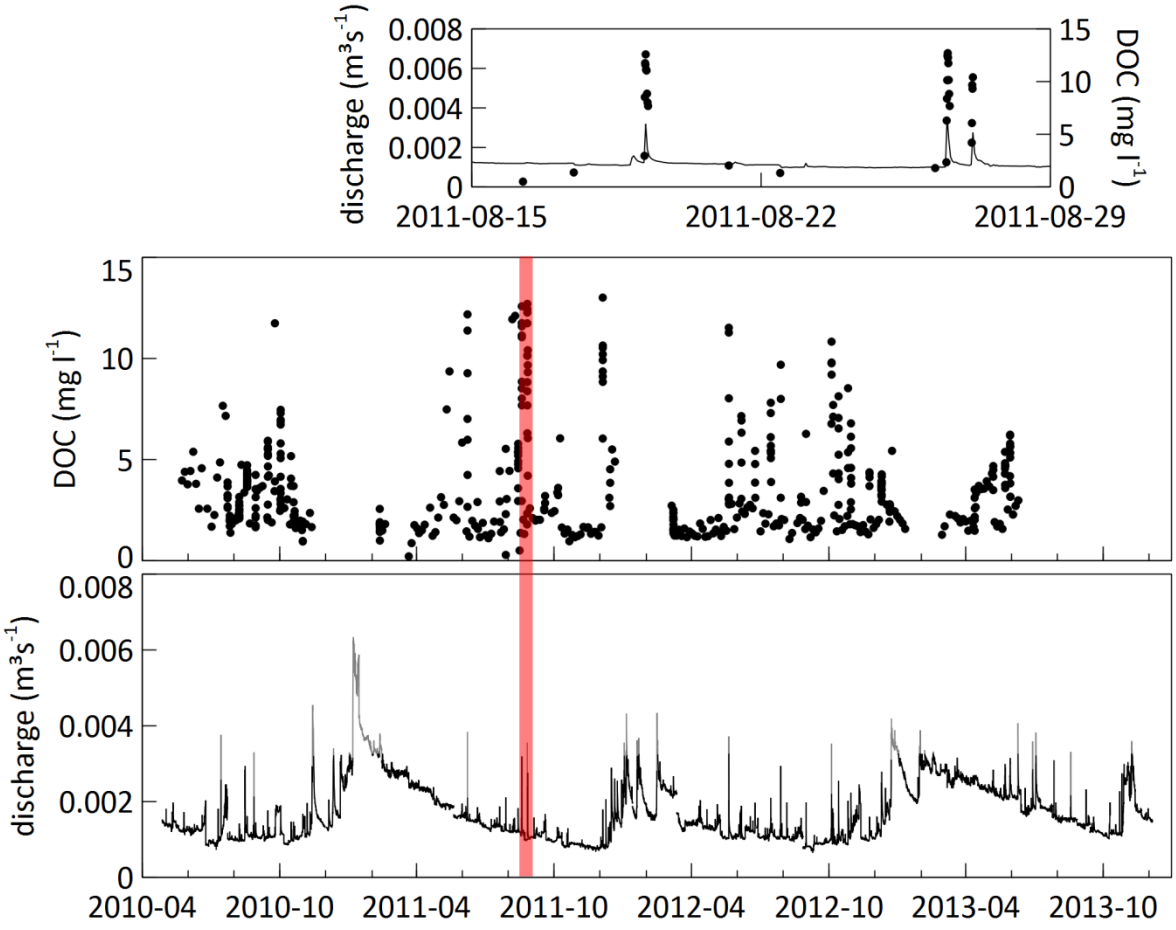

Figure 4.4. Stream water DOC concentrations measured during baseflow and peak flow conditions. The inset shows the enlargement of a two week period (indicated in red) in the summer of 2011, clearly illustrating the rising DOC concentrations during rain events.

Table 4.3. Mean values and standard deviations (in parentheses) of DOC concentrations measured in the stream water during baseflow conditions, soil pore water, groundwater, riparian water, seeps and precipitation samples. For stream water event samples minimum and maximum values are given.

Sample	DOC ($mg\ l^{-1}$)
Stream - baseflow conditions	2.2 (1.3)
Stream - event minimum	0.9
Stream - event maximum	13.0
Soil water†	25.9 (17.9)
Groundwater‡	8.3 (7.1)
Riparian water†	28.6 (10.4)
Seepage	1.9 (1.2)
Precipitation	3.9 (0.7)

† Mean values and standard deviations of the soil pore water and the riparian water were calculated using suction cup samples from all depths.

‡ Mean values and standard deviation of the groundwater were calculated using samples from all 3 piezometers.

4.3.3 Results of the FLEX hydrological model

4.3.3.1 Simulation of discharge

The calibration of the FLEX hydrological model using the DREAM algorithm yielded the parameter set that optimized the objective function (Table 4.4), as well as the underlying parameter posterior probability distribution. The posterior histograms (Figure 4.5) show most model parameters were well defined. Parameters L_P and k_S reached their lower bound.

Table 4.4. Parameter set with lowest sum of squared residuals, as inferred from the DREAM calibration procedure.

Parameter	Value	Unit
S_{Umax}	715.4823	mm
L_P	$1.5150*10^{-5}$	-
D	0.7404	-
λ	0.1616	-
β	23.6803	-
k_F	$1.3391*10^{-3}$	h^{-1}
k_S	$1.0048*10^{-4}$	h^{-1}
k_R	$4.1145*10^{-2}$	h^{-1}
f	$5.6410*10^{-3}$	-

Prediction of the discharge using the optimal parameter set (Figure 4.6) showed that the FLEX model under- or overestimated the measured discharge at several periods in time. Most notably, discharge was highly underestimated between December 2011 and April 2012. As stated previously (4.2.4.1), a considerable amount of snowfall was observed in the Blégny catchment during this winter period. Snowfall and subsequent thawing was not included in the model structure and thus can have caused this discrepancy. Between May 2013 and December 2013, the FLEX model results overestimated total measured discharge at the catchment outlet, for which no apparent reason was found. Overall, dry weather discharge was overestimated on the receding limbs of the hydrograph in the summer-fall periods. Also the short and flashy peak responses to rainfall events observed in the field were generally not well reproduced by the model. Modeled discharge did rise during rain events, but the peaks did not reach discharge values as high as observed values and discharge did not cease as fast

after a rain event as what was observed in the field. At most of the times that the model over- or underpredicted the measured discharge, measured discharge did not fall within the 95 % confidence intervals of the modeled discharge due to parameter uncertainty (Figure 4.6).

The coefficient of determination (R^2) of the measured versus the modeled discharge equaled 0.31, indicating the model was only a moderate fit to the measured discharge. The Pearson's linear correlation coefficient (P_{corr}) however was 0.89, meaning there was a high degree of correlation between the measured and the modeled values.

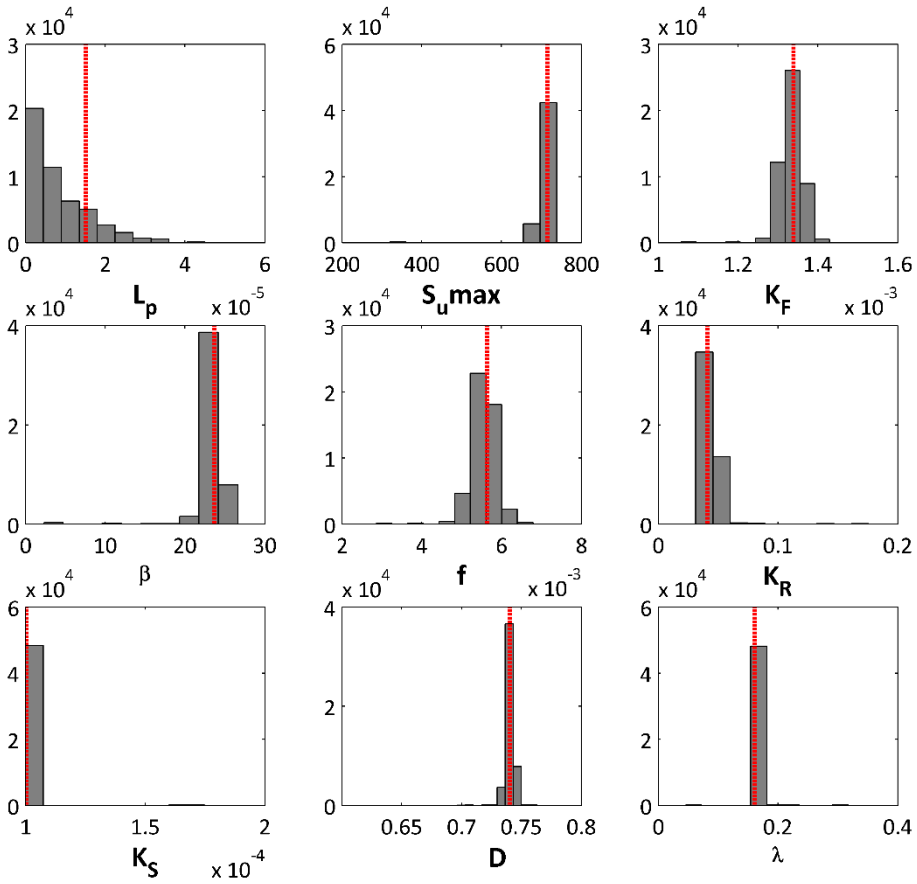

Figure 4.5. Histograms showing the parameter posterior probability distribution. The parameter set with the lowest sum of squared residuals, as inferred from the DREAM calibration procedure, is indicated in red.

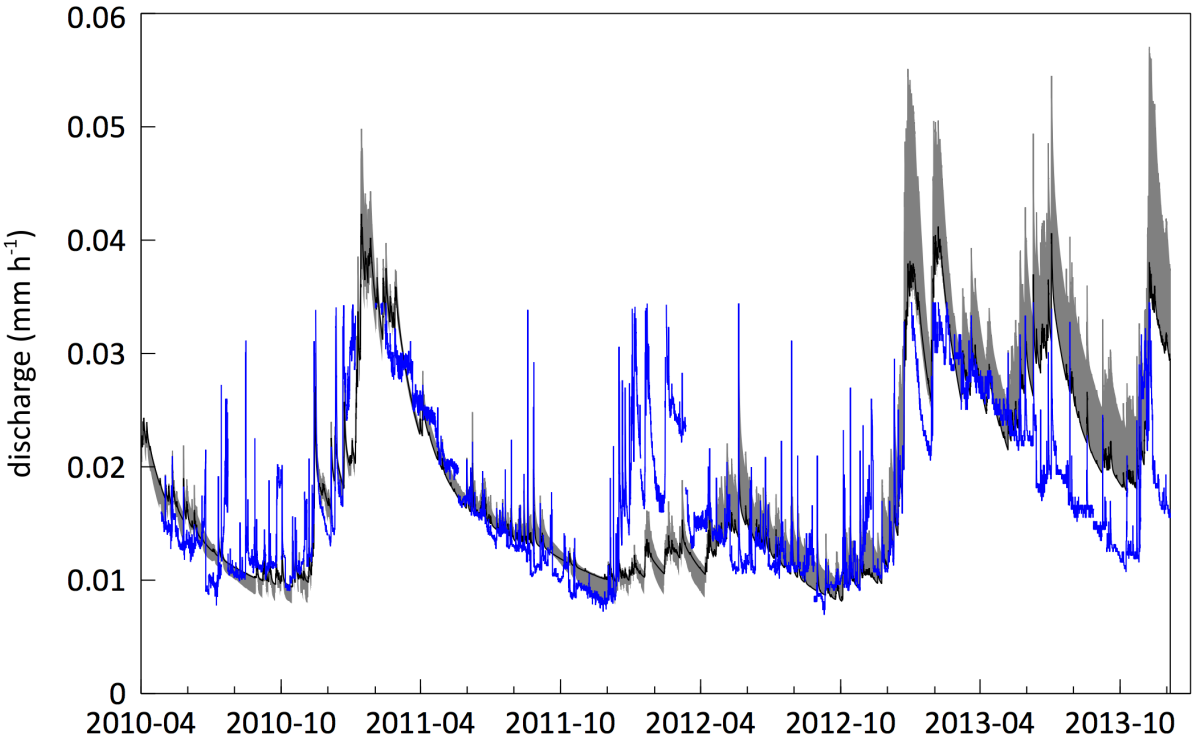

Figure 4.6. Hourly aggregated measured (full blue line) and modeled (FLEX, full black line) discharge data. The grey band indicates the 95 % confidence interval of the modeled discharge values due to parameter uncertainty.

The separate discharge components modeled by the FLEX model (Figure 4.7) showed that the slow component delivered vast quantities of water to the stream outlet year round, with the lowest slow component discharges around 0.01 mm h^{-1} in November and values up to almost twice as high around March. The slope of the seasonally receding limb of the slow component did however not follow the slope of the receding limb of the measured values, giving rise to the overestimation of baseflow discharge during the summer-fall periods. The higher simulated baseflow discharge between November and June compared to the rest of the year was caused by significant contributions of the fast component during that period. This fast component of the FLEX model represents water released over preferential flow paths and/or overland flow at times of high soil moisture contents. The fast component also accounted for part of the rise in discharge during rainfall events in the wettest periods of the year. Year round however, particularly the contributions of the riparian component caused discharge to peak in response to rainfall events. As contributions of this riparian component returned to pre-event values more slowly than total measured discharge (Figure 4.7, inset), modeled peaks were less flashy than what was observed in the field.

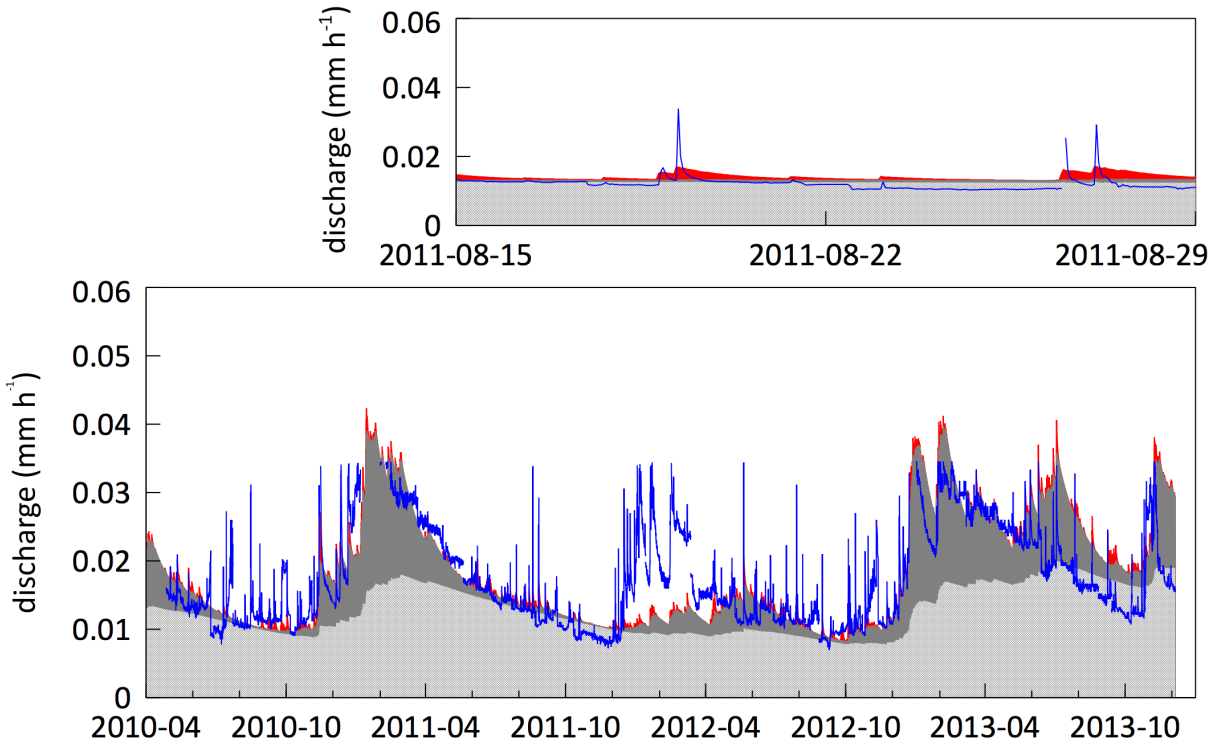

Figure 4.7. Hourly aggregated measured discharge values (full blue line) and discharge modeled by the FLEX model consisting of its three components namely Q_S (light grey), Q_F (dark grey) and Q_R (red). The inset shows the enlargement of the same two week period in the summer of 2011 as was the case in Figure 4.4.

4.3.3.2 Simulation of DOC dynamics

In chapter 3, we have reported that there is no seasonal variation in baseflow DOC concentrations measured at the stream outlet of the Blégny catchment. Based on a chemical analysis of the catchments waters, it was found that water originating from the seeps located on the hillslope is year round the dominant source of water delivered to the stream water. Therefore, for the calculation of DOC concentrations using the modeled subflow results of the FLEX model as described in 4.2.5, the DOC concentration in the slow discharge component and the fast discharge component, which both contribute to baseflow, were considered equal and to be represented by the average concentration measured at the seeps in the field (Table 4.3). As Chapter 3 showed that concentrations of DOC in both the precipitation water and the riparian zone soil pore water contributed to rising DOC concentrations during rainfall events, DOC concentrations in the FLEX riparian component were assumed to match the average of the concentrations measured in the precipitation samples and the riparian zone soil pore water samples collected at the field (16.265 mg l^{-1}, Table 4.3).

Modeled DOC concentrations in the stream (Figure 4.8) water had a minimum of 1.9 mg l^{-1}. This minimum value equals the average concentration measured in seepage water (Table 4.3), and was correspondingly predicted during times when the modeled discharge consists entirely of the slow and fast discharge components. It agrees well with the average concentration measured at the site during baseflow conditions (Table 4.3). Maximum modeled DOC concentrations reach 7.4 mg l^{-1}, and

were simulated during peak events, when water from the FLEX riparian component plays a considerable role. This modeled maximum value is somewhat lower than the maximum observed in the field (Table 4.3). Many of the higher measured DOC concentrations, observed during the discharge peaks as a response to rainfall events, were underestimated by the model (Figure 4.9). During the rainfall events, modeled DOC concentrations did rise compared to baseflow conditions (Figure 4.8, inset), but reached a peak concentration that was lower than what was observed in the field. Furthermore, modeled DOC concentration peaks were less flashy than measured ones.

Pearson's linear correlation coefficient of the measured versus the modeled concentrations (P_{corr}) equaled 0.58, indicating there is a moderate correlation between the measured and the modeled values.

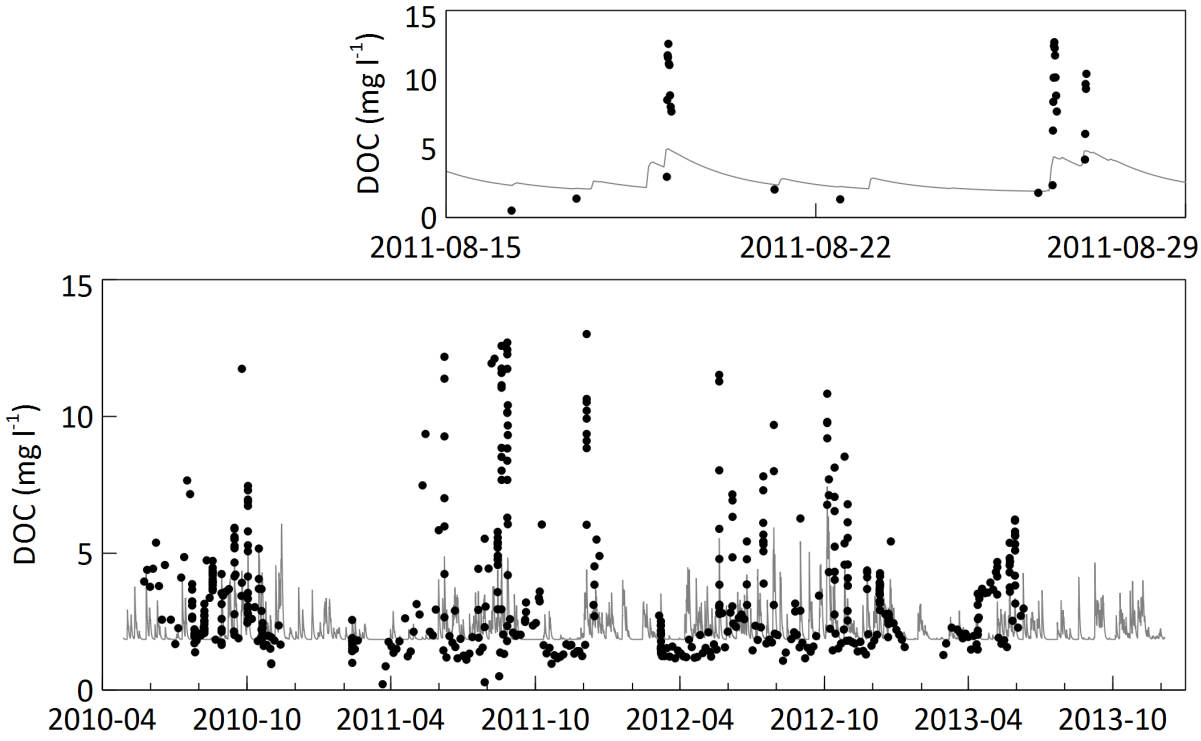

Figure 4.8. DOC concentration at the catchment outlet, with measured values represented by black dots and hourly modeled values using the FLEX subflow results represented by the full line. The inset shows the enlargement of the same two week period in the summer of 2011 as was the case in Figure 4.4.

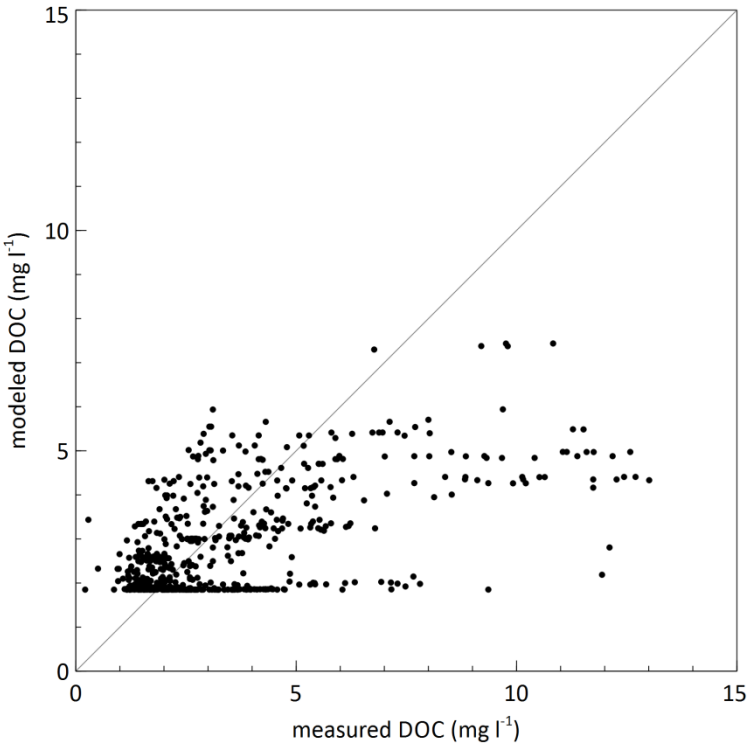

Figure 4.9. Measured DOC concentrations versus DOC concentrations modeled using the subflow results of the FLEX model.

4.3.4 Results of the WETSPRO hydrological model

4.3.4.1 Simulation of discharge

For the different subflow components of the WETSPRO model (slow flow, interflow, quick flow), the recession constant (k) and parameter w that represents the average fraction of the subflow volume over the total flow volumes, were calibrated (Table 4.5). The calibrated parameter values indicated that on average 86 % of the discharge observed at the outlet of the Blégny catchment could be attributed to slow flow. On average 10 % of the discharge originated from quick flow, whereas only an average of 4.2 % of the total discharge was attributed to interflow.

Table 4.5. Calibrated parameters of the WETSPRO filter for each subflow.

Subflow	Recession constant k (h)	Parameter w (-)
Slow flow	1180	0.86
Interflow	40	0.042
Quick flow	20	0.098

The slow flow and interflow components of the WETSPRO model were year round the main contributing fractions of water during baseflow conditions (Figure 4.10). Rising discharge during rainfall events was mainly caused by significant contributions of the quick flow component of the WETSPRO model (Figure 4.10, inset) which is a fast reacting component with a calibrated recession constant of just 20 h (Table 4.5). During rainfall events in winter-spring periods, the interflow component contributed to the rise in discharge as well.

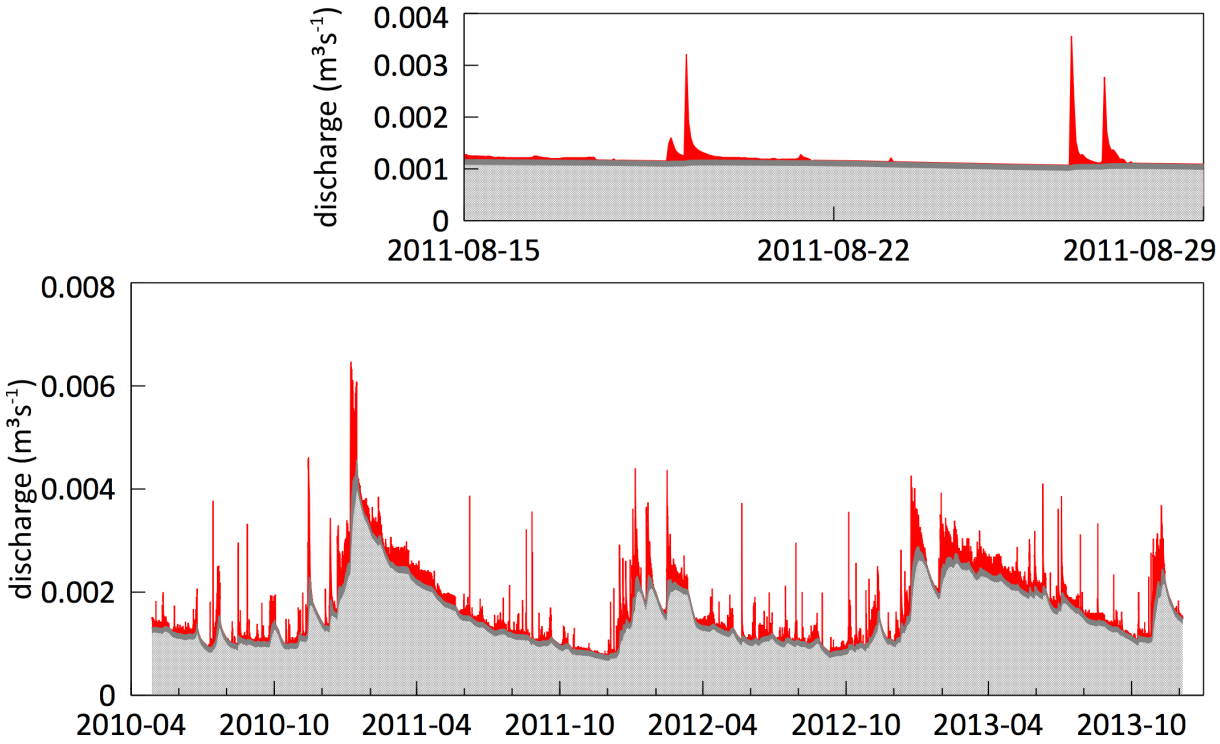

Figure 4.10. Hourly discharge consisting of its three subflow components separated by the WETSPRO tool: slow flow (light grey), interflow (dark grey) and overland flow (red). The inset shows the enlargement of the same two week period in the summer of 2011 as was the case in Figure 4.4.

4.3.4.2 Simulation of DOC dynamics

For the calculation of DOC concentrations using the modeled WETSPRO subflow results as described in 4.2.5, the DOC concentration in the slow flow and interflow component were considered equal. As the groundwater table in the Blégny catchment is very shallow (Chapter 3), groundwater is present in different layers of the soil, each with its own hydrological properties. Therefore, water from the interflow component, although differing from the slow flow component in dynamics, essentially has the same origin and therefore the same DOC concentration. DOC concentrations in both the slow flow and interflow component were therefore assigned to be equal to the concentrations measured at the seeps in the field (1.9 mg l^{-1}, Table 4.3). In Chapter 3, we additionally showed that both DOC concentrations measured in the precipitation water and the riparian zone soil pore water contributed to a rise in stream water DOC concentrations during peak events. Therefore, the DOC concentration of the quick flow component of the WETSPRO model, which is the main cause for rising discharge values during rainfall events, was assumed to be the average of the concentrations measured in the precipitation samples and the riparian zone soil pore water samples collected at the field (16.3 mg l^{-1}, Table 4.3).

Modeled DOC concentrations in the stream water using the subflow results of the WETSPRO model (Figure 4.11) correspond well with measured values at the field. At times when modeled discharge consist entirely of slow flow and interflow, modeled DOC concentrations are lowest (1.9 mg l^{-1}) and agree well with the average concentration measured at the site during baseflow (Table 4.3). As was the case for measured DOC concentrations, modeled DOC concentrations rose during rainfall events

and reached a peak when discharge was at its highest point (Figure 4.11, inset). The highest modeled DOC concentrations reached values up to 12.7 mg l^{-1}, which is very similar to the observed maximum DOC concentration in the stream of 13 mg l^{-1} (Table 4.3). Modeled DOC concentrations decreased after the rainfall event with a similar rate as measured DOC concentrations (Figure 4.11, inset).

Pearson's linear correlation coefficient of the measured versus the modeled concentrations (P_{corr}) was 0.70, indicating a good correlation between the measured and the modeled values (Figure 4.12).

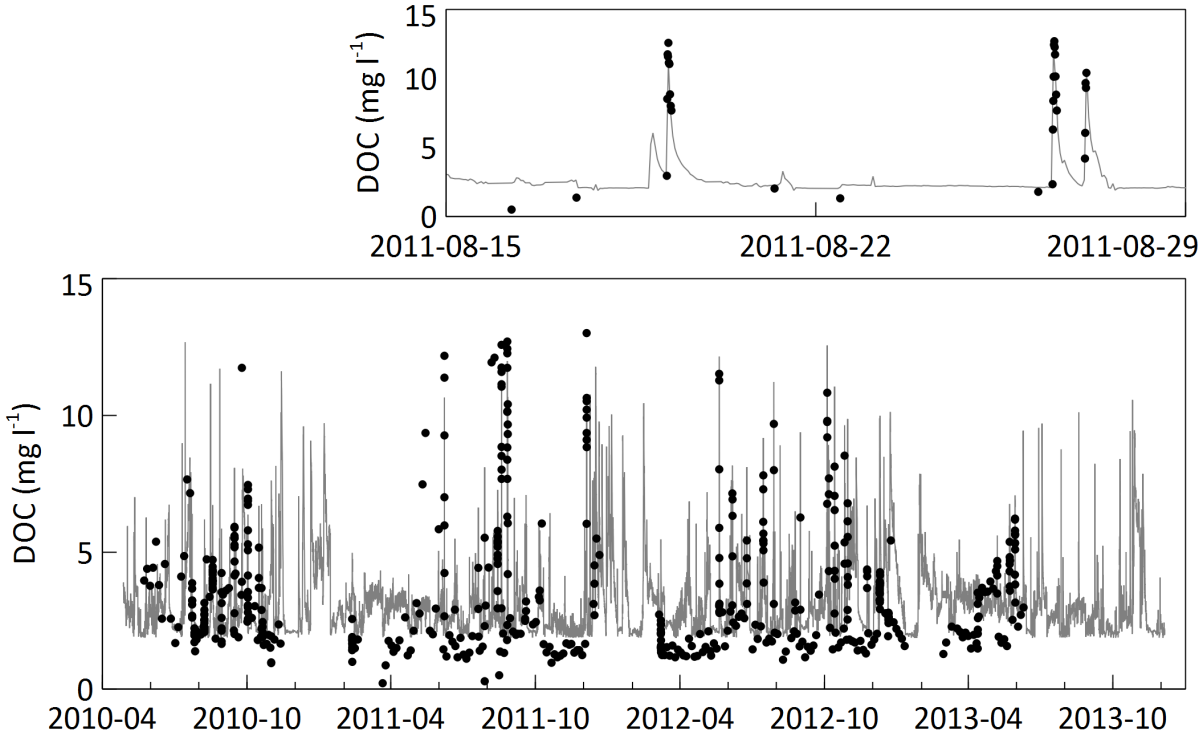

Figure 4.11. DOC concentration at the catchment outlet, with measured values represented by black dots and hourly modeled values using the WETSPRO subflow results represented by the full line. The inset shows the enlargement of the same two week period in the summer of 2011 as was the case in Figure 4.4.

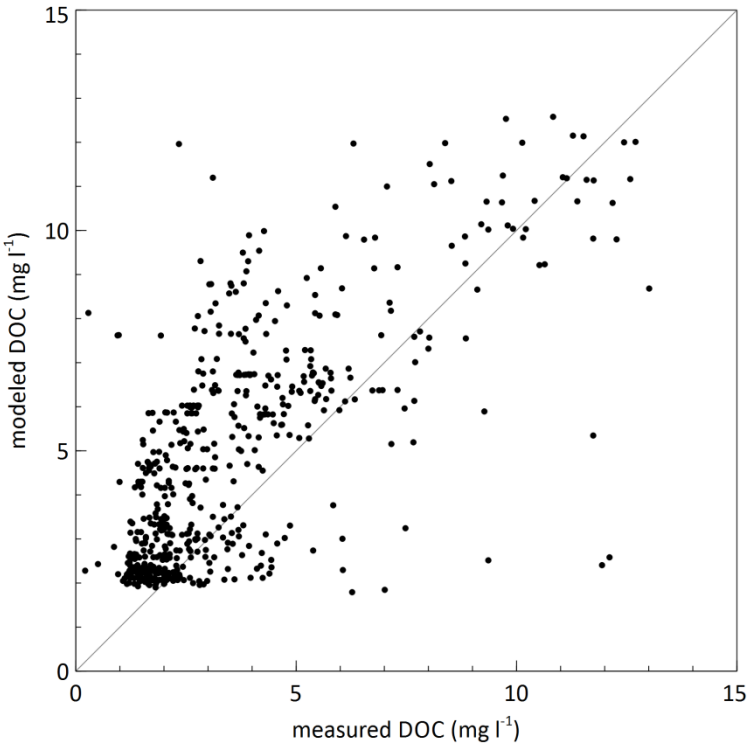

Figure 4.12. Measured DOC concentrations versus DOC concentrations modeled using the subflow results of the WETSPRO model.

4.4 Discussion

The FLEX hydrological model did in the current work not allow a good prediction of the temporal discharge variations observed in the field. As was reported earlier (Chapter 3), discharge measured at the Blégny catchment outlet showed both seasonal variation under baseflow conditions, and considerable temporal changes as a response to rainfall events. During baseflow conditions, the FLEX model periodically overestimated total discharge values. During rainfall events on the other hand, total discharge was often underestimated by the model. The different modeled subflow components did not succeed in reproducing the flashy discharge peaks observed in the field during rainfall events. Overall, although the structure of the FLEX model used in this work proved in an early calibration procedure to be the model structure that fitted the observed data best, the calibrated parameter values (Table 4.4) and the discharge results obtained using the optimal parameter set (Figure 4.6 and Figure 4.7) pointed out several issues concerning the use of the applied FLEX model structure to simulate discharge measured in the Blégny catchment. As the storage coefficient of the slow component K_S reached its lower bound in the calibration and the storage coefficient of the fast component K_F (0.03 day^{-1}, Table 4.4) was fairly low and reached a value rather associated with groundwater flow than overland or preferential flow, it appeared the FLEX model structure used both the slow responding and the fast responding component of the model to explain baseflow dynamics observed in the field. This could be due to the fact that the groundwater table in the Blégny catchment is very shallow and might be present in soil layers with different hydrological dynamics. However, as the fast component of the FLEX model was needed in addition to the slow component to explain baseflow dynamics, only contributions of the riparian component of the FLEX model structure allowed the prediction of discharge peaks during rainfall events. In that, a second

issue arose. To simulate larger contributions of flow from the riparian component, the proportion of catchment covered by the riparian zone (parameter f, Table 4.2) would have to increase. Larger f values however also lead to higher total actual evapotranspiration from the riparian zone, which affects the overall water balance and is heavily penalized by the objective function in the calibration procedure. Therefore, calibrated parameter f and thus contributions of the riparian component remained very limited. We argue that to accurately model discharge at the Blégny catchment, the FLEX model structure used in this work would have to be adapted, for example by adding an additional fast reservoir that contributes to the stream discharge during discharge peaks. The adjustment of the FLEX model structure however was out of the scope of this work.

The separation of total discharge in hydrological components contributing water to the catchment outlet using the simpler WETSPRO filter correspond well with the findings presented in previous work (Chapter 3), where discharge was separated based on an end-member mixing analysis using the chemical concentrations of several elements. In the Blégny catchment, during baseflow conditions, water originates mostly from a shallow groundwater component delivering water at the catchment outlet. Due to high groundwater tables in the catchment also an interflow discharge component contributes to stream flow during baseflow conditions. The rises in discharge in response to a rainfall event are mainly attributed to contributions of water from a quick flow component. During the wettest periods of the year, the contributions of interflow rise during rainfall events as well.

As was the case in other work (Lewis and Grant, 1979; Dawson et al., 2002, 2011; McGlynn and McDonnell, 2003), the observed variations in streamflow discharge at the Blégny catchment outlet were linked to temporal changes in stream DOC concentrations. In our study catchment, no seasonal variation in DOC concentrations was observed, which is in contrast with the findings of Mcdowell and Likens (1988), Dawson et al. (2002, 2008a, 2011) and Halliday et al. (2012). We did however clearly measure rising DOC concentrations during periods of elevated discharge caused by rainfall events, in agreement with what was reported earlier by Mcdowell and Likens (1988), Hagedorn et al. (2000), Dawson et al. (2002), Kaiser and Guggenberger (2005), Shanley et al. (2011) and Halliday et al. (2012).

Using the combination of predicted discharge subflows and DOC concentrations measured at several source locations in the field, we showed that the observed variation in DOC concentrations at the Blégny catchment outlet can be explained by varying contributions of water from different transport pathways, each with its own geochemical signal. This confirms previous research in the study catchment (Chapter 3) as well as work of other authors (Holloway and Dahlgren, 2001; Shanley et al., 2011; Halliday et al., 2012). As the FLEX hydrological model results did not agree well with measured discharge and in particular modeled discharge during rainfall events was underestimated and less flashy than what was observed in the field, the use of predicted FLEX subflows to estimate DOC concentrations in the catchment stream did not lead to a good agreement between measured and modeled DOC concentrations. This indicates that a good prediction of discharge subflows is needed to explain DOC concentrations in the stream as a combination of DOC concentrations delivered to the catchment outlet by varying contributions of different water transport pathways. Results of the WETSPRO model on the other hand successfully allowed to reproduce the DOC concentrations measured at the catchment outlet. Low, relatively constant DOC concentrations measured during baseflow conditions typically indicate the dominance of groundwater flow (Hornberger et al., 1994; Halliday et al., 2012). In the Blégny catchment, the WETSPRO hydrological model indicated that both

a slow flow hydrological component and an interflow component contribute to dry weather baseflow discharge and thus baseflow DOC concentrations. This can be explained by the fact that although hydrologically reacting differently, these two components do not differ in DOC concentrations. We argue that the WETSPRO slow flow component modeled in this work represents the shallow groundwater that intersects the stream as well as being discharged at hillslope seeps observed in the Blégny catchment. As groundwater levels are close to the soil surface, a part of the shallow groundwater however enters the stream via preferential or subsurface flow, represented by the WETSPRO interflow component. As water in this interflow component essentially has the same origin as the shallow groundwater, it has similar DOC concentrations.

High DOC concentrations measured in the stream during peak events have in previous research been attributed to increased contributions of near-surface pathways interacting with organic carbon-rich surficial soil layers (Boyer et al., 1997; Hagedorn et al., 2000; Inamdar and Mitchell, 2006; Chapter 3). This corresponds well with what we observed in the current work. During discharge peaks in response to rainfall events, the WETSPRO hydrological filter described large contributions of the quick flow component. In this work, we presumed the composition of this quick flow to be a mixture of water from the riparian zone and precipitation water, the latter accounting for a surficial runoff pathway through the organic rich top soil layer, as was the case for Shanley et al. (2011) and in Chapter 3. Due to high concentrations of DOC in the quick flow component, elevated contributions of this discharge component during rainfall events caused stream water DOC concentrations to peak. This is both in agreement with Laudon et al. (2007) and Mei et al. (2014) who showed the importance of the riparian zone for the delivery of DOC to a stream during storm events and with Brown et al. (1999) who found not throughfall itself but a transport pathway with a similar composition to cause DOC concentrations to rise during peak events.

4.5 Conclusion

Total discharge observed at the Blégny catchment outlet was modeled as a combination of subflow from different components, using the FLEX hydrological model and the WETSPRO filter. By linking the contribution of the discharge components with the measured average DOC concentration for each component, the temporal trends in DOC concentrations in the stream were predicted. The FLEX hydrological model did not succeed in an accurate prediction of measured discharge and due to the lack of fit of the hydrological model during peak events, peak DOC concentrations during discharge events caused by rainfall were highly underestimated and less flashy than what was observed in the field. Modeled DOC concentrations using the subflow results of the WETSPRO model did agree well with measured values. This work shows the need for detailed hydrological modeling in order to adequately predict DOC concentrations as a mixture of DOC from different discharge components delivering water at the stream outlet.

Chapter 5. General discussion, conclusions and future perspectives

This work set out to determine the controlling factors for the transport of dissolved organic carbon from the soil to the surface water and to identify and model the transport pathways. Therefore, experiments were conducted at different temporal and spatial scales. Monitoring at catchment level provided insight to the transport pathways delivering DOC towards the surface water and the temporal variation in stream water DOC concentrations and quality over the seasons as well as during single rainfall events. At the plot scale, the surface runoff pathway for the export of DOC from agricultural land was studied in more detail.

The research questions and accompanying hypotheses identified in the introductory chapter are used as a basis to put the results obtained in this work into a larger context and to formulate the major conclusions of this thesis.

Q1. What are the controls for the transport of DOC through surface runoff from arable land? What is the effect of soil properties, hydrological conditions and field characteristics on the concentrations and quality of DOC in surface runoff?

To assess the effect of soil properties, hydrological conditions and field characteristics on the concentrations and quality of DOC in surface runoff during a rainfall event at the interrill plot scale, we have reported rainfall experiments conducted on arable land in the Belgian loam belt. The results from both laboratory and field rainfall experiments, presented in Chapter 2, showed that the most important control on DOC concentration and quality in runoff water was the antecedent rainfall, which determined the initial soil moisture conditions of the field site at the time of the rainfall experiment. Greater amounts of precipitation in the period before the experiment, or higher initial soil moisture content, led to lower mean DOC concentrations and higher mean SUVA values in the runoff during the experiments. Similar results have been reported for the vertical transport of DOC in the soil (De Troyer, 2011, Don and Schulze, 2008 and Mertens et al., 2007). This confirms our hypothesis (H1) that the export of DOC via surface runoff from agricultural fields in the Belgian loam belt is limited by the source term or the DOC production rate in the surface soil. As this source term does not increase with more frequent and more intense rainfall, greater volumes of surface runoff will contain lower DOC concentrations. Hence, greater antecedent soil moisture contents and higher rainfall intensities lead to lower DOC concentrations in surface runoff, confirming hypothesis (H1.1.). The hydrological conditions also determine the temporal variation observed in DOC concentration and quality in surface runoff during a single rainfall event. Following a dry period, large amounts of low aromatic DOC are released at the beginning of a runoff period, with a gradual shift towards lower DOC concentrations and higher DOC aromaticity.

Our work additionally evidenced that soil properties, tillage technique and field characteristics only have a limited effect on DOC concentrations and quality in runoff waters from agricultural soils located in the Belgian loam belt. For the range of considered soil types, no correlation was found between the soil C content and the DOC concentration in runoff water. The effect of reduced tillage on DOC concentrations in surface runoff was ambiguous, with effects differing between experimental

field sites. In the laboratory experiments, the incorporation of crop residues in the top soil layer as is custom in reduced tillage practices, significantly increased the DOC concentrations and decreased the SUVA values. However, under field conditions, tillage practices influence many soil properties, which can interact and counterbalance. This also agrees well with previously reported results for vertical transport of DOC in the soil, whereby De Troyer (2011) showed that environmental conditions and land management practices only have a limited effect. The hypothesis (H1.2.) that field management characteristics such as tillage technique affect the DOC concentrations measured in surface runoff from agricultural fields in the Belgian loam belt, whereby reduced tillage leads to greater DOC concentrations in the surface runoff water, could thus not be confirmed in this work.

The results from the rainfall experiments on the field indicated that the concentrations of DOC observed in surface runoff from arable land in the Belgian loam belt varied between 1.90 mg l^{-1} and 17.85 mg l^{-1}, with an average value of 8.54 mg l^{-1}. This is higher than concentrations typically observed in other transport pathways for DOC such as groundwater flow, soil pore water flow or precipitation (Table 1.1) and confirms the findings of Cronan et al. (1999) and Royer et al. (2007) who indicated that DOC concentrations in surface runoff are at least of the same magnitude as those found in subsurface flow or groundwater flow. Based on the average DOC concentrations in surface runoff observed in this work and taking into account that (1) the area receives a mean annual precipitation of ca. 800 mm and (2) from the data presented by Van Oost et al. (2005) the average runoff coefficient on similar loamy agricultural fields in the area can be calculated to be 5.47 %, the total annual flux of DOC that is transported via the surface runoff from arable fields in the Belgian loam belt is estimated to be 3.76 kg ha^{-1} $year^{-1}$. This is in the same order of magnitude as the total annual DOC export from agricultural catchments reported by others (Royer et al., 2005 and Stedmon et al., 2006), and thus clearly indicates that on soils generating considerable surface runoff during rainfall events, the surface runoff pathway can be an important transport pathway for the export of DOC from the soil to the surface water.

Q2. At the catchment scale, what are the factors controlling the temporal variation in DOC concentrations and quality observed at the stream outlet?

DOC concentrations and quality were monitored over a 3.5 years time period in four headwater catchments in central Belgium, differing in land use and hydrogeology. The results presented in Chapter 3 showed that during rainfall events, both DOC concentrations and SUVA values increased with discharge, reached a maximum and decreased again as discharge returned to pre-event baseflow values. These changes in concentrations and quality of DOC as well as concentrations of other solutes such as Si and major cations during discharge events could be attributed to a change in contributions of transport pathways of water to the stream. High stream concentrations of DOC and K during a rain event originated from flow pathways through upper soil layers where these solutes are concentrated by nutrient cycling, while elevated concentrations of Ca and Si during baseflow indicated the dominance of shallow groundwater. These results confirm our hypothesis (H2) that the temporal variation in DOC concentrations and quality observed in the stream during periods of elevated discharge caused by rain events, can be explained by a change in contributions of different pathways delivering water and thus DOC at the catchment outlet.

The finding that changes in concentrations and quality of DOC and other solutes measured in the stream during discharge events are caused by a change in contributions from different water transport pathways, is further endorsed by measurements of water isotopes ratios in the stream water of the Meerdaal catchment and the Blégny catchment. Starting from April 2011, all river water samples collected during baseflow conditions were analyzed for stable oxygen and hydrogen isotope ratios. In addition, the samples collected during a limited number of rainfall events in 2011 were analyzed. The stable isotope analyses were performed with a liquid water isotope analyzer method (LWIA) using an off-axis integrated cavity output spectroscope (OA-ICOS), model DLT-100, manufactured by Los Gatos Research Inc. The analyses were conducted at the Faculty of Civil Engineering and Geosciences at the Delft University of Technology in the Netherlands.

Measurements of $^{2}H/H$ and $^{18}O/^{16}O$ ratios are commonly expressed in δ units (Eq. 5.1 and Eq. 5.2)

$$\delta\,^{18}O = \left(\frac{\left(\frac{^{18}O}{^{16}O}\right)_{sample}}{\left(\frac{^{18}O}{^{16}O}\right)_{standard}} - 1 \right) * 1000 \qquad (5.1)$$

$$\delta\,^{2}H = \left(\frac{\left(\frac{^{2}H}{^{1}H}\right)_{sample}}{\left(\frac{^{2}H}{^{1}H}\right)_{standard}} - 1 \right) * 1000 \qquad (5.2)$$

whereby δ is in ‰, and the subscripts *sample* and *standard* refer to isotope ratios in the water sample collected in the field and in the Vienna standard mean ocean water (V-SMOW) standard respectively.

Oxygen and hydrogen isotope ratios observed in the Meerdaal catchment (Figure 5.1) and the Blégny catchment (Figure 5.2) showed limited variation between samples collected during baseflow conditions. During discharge peaks following a rain event however, both $\delta^{18}O$ and $\delta^{2}H$ increased to less negative values, which is in agreement with changes in isotope ratios during rainfall events observed by Laudon and Slaymaker (1997) and Sklash and Farvolden (1979). Both in the Meerdaal and the Blégny catchment, the highest $\delta^{18}O$ and $\delta^{2}H$ values were measured at peak discharge (Figure 5.3 and Figure 5.4).

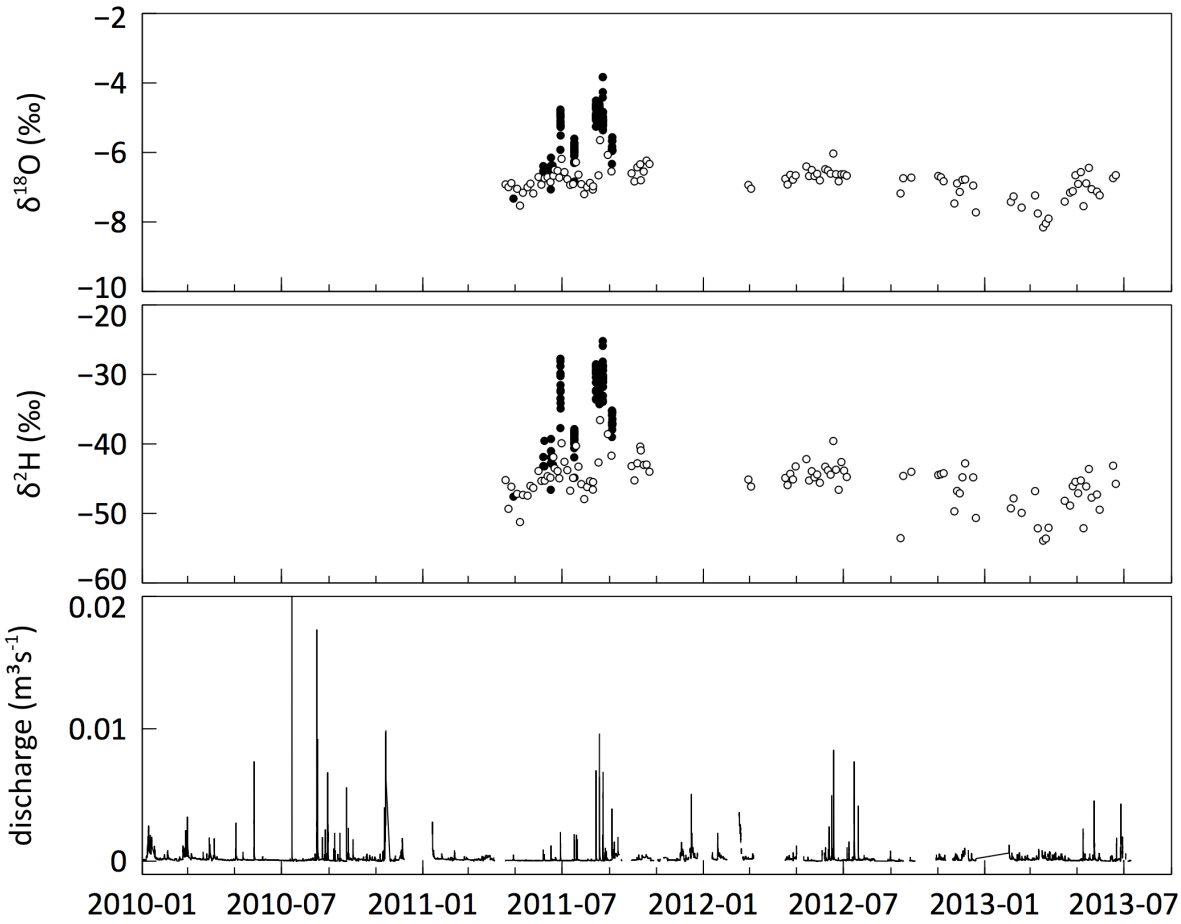

Figure 5.1. Discharge, $\delta^{18}O$ and $\delta^{2}H$ measured in the stream outlet of the Meerdaal catchment. Open circles indicate values measured in samples collected during baseflow conditions, full circles indicate values measured in event samples.

Measurements of isotope ratios are commonly used to separate the stream hydrograph observed during peak events into its different time-source components (Hooper and Shoemaker, 1986, Sklash and Farvolden, 1979, Tetzlaff et al., 2007). Thereby, 'event water' falling as precipitation during a particular storm, is distinguished from 'pre-event water' stored in the watershed before the start of the storm (Kendall and McDonnell, 1998). This hydrograph separation differs from the end-member mixing analysis applied in Chapter 3 in that the latter divided the stream discharge into its geographic-source components, thereby determining contributions of water from different source waters present in the catchment, such as groundwater, pore water, riparian zone water or precipitation water. For the separation of the hydrograph into pre-event and event water, a simple mixing equation is applied, whereby the pre-event isotopic ratio is based on measurements in the stream during dry weather conditions or on analysis of groundwater and the event-water isotopic ratio is based on observations of precipitation water.

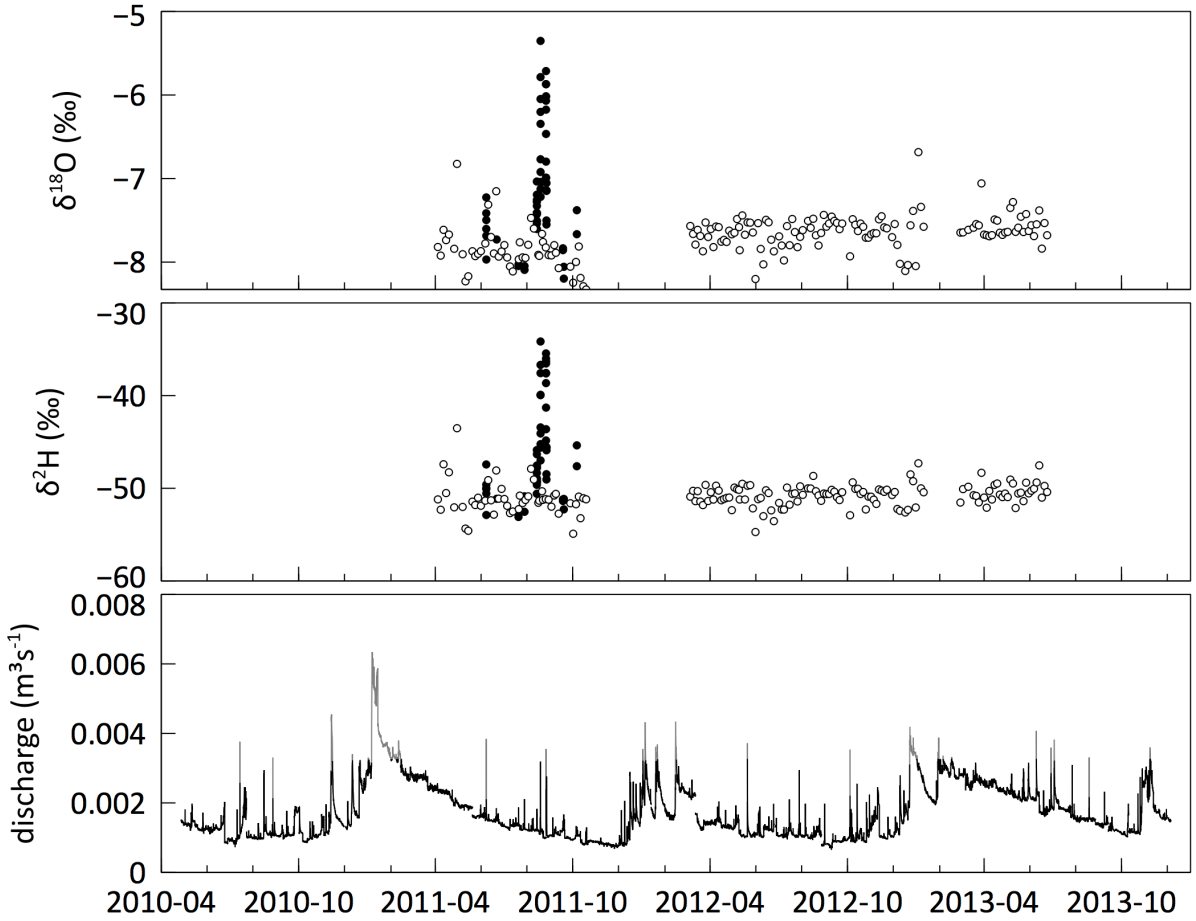

Figure 5.2. Discharge, $\delta^{18}O$ and $\delta^{2}H$ measured in the stream outlet of the Blégny catchment. Open circles indicate values measured in samples collected during baseflow conditions, full circles indicate values measured in event samples.

During the rainfall events in the Meerdaal and the Blégny catchment for which collected stream flow event samples were analyzed for oxygen and hydrogen isotopes, no isotopic analysis of the precipitation water was performed, which did not allow us to identify the contributions of pre-event and event water during the peak discharge events based on the isotopic ratios measured in the stream water. The change in isotopic ratios observed (Figure 5.3 and Figure 5.4) however, clearly indicated a role for event water during peak discharges caused by rainfall events. If all water reaching the catchment outlet during peak discharge would originate from pre-event water already stored in the watershed before the start of the storm, no change in isotopic ratios would be observed. Furthermore, as summer precipitation is generally enriched and thus has less negative values of $\delta^{18}O$ and $\delta^{2}H$ compared to winter precipitation (IAEA, 2005), contributions of event water can explain the rise in $\delta^{18}O$ and $\delta^{2}H$ observed in the Meerdaal and the Blégny catchment during rain storms. This additionally endorses the importance of contributions from the precipitation/throughfall end-member that was observed in our study catchments and that represented a transport pathway through the organic rich top soil layer.

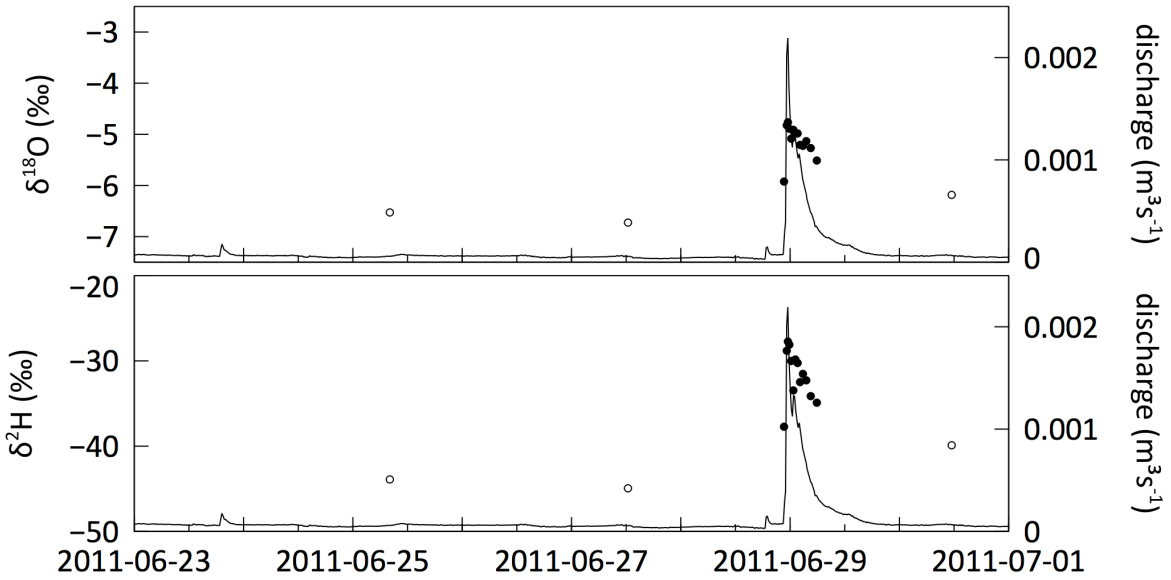

Figure 5.3. Discharge, $\delta^{18}O$ and $\delta^{2}H$ measured in the stream outlet of the Meerdaal catchment during a rainfall event. Open circles indicate values measured in samples collected during baseflow conditions, full circles indicate values measured in event samples.

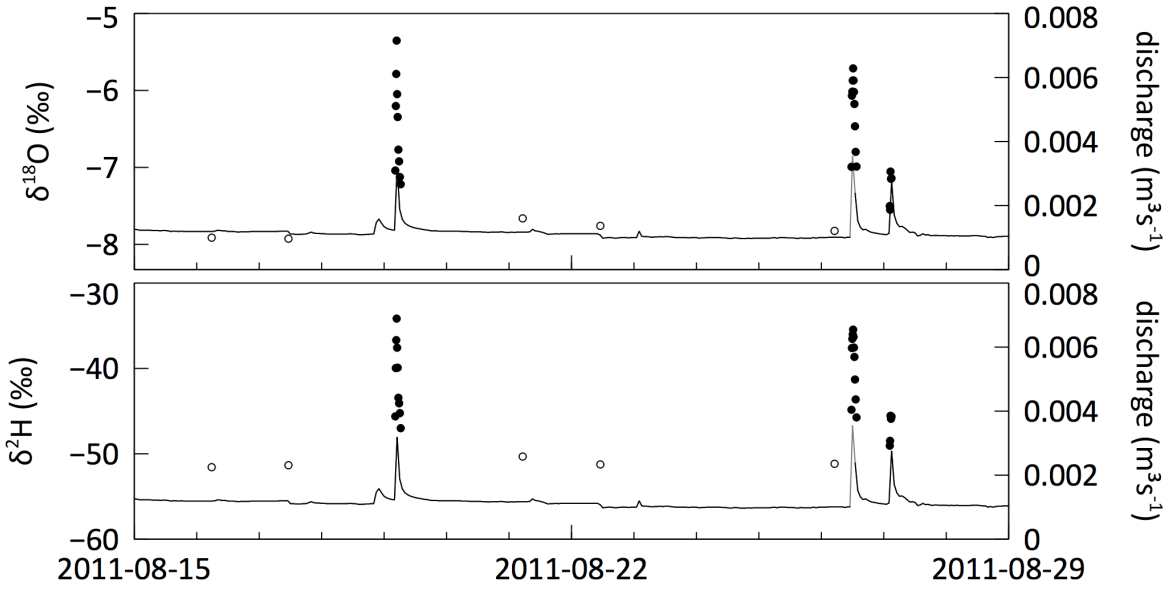

Figure 5.4. Discharge, $\delta^{18}O$ and $\delta^{2}H$ measured in the stream outlet of the Blégny catchment during a two-week period in the summer of 2011. Open circles indicate values measured in samples collected during baseflow conditions, full circles indicate values measured in event samples.

Q3. Which transport pathways contribute to the transport of DOC to the surface water at the watershed scale during baseflow conditions and during discharge peak events?

In both the Meerdaal and the Blégny study catchment, our results indicate the importance of discharge events caused by rainfall for the total yearly export of DOC at the catchment scale. It was estimated that 70 % and 72% of the total annual export of DOC was transported at times when discharge was elevated in response to a rainfall event, for Meerdaal and Blégny respectively. Confirming the findings of Shanley et al. (2011) and Halliday et al. (2012), this clearly indicates the added value of our work, focusing both on long-term regular sampling during dry weather conditions and more frequent sampling during a great number of rainfall events, for the total understanding of DOC transport at the catchment scale.

The pathways contributing to the transport of DOC to the stream water in the Meerdaal and Blégny catchment during these different flow regimes were identified in Chapter 3 using an end-member mixing analysis. Results showed that during dry weather baseflow conditions, the greatest contributions of discharge to the stream in the Blégny and the Meerdaal catchment came from the groundwater or shallow groundwater discharged at seeps. The rise in DOC concentrations measured in the streams during rainfall events, accompanied by a rise in SUVA values, was caused by additional contributions of water from the riparian zone and from the precipitation/throughfall end-member that represented a transport pathway through the organic rich top soil layer.

The changing contributions of water reaching the catchment outlet via different pathways also determined the timing of the solutes peak during rainfall events. In the Blégny catchment, the peak in DOC concentrations and quality, as well as the minimum or maximum of other solute concentrations during a rainfall event, coincided with the discharge peak. This indicated that the maximum contribution of the different transport pathways occurred at the same moment as the peak in total stream discharge. In the Meerdaal catchment however, the peak in DOC concentrations and quality and K concentrations during rainfall events was only observed on the descending limb of the hydrograph, while Si, Mg, K and S concentrations had a minimum at the time of maximum discharge. It was found that the maximum contribution of the throughfall end-member representing a surficial runoff pathway coincided with the peak discharge, while the maximum contribution of the riparian zone water occurred only after the peak in stream discharge.

In the Blégny catchment, changing solute concentrations during rainfall events occurring in spring and summer were attributed to equal contributions of precipitation and riparian zone water. In the fall or winter period on the other hand, when groundwater tables are high and soils are (almost) completely saturated, contributions of water from the riparian zone were more important than contributions of the precipitation end-member during rainfall events. These larger contributions of riparian zone water in winter were attributed to increased volumes of water stored in the soil around the river and thus a larger saturated riparian zone. For the Meerdaal and the Blégny catchment, Verheyen et al. (2015) showed that the transport pathways described here were also able to describe the transport of dissolved phosphorus to the surface water. This additionally evidences that for our study catchments, hypotheses (H2.1.) and (H2.2.) could be confirmed. Discharge to the stream during baseflow conditions is mainly via groundwater flow. During discharge peaks caused by rainfall events, additional transport pathways such as precipitation/throughfall and riparian zone water additionally contribute to the transport of DOC to the surface water. The end-member mixing analysis using

cation and DOC concentrations measured in the different transport pathways, allowed the identification of the contribution of each pathway for the transport of DOC to the surface water at different flow regimes.

As we have shown that the greatest part of the total annual DOC flux from the Meerdaal and the Blégny catchment was transported during rainfall events, it are consequently the end-members that play a significant role to the stream discharge during rainfall events that contribute most to the total annual DOC export from the catchments. The greatest part of the total annual export of DOC from the Meerdaal catchment originated from the throughfall end-member that represents a transport pathway through the organic rich top soil layers. In the Blégny catchment, the main contributions to the total annual DOC flux originated from the riparian zone, which is in agreement with Lambert et al. (2013) and Sanderman et al. (2009) who also reported the dominant role of a shallow riparian source in contributing the majority of the annual DOC flux. Overall, our results from the Blégny and the Meerdaal catchment show that the transport pathways that contribute most to the total annual water flux of the catchment (the groundwater or shallow groundwater discharged at seeps) are not necessarily the pathways delivering the greatest part of the total annual DOC flux. On the contrary, at the catchment scale a transport pathway that has only limited contributions to the total annual water flux, can be responsible for the greatest part of the total annual DOC flux.

Q4. Can hydrological modeling of the different water pathways at the catchment scale lead to an adequate modeling of DOC concentrations in the stream outlet during different flow regimes?

Using the FLEX hydrological model and the WETSPRO filter in Chapter 4, observed discharge in the small Blégny headwater catchment was modeled as a combination of water from different discharge components. The combination of the contribution from each component delivering water at the stream outlet and the average DOC concentration measured in the different transport pathways (Chapter 3), allowed the modeling of DOC concentrations in the stream water as a mixture of DOC from the different transport components. As the FLEX hydrological model did not lead to a good fit between measured and modeled discharge, especially during discharge peak events, peak DOC concentrations during rainfall events were underestimated and less flashy than what was observed in the field. Using the discharge subflow results of the WETSPRO model however, we were able to reproduce measured DOC concentrations well. The low, relatively constant DOC concentrations observed during baseflow discharge originated from the WETSPRO slow flow and interflow components, both carrying only low DOC concentrations, as represented by the DOC concentrations measured at the seeps in the field. During discharge peaks caused by rainfall events, the model was able to describe the temporal rising and falling pattern in DOC concentrations observed in the stream. The peak in DOC concentrations during discharge peaks was caused by considerable contributions of the quick flow component, of which the composition was a mixture of water from the riparian zone and precipitation water, the latter accounting for a transport pathway through the organic rich top soil layer. The results of the WETSPRO filter allow us to confirm the hypothesis (H2.3.) that in a small headwater catchment with quick discharge responses to rainfall events, stream water DOC concentrations can be adequately predicted by hydrological modeling of the different water pathways combined with a simple mixing equation of DOC concentrations measured in these transport pathways.

Combining the modeled time series of contributions of the transport pathways (Chapter 4) with average DOC concentrations measured in each pathway (Chapter 3), additionally allowed to calculate the contribution of each WETSPRO flow component to the total annual export of DOC from the Blégny catchment. Using the contributions from each component modeled by the WETSPRO filter, the total annual DOC flux from the Blégny catchment was calculated to be 5.28 kg ha^{-1} $year^{-1}$. This agrees well with the estimation of the total annual flux in Chapter 3 (6.79 kg ha^{-1} $year^{-1}$), which was calculated using the time-based separation of actual measured discharge values into discharge originating from the different end-members during baseflow conditions and during peak event conditions, in combination with average DOC concentrations measured in end-member samples. It is almost double of what is reported for other grassland catchments (Table 1.2), but smaller than typical values observed in catchments with different land uses, which is in agreement with Mattsson et al. (2009). The WETSPRO results indicated that 47.2 %, 4.0 % and 48.8 % of the total annual DOC flux originated from the WETSPRO slow flow component, interflow component and quick flow component respectively. Although the quick flow component of the WETSPRO filter on average only contributed 10 % of the discharge in the stream, it is thus an important transport mechanism for DOC towards the surface water. This agrees well with the findings reported in Chapter 3, where we observed that as the greatest part of the total annual DOC flux in the Blégny catchment is transported at times when discharge is elevated in response to rainfall event, it are the end-

members that particularly contribute to the stream discharge during these peak events, that contribute most to the total annual DOC export.

Overall, the modeling results presented in the current work indicate the importance of adequate modeling of the catchment hydrology for the prediction of DOC transport from the soil to the surface water. We showed that with a good prediction of the contributing hydrological transport pathways, we were able to reproduce DOC concentrations observed during baseflow conditions as well as variations in stream DOC concentrations during peak discharges.

5.1 Suggestions for future research

The current work has clearly showed the importance of the surface runoff pathway for the transport of dissolved organic carbon from loamy agricultural fields in the Belgian loam belt and has gained unique insights in the factors controlling the transport via this pathway. Although the limited effect of soil properties and land management on DOC concentrations in surface runoff that was observed is in agreement with what is previously reported for vertical transport of DOC, the rainfall experiments carried out in this work did not allow to completely exclude the effect of soil properties and land management strategies on DOC concentrations in surface runoff, as the range of soil types studied was limited. Similar rainfall experiments carried out on soils with a larger range in soil properties would gain additional insight on DOC transport through surface runoff from different soil types. As rainfall experiments carried out in the lab under similar conditions as rainfall experiments on the field in this work led to lower average DOC concentrations in surface runoff, rainfall experiments on the field should get preference.

For the transport of DOC on the catchment scale, the current work indicated that solute concentrations (such as Si, K, Ca, Mg, S) measured at the field in the different transport pathways delivering DOC at the catchment outlet yield great insight in the transport pathways and the controlling factors for DOC transport to the catchment outlet during different hydrological conditions. A suggestion for future work would be to incorporate the (conservatively mixing) solute concentrations measured in the different contributing water sources at the field into the hydrological model, as a way to even better constrain model parameters. This would not only improve the calibration of the hydrological model. As the separation of the total discharge observed at the catchment outlet by the hydrological model can be used to predict the stream DOC concentrations, the incorporation of solute concentrations for the model calibration would also affect the possibility of accurately predicting DOC concentrations in the stream. In a small headwater catchment with quick discharge responses to rainfall events such as the Blégny catchment, a hydrological model that captures variation in stream discharge in detail will most likely lead to a very accurate description of DOC concentration variations in the stream.

Overall, our work has demonstrated the importance of short term peak discharges for the transport of DOC from the soil to the surface water. Future work concerning the long-term increases in DOC concentrations observed in surface waters in the UK, northern Europe and North America over the last decades should therefore not overlook the large quantities of DOC transported during discharge peaks caused by rainfall events.

References

Aitkenhead, J.A., D. Hope, and M.F. Billett. 1999. The relationship between dissolved organic carbon in stream water and soil organic carbon pools at different spatial scales. Hydrol. Process. 13(8): 1289–1302.

Aitkenhead, J.A., and W.H. McDowell. 2000. Soil CN ratio as a predictor of annual riverine DOC flux at local and global scales. Global Biogeochem. Cy. 14: 127–138.

Akaike, H. 1974. A New Look at the Statistical Model Identification. IEEE Trans. Automat. Contr. 19: 716–723.

Akkanen, J. 2002. Does dissolved organic matter matter ? – Implications for bioavailability of organic chemicals. PhD dissertation University of Joensuu. : 118.

Amery, F., F. Degryse, K. Cheyns, I. De Troyer, J. Mertens, R. Merckx, and E. Smolders. 2008. The UV-absorbance of dissolved organic matter predicts the fivefold variation in its affinity for mobilizing Cu in an agricultural soil horizon. Eur. J. Soil Sci. 59(6): 1087–1095.

Amery, F., F. Degryse, W. Degeling, E. Smolders, and R. Merckx. 2007. The copper-mobilizing-potential of dissolved organic matter in soils varies 10-fold depending on soil incubation and extraction procedures. Environ. Sci. Technol. 41(7): 2277–81.

Amery, F., C. Vanmoorleghem, and E. Smolders. 2009. Adapted DAX-8 fractionation method for dissolved organic matter (DOM) from soils: development, calibration with test components and application to contrasting soil solutions. Eur. J. Soil Sci. 60(6): 956–965.

Bajracharya, R.M., R. Lal, and J.M. Kimble. 1998. Soil organic carbon dynamics under simulated rainfall as related to erosion and management in central Ohio. Adv. Geoecol. 31: 231–238.

Benning, R., Schua, K., Schwärzel, K. and Feger, K.H. 2012. Fluxes of Nitrogen, Phosphorus, and Dissolved Organic Carbon in the inflow of the Lehnmühle reservoir (Saxony) as compared to streams draining three main land-use types in the catchment. Adv. Geosci., 32: 1-7.

Bertol, I., F.L. Engel, A.L. Mafra, O.J. Bertol, and S.R. Ritter. 2007. Phosphorus, potassium and organic carbon concentrations in runoff water and sediments under different soil tillage systems during soybean growth. Soil Tillage Res. 94(1): 142–150.

Bertol, I., D. Leite, J.C. Guadagnin, and S.R. Ritter. 2004. Erosão hídrica em um Nitossolo Háplico submetido a diferentes sistemas de manejo sob chuva simulada. II - Perdas de nutrientes e carbono orgânico. Rev. Bras. Ciência do Solo 28: 1045–1054.

Bishop, K., J. Seibert, S. Köhler, and H. Laudon. 2004. Resolving the Double Paradox of rapidly mobilized old water with highly variable responses in runoff chemistry. Hydrol. Process. 18(1): 185–189.

Borselli, L., D. Torri, J. Poesen, and P. Salvador Sanchis. 2001. Effects of water quality on infiltration, runoff and interrill erosion processes during simulated rainfall. Earth Surf. Process. Landforms 26(3): 329–342.

Boyer, E.W., G.M. Hornberger, K.E. Bencala, and D.M. McKnight. 1996. Overview of a simple model describing variation of dissolved organic carbon in an upland catchment. Ecol. Modell. 86(2-3): 183–188.

Boyer, E.W., G.M. Hornberger, K.E. Bencala, and D.M. McKnight. 1997. Response characteristics of DOC flushing in an alpine catchment. Hydrol. Process. 11(12): 1635–1647.

Boyer, E.W., G.M. Hornberger, K.E. Bencala, and D.M. Mcknight. 2000. Effects of asynchronous snowmelt on flushing of dissolved organic carbon: a mixing model approach. Hydrol. Process. 14: 3291–3308.

Brown, V. A., J.J. McDonnell, D. A. Burns, and C. Kendall. 1999. The role of event water, a rapid shallow flow component, and catchment size in summer stormflow. J. Hydrol. 217(3-4): 171–190.

Burns, D.A., J.J. McDonnell, R.P. Hooper, N.E. Peters, J.E. Freer, C. Kendall, and K. Beven. 2001. Quantifying contributions to storm runoff through end-member mixing analysis and hydrologic measurements at the Panola Mountain Research Watershed (Georgia, USA). Hydrol. Process. 15(10): 1903–1924.

Chantigny, M. 2003. Dissolved and water-extractable organic matter in soils: a review on the influence of land use and management practices. Geoderma 113(3-4): 357–380.

Christopher, S.F., R. Lal, and U. Mishra. 2009. Regional study of no-till effects on carbon sequestration in the Midwestern United States. Soil Sci. Soc. Am. J. 73(1): 207.

Christophersen, N., and R.P. Hooper. 1992. Multivariate analysis of stream water chemical data: The use of principal components analysis for the end-member mixing problem. Water Resour. Res. 28(1): 99–107.

Christophersen, N., C. Neal, R.P. Hooper, R.D. Vogt, and S. Andersen. 1990. Modelling streamwater chemistry as a mixture of soilwater end-members - a step towards second-generation acidification models. J. Hydrol. 116: 307–320.

Clymans, W. 2012. Land use related silica dynamics in terrestrial ecosystems. PhD dissertation KU Leuven, Leuven, Belgium: 178.

Clymans, W., G. Govers, E. Frot, B. Ronchi, B. Van Wesemael, and E. Struyf. 2013. Temporal dynamics of bio-available Si fluxes in a temperate forested catchment (Meerdaal forest, Belgium). Biogeochemistry 116(1-3): 275–291.

Cookson, W.R., D. V. Murphy, and M.M. Roper. 2008. Characterizing the relationships between soil organic matter components and microbial function and composition along a tillage disturbance gradient. Soil Biol. Biochem. 40(3): 763–777.

Cronan, C.S., J.T. Piampiano, and H.H. Patterson. 1999. Influence of land use and hydrology on exports of carbon and nitrogen in a Maine river basin. J. Environ. Qual. 28(3): 953–961.

Currie, W.S., and J.D. Aber. 1997. Modeling leaching as a decomposition process in humid montane forests. Ecology 78(6): 1844–1860.

Dalzell, B., T. Filley, and J. Harbor. 2007. The role of hydrology in annual organic carbon loads and terrestrial organic matter export from a midwestern agricultural watershed. Geochim. Cosmochim. Acta 71(6): 1448–1462.

Dawson, J.J.C., M.F. Billett, C. Neal, and S. Hill. 2002. A comparison of particulate , dissolved and gaseous carbon in two contrasting upland streams in the UK. J. Hydrol. 257: 226–246.

Dawson, J.J.C., C. Soulsby, D. Tetzlaff, M. Hrachowitz, S.M. Dunn, and I.A. Malcolm. 2008a. Influence of hydrology and seasonality on DOC exports from three contrasting upland catchments. Biogeochemistry 90: 93–113.

Dawson, J.J.C., C. Soulsby, D. Tetzlaff, M. Hrachowitz, S.M. Dunn, and I. a. Malcolm. 2008b. Influence of hydrology and seasonality on DOC exports from three contrasting upland catchments. Biogeochemistry 90(1): 93–113.

Dawson, J.J.C., D. Tetzlaff, M. Speed, M. Hrachowitz, and C. Soulsby. 2011. Seasonal controls on DOC dynamics in nested upland catchments in NE Scotland. Hydrol. Process. 25(10): 1647–1658.

Dawson, H.J., F.C. Ugolini, B.F. Hrutfiord, and J. Zachara. 1978. Role of soluble organics in soil processes of a Podzol, central Cascades,Washington. Soil Sci. 126: 290–296.

Deckers, J., R. Langohr, J. Poesen, and K. Vancampenhout. 2009. Natuur en cultuur volgens de bodem 34-45. *In* De Bie, H., M. Hermy and P. Van den Bremt (eds). Miradal, Erfgoed in Heverleebos en Meerdaalwoud. Davidsfonds, Leuven, Belgium.

IAEA. 2005. Isotopic composition of precipitation in the mediterranean basin in relation to air circulation patterns and climate. IAEA, Vienna, Austria.

De Troyer, I. 2011. Genesis and dynamics of dissolved organic matter in agricultural soils. PhD dissertation KU Leuven, Leuven, Belgium: 177.

De Troyer, I., R. Merckx, F. Amery, and E. Smolders . 2014. Factors controlling the dissolved organic matter concentration in pore waters of agricultural soils. Vadose Zone J. 13(7).

Don, A., and E.-D. Schulze. 2008. Controls on fluxes and export of dissolved organic carbon in grasslands with contrasting soil types. Biogeochemistry 91(2-3): 117–131.

Evans, C.D., D.T. Monteith, and D.M. Cooper. 2005. Long-term increases in surface water dissolved organic carbon: observations, possible causes and environmental impacts. Environ. Pollut. 137(1): 55–71.

Fenicia, F., D. Kavetski, and H.H.G. Savenije. 2011. Elements of a flexible approach for conceptual hydrological modeling: 1. Motivation and theoretical development. Water Resour. Res. 47(11): 1–13.

Fenicia, F., H.H.G. Savenije, P. Matgen, and L. Pfister. 2006. Is the groundwater reservoir linear ? Learning from data in hydrological modelling. Hydrol. Earth Syst. Sci. 10: 139–150.

Fenicia, F., H.H.G. Savenije, P. Matgen, and L. Pfister. 2008. Understanding catchment behavior through stepwise model concept improvement. Water Resour. Res. 44: 1–13.

Fierer, N.G., and E.J. Gabet. 2000. Carbon and nitrogen losses by surface runoff following changes in vegetation. J. Environ. Qual. 31(4): 1207–13.

Freeman, C., C.D. Evans, D.T. Monteith, B. Reynolds, and N. Fenner. 2001. Export of organic carbon from peat soils. Nature 412(6849): 785.

Freeman, C., N. Fenner, N.J. Ostle, H. Kang, D.J. Dowrick, B. Reynolds, M. a Lock, D. Sleep, S. Hughes, and J. Hudson. 2004. Export of dissolved organic carbon from peatlands under elevated carbon dioxide levels. Nature 430(6996): 195–8.

Futter, M.N., D. Butterfield, B.J. Cosby, P.J. Dillon, a. J. Wade, and P.G. Whitehead. 2007. Modeling the mechanisms that control in-stream dissolved organic carbon dynamics in upland and forested catchments. Water Resour. Res. 43(2): 1–16.

Gelman, A., and D.B. Rubin. 2007. lnference from Iterative Simulation Using Multiple Sequences. Simulation 7(4): 457–472.

Govers, G. 1991. A field study on topographical and topsoil effects on runoff generation. Catena 18: 91–111.

Grieve, I.C. 1991a. A model of dissolved organic carbon concentrations in soil and stream waters. Hydrol. Process. 5: 301–307.

Grieve, I.C. 1991b. Dissolved organic carbon trends in small streams, land use effects and models of temportal variation. *In* "Sediment and stream water quality in a changing environment: Trends and explanation." Proceedings of the Vienna Symposium, August, 1991. IAHS Publication. 203: 201-208.

Gruau, G., and E. Jardé. 2005. Export of DOM by rivers: Assessing the relative effects of climate change and human activities using long-term records. p. A759. *In* Goldschmidt Conference Abstracts 2005 Watershed Scale Geochemistry.

Guggenberger, G., and K. Kaiser. 2003. Dissolved organic matter in soil: challenging the paradigm of sorptive preservation. Geoderma 113(3-4): 293–310.

Hagedorn, F., P. Schleppi, P. Waldner, and H. Flühler. 2000. Export of dissolved organic carbon and nitrogen from Gleysol dominated catchments – the significance of water flow paths. Biogeochemistry 50: 137–161.

Halliday, S.J., A.J. Wade, R.A. Skeffington, C. Neal, B. Reynolds, P. Rowland, M. Neal, and D. Norris. 2012. An analysis of long-term trends , seasonality and short-term dynamics in water quality data from Plynlimon, Wales. Sci. Total Environ. 434: 186–200.

Haynes, R.J. 2000. Labile organic matter as an indicator of organic matter quality in arable and pastoral soils in New Zealand. Soil Biol. Biochem. 32: 211–219.

Hermle, S., T. Anken, J. Leifeld, and P. Weisskopf. 2008. The effect of the tillage system on soil organic carbon content under moist, cold-temperate conditions. Soil Tillage Res. 98(1): 94–105.

Hernes, P., R. Spencer, R. Dyda, B. Pellerin, P. Bachand, and B. Bergamaschi. 2008. The role of hydrologic regimes on dissolved organic carbon composition in an agricultural watershed. Geochim. Cosmochim. Acta 72(21): 5266–5277.

Hinton, M.J., S.L. Schiff, and M.C. English. 1997. The significance of storms for the concentration and export of dissolved organic carbon from two Precambrian Shield catchments. Biogeochemistry 36: 67–88.

Hinton, M.J., S.L. Schiff, and M.C. English. 1998. Sources and flowpaths of dissolved organic carbon during storms in two forested watersheds of the Precambrian Shield. Biogeochemistry 41: 175–197.

Holland, J.M. 2004. The environmental consequences of adopting conservation tillage in Europe: reviewing the evidence. Agric. Ecosyst. Environ. 103(1): 1–25.

Holloway, J.M., and R.A. Dahlgren. 2001. Seasonal and event-scale variations in solute chemistry for four Sierra Nevada catchments. J. Hydrol. 250: 106–121.

Hooper, R.P. and C. Shoemaker. 1986. A comparison of chemical and isotopic hydrograph separation. Water Resour. Res. 22(10): 1444-1454.

Hooper, R.P. 2003. Diagnostic tools for mixing models of stream water chemistry. Water Resour. Res. 39(3).

Hope, D., M.F. Billett, and M.S. Cresser. 1997. Exports of organic carbon in two river systems in NE Scotland. J. Hydrol. 193(1-4): 61–82.

Hornberger, G.M., K.E. Bencala, and D.M. McKnight. 1994. Hydrological controls on dissolved organic-carbon during snowmelt in the Snake River near Montezuma, Colorado. Biogeochemistry 25: 147–165.

Inamdar, S.P., and M.J. Mitchell. 2006. Hydrologic and topographic controls on storm-event exports of dissolved organic carbon (DOC) and nitrate across catchment scales. Water Resour. Res. 42: 1–16.

Jaffrain, J., F. Gérard, M. Meyer, and J. Ranger. 2007. Assessing the Quality of Dissolved Organic Matter in Forest Soils Using Ultraviolet Absorption Spectrophotometry. Soil Sci. Soc. Am. J. 71(6): 1851–1858.

Jardine, P.M., M.A. Mayes, P.J. Mulholland, P.J. Hanson, J.R. Tarver, R.J. Luxmoore, J.F. McCarthy, and G. V. Wilson. 2006. Vadose zone flow and transport of dissolved organic carbon at multiple scales in humid regimes. Vadose Zone J. 5(1): 140.

Kaiser, K., and G. Guggenberger. 2005. Storm flow flushing in a structured soil changes the composition of dissolved organic matter leached into the subsoil. Geoderma 127(3-4): 177–187.

Kaiser, K., and K. Kalbitz. 2012. Cycling downwards – dissolved organic matter in soils. Soil Biol. Biochem. 52: 29–32.

Kalbitz, K., S. Solinger, J.. Park, B. Michalzik, and E. Matzner. 2000. Controls on the dynamics of dissolved organic matter in soils: a review. Soil Sci. 165(4): 277–304.

Kavetski, D., and F. Fenicia. 2011. Elements of a flexible approach for conceptual hydrological modeling: 2. Application and experimental insights. Water Resour. Res. 47(11): 1–19.

Kendall C. and J. J. McDonnell (eds.). 1998. Isotope Tracers in Catchment Hydrology. Elsevier Science B.V., Amsterdam.

Kirchner, J.W., X. Feng, C. Neal and A.J. Robson. 2004. The fine structure of water-quality dynamics: the (high-frequency) wave of the future. Hydrol. Process. 18: 1353–1359.

Kirchner, J.W. 2009. Catchments as simple dynamical systems : Catchment characterization , rainfall-runoff modeling , and doing hydrology backward. Water Resour. Res. 45: 1–34.

Kvalseth, T.O. 1985. Cautionary note about R^2. Am. Stat. 39(4): 279–285.

Lambert, T., A.-C. Pierson-Wickmann, G. Gruau, A. Jaffrezic, P. Petitjean, J.-N. Thibault, and L. Jeanneau. 2013. Hydrologically driven seasonal changes in the sources and production mechanisms of dissolved organic carbon in a small lowland catchment. Water Resour. Res. 49(9): 5792–5803.

Langhans, C., G. Govers, J. Diels, A. Leys, W. Clymans, A. Van Den Putte, and J. Valckx. 2011. Experimental rainfall–runoff data: Reconsidering the concept of infiltration capacity. J. Hydrol. 399(3-4): 255–262.

Laudon, H. and O. Slaymaker. 1997. Hydrograph separation using stable isotopes, silica and electrical conductivity: an alpine example. J. Hydrol. 201: 82-101.

Laudon, H., S. Köhler, and I. Buffam. 2004. Seasonal TOC export from seven boreal catchments in northern Sweden. Aquat. Sci. 66: 223–230.

Laudon, H., V. Sjoblom, I. Buffam, J. Seibert, and M. Morth. 2007. The role of catchment scale and landscape characteristics for runoff generation of boreal streams. J. Hydrol. 344(3-4): 198–209.

Ledesma, J.L.J., S.J. Köhler, and M.N. Futter. 2012. Long-term dynamics of dissolved organic carbon: Implications for drinking water supply. Sci. Total Environ. 432: 1–11.

Leenheer, J.A., and J.-P. Croué. 2003. Characterising aquatic dissolved organic matter. Evironmental Sci. Technol. 37: 18A–26A.

Lewis, W.M., and M.C. Grant. 1979. Relationships between stream discharge and yield of dissolved substances from a Colorado mountain watershed. Soil Sci. 128(6): 353–363.

Leys, A., G. Govers, K. Gillijns, E. Berckmoes, and I. Takken. 2010. Scale effects on runoff and erosion losses from arable land under conservation and conventional tillage: The role of residue cover. J. Hydrol. 390(3-4): 143–154.

Leys, a., G. Govers, K. Gillijns, and J. Poesen. 2007. Conservation tillage on loamy soils: explaining the variability in interrill runoff and erosion reduction. Eur. J. Soil Sci. 58(6): 1425–1436.

Liang, L., and P.C. Singer. 2003. Factors influencing the formation and relative distribution of haloacetic Acids and trihalomethanes in drinking water. Environ. Sci. Technol. 37(13): 2920–2928.

Littell, R.C. 2002. Analysis of unbalanced mixed model data: A case study comparison of ANOVA versus REML/GLS. J. Agric. Biol. Environ. Stat. 7(4): 472–490.

Littell, R.C., G.. Milliken, W.W. Stroup, R.D. Wolfinger, and O. Schabenberger. 2006. SAS for mixed models, second edition. Cary, NC: SAS Institute Inc.

Lundquist, E.J., L.E. Jackson, and K.M. Scow. 1999. Wet- dry cycles affect dissolved organic carbon in two California agricultural soils. Soil Biol. Biochem. 31: 1031–1038.

Mattsson, T., P. Kortelainen, A. Laubel, D. Evans, M. Pujo-Pay, A. Räike, and P. Conan. 2009. Export of dissolved organic matter in relation to land use along a European climatic gradient. Sci. Total Environ. 407(6): 1967–76.

McDowell, W.H., and G.E. Likens. 1988. Origin , Composition , and Flux of Dissolved Organic Carbon in the Hubbard Brook Valley. Ecol. Monogr. 58(3): 177–195.

McGlynn, B.L., and J.J. McDonnell. 2003. Role of discrete landscape units in controlling catchment dissolved organic carbon dynamics. Water Resour. Res. 39(4).

Mei, Y., G.M. Hornberger, L.A. Kaplan, J.D. Newbold, and A.K. Aufdenkampe. 2014. The delivery of dissolved organic carbon froma forested hillslope to a headwater streamin southeastern Pennsylvania, USA. Water Resour. Res. 50: 5774–5796.

Merckx, R., K. Brans, and E. Smolders. 2001. Decomposition of dissolved organic carbon after soil drying and rewetting as an indicator of metal toxicity in soils. Soil Biol. Biochem. 33(2): 235–240.

Mertens, J., J. Vanderborght, R. Kasteel, T. P., R. Merckx, J. Feyen, and E. Smolders. 2007. Dissolved organic carbon fluxes under bare Soil. J. Environ. Qual. 36(2001): 597–606.

Meybeck, M. 1982. Carbon, nitrogen, and phosphorus transport by world rivers. Am. J. Sci. 282: 401–450.

Morris, D.P., H. Zagarese, C.E. Williamson, E.G. Balseiro, B.R. Hargreaves, B. Modenutti, R. Moeller, and C. Queimalinos. 1995. The attenuation of solar UV radiation in lakes and the role of dissolved organic carbon. Limnol. Oceanogr. 40(8): 1381–1391.

Mulholland, P.J., and W.R. Hill. 1997. Seasonal patterns in streamwater nutrient and dissolved organic carbon concentrations: Separating catchment flow path and in-stream effects. Water Resour. Res. 33(6): 1297.

Neff, J.C., and G.P. Asner. 2001. Dissolved Organic Carbon in Terrestrial Ecosystems: Synthesis and a Model. Ecosystems 4(1): 29–48.

Peeters, L. 2010. Groundwater and geochemical modelling of the unconfined Brussels aquifer, Belgium. PhD dissertation KU Leuven, Leuven, Belgium. (January): 205.

Poesen, J. 1984. The influence of slope angle on infiltration rate and Hortonian overland flow volume. Zeitschrift fur Geomorphol. (Suppl. Bd. 49): 117–131.

Poesen, J., F. Ingelmo-Sanchez, and H. Mücher. 1990. The hydrological response of soil surfaces to rainfall as affected by cover and position of rock fragments in the top layer. Earth Surf. Process. Landforms 15: 653–671.

Qualls, R.G., and B.L. Haines. 1991. Geochemistry of Dissolved Organic Nutrients in Water Percolating through a Forest Ecosystem. Soil Sci. Soc. Am. J. 55: 1112–1123.

Regnier, P., P. Friedlingstein, P. Ciais, F.T. Mackenzie, N. Gruber, I.A. Janssens, G.G. Laruelle, R. Lauerwald, S. Luyssaert, A.J. Andersson, S. Arndt, C. Arnosti, A. V. Borges, A.W. Dale, A. Gallego-Sala, Y. Goddéris, N. Goossens, J. Hartmann, C. Heinze, T. Ilyina, F. Joos, D.E. LaRowe, J. Leifeld, F.J.R. Meysman, G. Munhoven, P. a. Raymond, R. Spahni, P. Suntharalingam, and M. Thullner. 2013. Anthropogenic perturbation of the carbon fluxes from land to ocean. Nat. Geosci. 6: 597–607.

Ronchi, B. 2014. Controlling factors of dissolved silicon in upstream catchments with different land uses. PhD dissertation KU Leuven, Leuven, Belgium: 110.

Roper, M.M., V.V.S.R. Gupta, and D. V Murphy. 2010. Tillage practices altered labile soil organic carbon and microbial function without affecting crop yields. Aust. J. Soil Res.: 274–285.

Royer, T.V. and M.B. David. 2005. Export of dissolved organic carbon from agricultural streams in Illinois, USA. Aquat. Sci. 67: 465-471.

Royer, I., D.A. Angers, M. Chantigny, R.R. Simard, and D. Cluis. 2007. Dissolved organic carbon in runoff and tile-drain water under corn and forage fertilized with hog manure. J. Environ. Qual. 36(3): 855–63.

Ruthy, I., and A. Dassargues. 2008. Notice explicative, Carte hydrogéologique de Wallonie 42/3-4 (Dalhem-Herve). Université de Liège, Liège, Belgium. 50p.

Sanderman, J., K. A. Lohse, J. A. Baldock, and R. Amundson. 2009. Linking soils and streams: Sources and chemistry of dissolved organic matter in a small coastal watershed. Water Resour. Res. 45.

Shanley, J.B., W.H. McDowell, and R.F. Stallard. 2011. Long-term patterns and short-term dynamics of stream solutes and suspended sediment in a rapidly weathering tropical watershed. Water Resour. Res. 47.

Siemens, J., M. Haas, and M. Kaupenjohann. 2003. Dissolved organic matter induced denitrification in subsoils and aquifers? Geoderma 113(3-4): 253–271.

Sklash, M.G. and R.N. Farvolden. 1979. The role of groundwater in storm runoff. J. Hydrol. 43: 45-65.

Stedmon C.A., S. Markager, M. Søndergaard, T. Vang, A. Laubel, N.H. Borch and A. Windelin. 2006. Dissolved organic matter (DOM) export to a temperate estuary: seasonal variations and implications of land use. Estuaries and Coasts 29: 388–400.

Tate, C.M., and J.L. Meyer. 1983. The influence of hydrologic conditions and successional state on dissolved organic carbon export from forested watersheds. Ecology 64(1): 25–32.

Tetzlaff, D., C. Soulsby, S. Waldron, I.A. Malcolm, P.J. Bacon, S.M. Dunn, A. Lilly and A.F. Youngson. 2007. Conceptualization of runoff processes using a geographical information system and tracers in a nested mesoscale catchment. Hydrol. Process. 21: 1289-1307.

Thurman, E. 1985. Organic geochemistry of natural waters. Kluwer, Dordrecht.

Tipping, E. 1993. Modeling the competition between alkaline-earth cations and trace-metal species for binding by humic substances. Environ. Sci. Technol. 27(3): 520–529.

Tipping, E., C. Woof, E. Rigg, A.F. Harrison, P. Ineson, K. Taylor, D. Benham, J. Poskitt, A.P. Rowland, R. Bol, and D.D. Harkness. 1999. Climatic influences on the leaching of dissolved organic matter from upland UK moorland soils, investigated by a field manipulation experiment. Environ. Int. 25(1): 83–95.

VandenBygaart, A.J., E.G. Gregorich, and D.A. Angers. 2003. Influence of agricultural management on soil organic carbon: A compendium and assessment of Canadian studies. Can. J. Soil Sci. 83(4): 363–380.

Van den Putte, A., G. Govers, J. Diels, C. Langhans, W. Clymans, E. Vanuytrecht, R. Merckx, and D. Raes. 2012. Soil functioning and conservation tillage in the Belgian Loam Belt. Soil Tillage Res. 122: 1–11.

Van Oost, K., G. Govers, O. Cerdan, D. Thauré, A. Van Rompaey, A. Steegen, J. Nachtergaele, I. Takken and J. Poesen, 2005. Spatially distributed data for erosion model calibration and validation: the Ganspoel and Kinderveld datasets. Catena, 61: 105-121.

Verheyen, D., N. Van Gaelen, B. Ronchi, O. Batelaan, E. Struyf, G. Govers, R. Merckx, J. and Diels. 2015. Dissolved phosporus transport from soil to surface water in catchments with different land use. AMBIO 44, 228-240.

Vrugt, J.A., C.J.F. Braak, C.G.H. Diks, B.A. Robinson, J.M. Hyman, and D. Higdon. 2009. Accelerating Markov chain Monte Carlo simulation by differential evolution with self-adaptive randomized subspace sampling. Int. J. Nonlinear Sci. Numer. Simul. 10(3): 271–288.

Vrugt, J.A., C.J.F. Braak, H. V. Gupta, and B.A. Robinson. 2008a. Equifinality of formal (DREAM) and informal (GLUE) Bayesian approaches in hydrologic modeling? Stoch. Environ. Res. Risk Assess. 23(7): 1011–1026.

Vrugt, J.A., C.J.F. ter Braak, M.P. Clark, J.M. Hyman, and B.A. Robinson. 2008b. Treatment of input uncertainty in hydrologic modeling: Doing hydrology backward with Markov chain Monte Carlo simulation. Water Resour. Res. 44: 1–15.

Vrugt, J.A., H. V. Gupta, W. Bouten, and S. Sorooshian. 2003. A Shuffled Complex Evolution Metropolis algorithm for optimization and uncertainty assessment of hydrologic model parameters. Water Resour. Res. 39(8).

Wang, Z., G. Govers, K. Van Oost, W. Clymans, A. Van den Putte, and R. Merckx. 2013. Soil organic carbon mobilization by interrill erosion: Insights from size fractions. J. Geophys. Res. Earth Surf. 118.

Weishaar, J.L., G.R. Aiken, B. A. Bergamaschi, M.S. Fram, R. Fujii, and K. Mopper. 2003. Evaluation of specific ultraviolet absorbance as an indicator of the chemical composition and reactivity of dissolved organic carbon. Environ. Sci. Technol. 37(20): 4702–8.

Willems, P. 2009. A time series tool to support the multi-criteria performance evaluation of rainfall-runoff models. Environ. Model. Softw. 24(3): 311–321.

Worrall, F., R. Harriman, C.D. Evans, C.D. Watts, J. Adamson, C. Neal, E. Tipping, T. Burt, I. Grieve, D. Monteith, P.S. Naden, T. Nisbet, B. Reynolds, and P. Stevens. 2004. Trends in dissolved organic carbon in UK rivers and lakes. Biogeochemistry 70: 369–402.

Xenopoulos, M. a., D.M. Lodge, J. Frentress, T. A. Kreps, S.D. Bridgham, E. Grossman, and C.J. Jackson. 2003. Regional comparisons of watershed determinants of dissolved organic carbon in temperate lakes from the Upper Great Lakes region and selected regions globally. Limnol. Oceanogr. 48(6): 2321–2334.

Xu, N., J.E. Saiers, H.F. Wilson, and P. A. Raymond. 2012. Simulating streamflow and dissolved organic matter export from a forested watershed. Water Resour. Res. 48(5): 1–18.

Zhang, Z., T. Fukushima, Y. Onda, T. Gomi, T. Fukuyama, R. Sidle, K. Kosugi, and K. Matsushige. 2007. Nutrient runoff from forested watersheds in central Japan during typhoon storms : implications for understanding runoff mechanisms during storm events. Hydrol. Process. 1178: 1167– 1178.

Zsolnay, A., E. Baigar, M. Jimenez, B. Steinweg, and F. Saccomandi. 1999. Differentiating with fluorescence spectroscopy the sources of dissolved organic matte in soils subjected to drying. Science (80-.). 38(1): 45–50.

Publications

Van Gaelen, N., Verschoren, V., Clymans, W., Poesen, J., Govers, G., Vanderborght, J. and Diels, J. 2014. Controls on dissolved organic carbon export through surface runoff from loamy agricultural soils. Geoderma 226-227, 387-396.

http://dx.doi.org/10.1016/j.geoderma.2014.03.018

Van Gaelen, N., Verheyen, D., Ronchi, B., Struyf, E., Govers, G., Vanderborght, J. and Diels, J. 2014. Identifying the Transport Pathways of Dissolved Organic Carbon in Contrasting Catchments. Vadose Zone Journal 13 (7).

http://dx.doi.org/10.2136/vzj2013.11.0199

Verheyen, D., **Van Gaelen, N.**, Ronchi, B., Batelaan, O., Struyf, E., Govers, G, Merckx, R. and Diels, J. 2015. Dissolved phosporus transport from soil to surface water in catchments with different land use. AMBIO 44, 228-240.

http://dx.doi.org/10.1007/s13280-014-0617-5

Mboh, C.M., Huisman, J.A., **Van Gaelen, N.**, Rings, J. and Vereecken, H. 2012. Coupled hydrogeophysical inversion of electrical resistances and inflow measurements for topsoil hydraulic properties under constant head infiltration. Near Surface Geophysics 10, 413-426.

http://dx.doi.org/10.3997/1873-0604.2012009